Tuft cell-derived acetylcholine regulates epithelial fluid secretion and helminth clearance

Tyler Billipp

A dissertation

submitted in partial fulfillment of the

requirements for the degree of

Doctor of Philosophy

University of Washington

2023

Reading Committee:

Jakob von Moltke, Chair

Elia Tait Wojno

Daniel J. Campbell

Program authorized to offer degree:

Immunology

University of Washington

Abstract

Tuft cell-derived acetylcholine regulates epithelial fluid secretion and helminth clearance

Tyler Billipp

Chair of the Supervisory Committee:

Jakob von Moltke

Department of Immunology

Helminth, or parasitic worm, infection afflicts nearly one third of humans worldwide, resulting in massive suffering and comorbidity. The arm of the immune system responsible for combatting helminth infection, called “Type 2” immunity, is also responsible for causing a variety of allergic diseases. Understanding how Type 2 immunity is regulated has the potential to inform both better treatment for helminth infection as well as allergic disease.

Mucosal barrier tissues are the site of exposure to Type 2 stimuli and the locus of the ensuing immune response. Both the airways and the gastrointestinal tract are protected by a gradient of mucus, antimicrobial peptides, and fluid secreted by epithelial cells that contribute to host defense and enable key physiological functions of the tissues. The Type 2 immune response triggers epithelial remodeling that increases fluid

and mucus secretion as well as contractility of underlying smooth muscle in order to flush away helminths and allergens. Acetylcholine is a key regulator of both epithelial secretion and muscle contraction. Collectively this response is known as “weep and sweep” and familiar to anyone who experiences seasonal allergies.

While the effects of Type 2 immunity have been well understood for decades, the initiation of the response remained a mystery until recently, when tuft cells were discovered as the key sensors of intestinal helminth infection. Tuft cells are epithelial cells that possess chemosensory machinery linking sensing of lumenal stimuli via a suite of receptors to basolateral secretion of immune- and neuro-modulating factors including IL-25, leukotrienes, and acetylcholine (ACh). In response to small intestinal (SI) helminth infection or succinate, a metabolite produced by protist and bacterial colonization, tuft cells secrete IL-25 and leukotrienes to activate Group 2 innate lymphoid cells (ILC2s) that produce the hallmark Type 2 cytokines IL-5 and IL-13. IL-13 signals on the intestinal stem cell compartment to drive preferential differentiation of mucus-producing goblet cells and, intriguingly, tuft cells, which rapidly remodels the epithelium in a matter of days. This remodeling, and thus tuft cells, are required for helminth clearance. Additional functions of SI tuft cells or tuft-derived ACh are not known.

We show that in response to sensing of succinate or direct activation of the chemosensory ion channel TRPM5, SI tuft cells secrete ACh to induce epithelial fluid secretion in the intestine and airways, independently of neurons. Unlike other tissues where nearly 100% of tuft cells express the enzyme *Chat* required for ACh synthesis, the frequency of *Chat*+ SI tuft cells occurred in a gradient from the proximal to distal SI,

increasing from approximately 40% to 80% of tuft cells. Succinate-induced fluid secretion was restricted to the distal SI where *Chat*+ frequency and SUCNR1 expression was highest. Consistent with their high expression of *Sucnr1,* tuft cells in the trachea also responded to succinate by inducing ACh-dependent fluid secretion. In the proximal SI and colon tuft cell activation via the TRPM5 agonist Class 8 induced fluid secretion, but the exact ligands sensed by tuft cells in these tissues remains to be determined. Oral administration of Class 8 induced fluid secretion *in vivo* as measured by fecal water content.

During Type 2 tissue remodeling, *Chat*+ tuft cells increase in number, enhancing the fluid secretion response. Upon helminth infection, mice with *Chat*-deficient tuft cells experience delayed helminth clearance despite normal tuft-ILC2 circuit activation. We conclude that tuft cell-derived ACh regulates epithelial fluid secretion, and that this effector function can contribute to Type 2 immune responses during helminth infection. By coupling chemosensing to rapid epithelial fluid secretion, tuft cells coordinate an epithelium-intrinsic effector unit that can flush offending agents away from the tissue.

TABLE OF CONTENTS

LIST OF FIGURES

ACKNOWLEDGMENTS

I'd like to start by thanking Jakob for his trust as a mentor. Jakob trusted me in the lab before I trusted myself and this was key to tempering my fear of failure and developing confidence as an independent scientist. It was easy to return the trust—Jakob is such a level-headed and kind person that I never wondered for a second what his motives were or where I fit in. I am grateful to him for promoting an engaging, open-minded lab culture and I will deeply miss the wide-ranging discussions of our lab meeting. He also made running a lab look so easy. His commitment to working 9-5 set reasonable boundaries and the expectation that grad school doesn't have to consume you. It isn't easy to emulate him, but I'm trying. He's taught me to get to the root of the question and to identify the most critical experiments, pushing back on my tendency to get lost in the minutiae. His lack of paranoia about getting scooped and willingness to share data, mice, and reagents make science a better, more open, discipline. I'm proud of the gut immunology community that we have fostered across Seattle.

I thank my committee for their valuable feedback, flexibility, and kindness. I have looked forward to our meetings over the years and appreciated the perspectives they bring to my project, which isn't in anyone's wheelhouse. Perhaps most of all, I am grateful to my committee for telling me that I am enough—err, I mean that I have enough data! They kept me focused on what really matters in the PhD—getting out!

Thanks to the lab. Jack, Marija, Anna, and James oversaw my entry into academic science. I'll never forget what Jack said to me one time after I expressed amazement at his prodigious productivity in lab—"but doing experiments, that's the fun part!". I've tried to take that to heart. His example combined with Marija's fearlessness

and professionalism—remarkable for a student straight out of undergrad—showed me how to be in the lab. They were only one year above me, but they filled the role of much more senior scientists. The second phase of the lab, the true post-doc years, has been equally formative. It is so inspiring to have such smart, knowledgeable people in the lab to lean on and learn from. Thanks Aloe, Shan, Margaret, and Thornton. Thank you to Heber for keeping art and design on my mind and to the youth--Lily, Macy, Derek, Tuan, Danielle, and others—who keep me young(ish). Through the pandemic and everything else, this group of people has made every day worth going into lab. I can't thank you all enough!

Thanks to the department. Graduate school was not what I expected it to be, yet mostly what I needed it to be. I arrived in Seattle insecure about my place in immunology and motivated by external validation. The humble intensity and independent work ethic of my classmates and peers has slowly molded me over the years. Now, in my 22nd year of education I'm finally comprehending how to work for my own sake, for my own growth, pleasure, and benefit. I'm grateful to the many fantastic scientists in this program for this lesson and many others. The down-to-earth collegiality and impromptu social engagements and commiserations have fostered solidarity and given me the motivation to keep going. To my classmates specifically—thank you for being the perfect group of people to go through graduate school with. I'm grateful to have such kind and brilliant scientists so close to hand. Summer nights down at the Mohai docks will always have a special place in my heart. Class of '22-23 all the way!

I thank my many friends outside of science who have insisted on pulling me out of the lab, not taking my excuses, and making sure I experience the rest of what

Washington has to offer. It has been such a joy to explore the mountains on foot, bike, and ski and to cook meals, drink beer, and laugh with all of y'all. A special shoutout to my friend and longtime roommate Randall Stacy for our five years of cohabitating, adventuring, gardening, and hosting. It's been an absolute pleasure.

I'd also like to thank a number of people at my first job, Adimab. My transition from ecology and evolution to molecular and cell biology was made possible by the willingness of several important people to take a chance on me. From Beth Sharkey who hired me last-minute for my summer internship to Jon Belk and Kevin Schutz who took me on full-time as a "predoc", thank you for taking a chance on someone with next to no lab experience alongside graduates with extensive and impressive undergraduate research. I'm not sure I deserved it, but I sure am grateful. I am also indebted to Jen Symonds, Ross Connor, Cody Williams, William Roach, Cory Ahonen, Noel Pauli, and many others who gave me so much friendship and advice for graduate school and beyond. And to the immunologists—Noel, Cory, Laura Walker, Tony Cooper—thank you for the inspiration to join your ranks.

I'd like to thank my delightful partner Elaine Schmidt. I learn so much all the time being with her. Despite having lived here for a third of the time I have, she has opened my eyes to so many tiny wonders in the PNW, from the tidepool to the forest floor. Our adventures have been the best distraction from lab while reinvigorating my love for science overall. Her curiosity extends to my research, for which I am grateful and about which I promise to finally explain. I love you, Elaine!

Finally, I must thank my parents, Karen and Peter, without whom I could not have finished this degree. They raised me so gently and conscientiously and in doing so

allowed me the immense privilege of following my curiosity. I learned my love for nature and biology, and by extension my love of science, from them at our home surrounded by gardens, oaks, and so many frogs. They're the model of hard work that I use to motivate myself when my work piles up or I feel like procrastinating. Through the PhD they've kept my best interests at heart and helped make my lavish lifestyle possible on a grad student stipend. Their simultaneous concern with making sure I'm working enough and playing enough has kept me balanced and mostly sane. My visits home to Maine restore my resolve and when they visit it's exciting to show them around the beautiful state I now call home. Thank you for everything, I love you both so much!

CHAPTER 1
Introduction

Parts of this chapter are adapted from the following publication:

Billipp TE*, Nadjsombati MS*, von Moltke J. Tuning tuft cells: new ligands and effector functions reveal tissue-specific function. Current Opinion in Immunology. 2021. 68:98-106.

* Denotes equal contribution

1.1 Helminths and Type 2 immunity

Helminth, or parasitic worm, infection afflicts nearly one third of humans worldwide, resulting in massive suffering and comorbidity.[1] While helminth parasites are endemic to all latitudes, sanitation infrastructure and effective anti-helminthic drugs have rendered helminth infection a “disease of poverty” restricted primarily to the Global South. Thus, the poorest regions of the world must contend with the added burden of persistent parasitization. It is therefore crucial that we better understand the mechanisms by which helminths are controlled and expelled from the host.

The dynamic of host and parasite reflects a deep co-evolutionary relationship. Helminths have managed to parasitize all orders of animals from insects to mammals.[2] Analysis of ancient latrines and archaeological sites have confirmed that humans too have long contended with parasitization.[3] Consistent with this, one arm of the mammalian immune system, known as “Type 2” immunity, is believed to have evolved specifically to combat helminth infection.[4] This response is characterized by eosinophilia, CD4+ T helper 2 (Th2) cell polarization, IgE class-switching in B cells, and the production of the cytokines IL-4, IL-5, and IL-13.[5] In addition to targeting the worms directly, the Type 2 response remodels host organs to be inhospitable to worms and repairs others that have been damaged during their passage.[6] In the small intestine (SI), where many helminths traffic to mature and mate, Type 2 remodeling results in mucus overproduction from intestinal epithelial cells (IECs) and hypercontractility of the smooth muscle which together help to physically push the worms out in the feces: this response is known as “weep and sweep”.[5] In the intestine as well as the lungs, which

are damaged by the passage of some helminths, Type 2 responses target stromal cells and extracellular matrix to repair damage caused to these vital organs.[5]

While helminths can be killed or cleared by the Type 2 response, in many cases they chronically infect, and reinfect, their hosts. The apparent failure of the immune response reflects both the worm's exquisite ability to suppress Type 2 immunity as well as the host's regulation of Type 2 immunity to avoid immunopathology in cases of chronic infection.[7] Such a "failure" might actually be adaptive in light of epidemiological observations showing that as helminth infection rates have fallen in the Global North over the last 100 years, rates of allergic and autoinflammatory disease, including allergies, asthma, and psoriasis, have increased strikingly.[8,9] Somehow, despite apparently bearing little resemblance to helminths, allergens like pollen, peanuts, and house dust mites all trigger the same Type 2 immune response consisting of CD4+ Th2 cells, eosinophils, mast cells, and IgE.[10] The main difference between allergens and helminths appears to be the tolerogenic state that helminths induce, which protects the host from overblown Type 2 responses to both helminth and allergens.

Central to the initiation of an immune response is a sensing event in which the host detects the presence of the pathogen. Why these seemingly innocuous environmental and dietary factors are perceived as helminths by the immune system in the first place has long been a focus of research in the field. Yet, compared to viruses, bacteria, or fungi, little is known about how helminths or allergens are first detected by the host.

A recent breakthrough came in 2010 with the discovery of group 2 innate lymphoid cells, or ILC2s, which populate host barrier tissues such as the lung, skin, and

SI starting soon after birth.[11–14] ILC2s are considered the innate equivalent of CD4+ Th2 cells due to their shared gene expression and ability to produce the Type 2 effector cytokines IL-5 and -13.[15,16] Like Th2s, ILC2s become activated during both helminth infection and allergen exposure but via a distinct mode of activation. Instead of using a receptor specific for pathogen-associated antigens like the T cell receptor, ILC2s express a suite of surface receptors that instead detect signals produced by the host. The balance of these signals, some of which are activating (IL-25, IL-33, NMU, LTC4, etc.) while others suppressive (norepinephrine, CGRP, etc.), tunes the functional state of the ILC2, including the production of cytokines.[17] Thus, ILC2s sit poised in barrier tissues to monitor the state of the tissue and respond to cues released upon helminth infection as well as allergen exposure. One important cue is IL-25, which was discovered in 2016 to be produced in the SI by a little-studied epithelial cell type known as tuft cells.[18–20]

1.2 Tuft cells and Type 2

Tuft cells were first identified in the 1950s by their unique morphology — the eponymous apical tuft of long microvilli— in electron microscopy images of epithelial cells in rodent airways and gastro-intestinal tract.[21,22] Found in all endoderm-derived columnar epithelia, these morphologically similar cells were given different names in different tissues — microvillus cells in the olfactory epithelium, solitary chemosensory cells in the respiratory epithelium, brush cells in the trachea, tuft cells in the gastrointestinal tract — but share a common transcriptional and developmental identity driven by the transcription factor POU2F3 (POU Class 2 Homeobox 3).[20,23,24]

Tuft cells closely resemble taste cells by their shared expression of the chemosensory pathway required for bitter, sweet, and umami taste transduction.[25,26] Canonically, this pathway is activated in taste cells by G protein-coupled taste receptors (TAS1R, TAS3R, and the TAS2R family) signaling through GNAT3 (G Protein Subunit Alpha Transducin 3), PLCB2 (Phospholipase C Beta 2) and ITPR3 (Inositol 1,4,5-Trisphosphate Receptor Type 3). The resulting Ca^{2+} flux opens the membrane cation channel TRPM5 (Transient Receptor Potential Cation Channel Subfamily M Member 5), which depolarizes the cell and drives release of ATP to activate adjacent neurons, relaying the sensation of taste to the brain.[27] Tuft cells therefore appeared to extend the chemosensory function of taste cells beyond the oral cavity to the barrier epithelia of the body, where they could potentially serve as sentinel cells “tasting” foreign stimuli. Intriguingly, tuft cells also expressed the machinery to synthesize a variety of immune- and neuro-modulatory signaling molecules, including IL-25, inflammatory lipid signaling molecules called leukotrienes, and the neurotransmitter acetylcholine (ACh).[28]

In 2016, several groups identified tuft cells as the key sensors of helminth infection responsible for initiating the Type 2 immune response in the SI. The findings centered on SI tuft cells as the sole source of IL-25, an important activating ligand for ILC2s, as well as their chemosensory capacity via the ion channel TRPM5.[18,20,29] Upon infection by the helminths *Nippostrongylus brasiliensis*, *Heligmosomoides polygyrus*, and *Trichinella spiralis*, or colonization by protists in the *Tritrichomonas* genus, SI tuft cell-derived IL-25 directly activates ILC2s in the lamina propria. Another tuft-derived molecule, leukotriene C4 (LTC4), is also released during helminth infection, but not protist colonization, and synergizes with IL-25 to even more potently activate ILC2s.[30] In

both contexts, genetic knockout of TRPM5 prevents ILC2 activation, presumably by inhibiting release of IL-25 and/or LTC4.

Once activated, ILC2s produce the canonical type 2 cytokines IL-5, IL-9, and IL-13 to coordinate classic manifestations of Type 2 inflammation. Among its many targets, IL-13 signals to the intestinal epithelial stem cell compartment, biasing lineage commitment toward tuft and goblet cells and resulting in hyperplasia of both cell types and initiation of a feed-forward tuft-ILC2 circuit.[19] Since the intestinal epithelium is almost completely renewed every 5 days, activation of the tuft-ILC2 circuit results in rapid remodeling of the intestinal epithelium which contributes to helminth clearance in part due to increased mucus secretion from increased numbers of goblet cells. The dramatic increase in tuft cell numbers suggests that tuft cells might perform additional functions during helminth infection, since it otherwise seems to be an inefficient way to achieve greater ILC2 activation. We are concerned with understanding what these additional functions of tuft cells in the SI might be.

1.3 Succinate sensing

While the exact helminth ligand detected by SI tuft cells—if it is a ligand at all—remains unknown, the discovery that *Tritrichomonas* sp. protists and certain bacteria produce succinate has helped to uncover more tuft cell biology.[31–33] Succinate, sensed by the succinate receptor (SUCNR1), is the first and best characterized ligand discovered for SI tuft cells. Succinate is a TCA cycle intermediate found in host cells as well as a metabolite produced by the protists and bacteria. But why detect succinate? Succinate can function as a damage-associated molecular pattern (DAMP) indicative of

mitochondrial and cellular stress when encountered by dendritic cells in the extracellular spaces within tissues, but this usually drives a pro-inflammatory Type 1 response.[34] Instead, when sensed by tuft cells in the intestinal lumen, succinate seems to indicate microbial dysbiosis, as perturbations to the microbiome induced by antibiotic or laxative treatment can result in spikes of succinate, likely due to imbalances in microbial energy consumption webs.[31] The resulting Type 2 epithelial remodeling and mucus production may help to encourage the re-growth of stable bacterial communities. In the case of the protists, the function of succinate sensing is not so clear—while protists induce potent immune responses in the SI (Type 2) and large intestine (LI; Type 1 and 17) they don't appear to harm the host in any obvious ways, nor do the immune responses have much effect on protist abundance.[18,35,36] Their presence does offer some collateral immunity towards bacterial and helminth infection in each respective tissue, however.[33,36] Surprisingly, even though several helminths also produce succinate as a metabolite, sensing of succinate via SUCNR1 is not important, or at least redundant, for activation of a robust Type 2 response and timely worm clearance.[32]

Tuft cells express SUCNR1 in other tissues besides the SI, including the trachea where tuft cells express the receptor at the highest level of any tissue.[32] It remains to be tested whether tracheal tuft cells can sense succinate, what the potential source of succinate is, and the purpose of succinate sensing in the trachea.

1.4 Tuft cells and acetylcholine

Before SI tuft cells were linked to helminths and Type 2 immunity, the paradigm around tuft cells centered on sensing of noxious environmental ligands and bacterial

products via the TAS2R family of bitter taste receptors and responding rapidly via a variety of anti-bacterial and neurogenic responses.[37] Previous studies focused on tuft cells in barrier tissues outside of the SI, namely the nasal passages, trachea, and urogenital tract, and many identified acetylcholine (ACh) as the key secreted factor from tuft cells coordinating these responses.[38–40] ACh is produced by the enzyme choline acetyltransferase (ChAT), and expression of *Chat* defines not only cholinergic neurons but also tuft cells across all tissues as part of their global signature.[26] In the airways and urogenital tract nearly 100% of tuft cells express *Chat* transcript. As a neurotransmitter, ACh typically signals over the short distance between neurons and is rapidly degraded by acetylcholinesterases (AChEs) outside of the synapse. Many questions remain about the production and regulation of non-neuronal ACh, however.

Bitter ligands are a signal that a substance is noxious or toxic and to be avoided.[41] In the airways tuft cells are approached by sensory neuronal fibers and closely contacted by synapse-like structures,[38,39] raising the possibility that tuft cells signal to neurons to regulate distal or whole tissue function. Indeed, ACh from tracheal tuft cells signals to peptidergic sensory neurons expressing nicotinic ACh receptors (nAChRs) to mediate evasion of noxious substances via transient breathing cessation.[39] Sensing of the same ligands as well as some bacterial ligands, specifically quorum-sensing molecules (QSMs), via the same TAS2R receptors also results in signaling to sensory neurons through nAChRs. In the nasal passages this results in neuronal release of peptides that cause local inflammation by inducing mucosal mast cell degranulation and vascular leakage, possibly in anticipation of bacterial overgrowth into the tissue.[40] In the urethra, sensing of bitter compounds results in neuronally-mediated

contraction of the bladder detrusor muscle, potentially stimulating urination to prevent bacterial colonization of the renal system.[42]

Consistent with the theme of sensing dangerous bacterial growth, tracheal tuft cells also detect formylated peptides produced by a variety of pathogenic bacteria of the lung.[43] Stimulation of explanted tracheas with formylated peptides drives rapid mucociliary clearance, an innate immune process that sweeps bacteria up and out of the trachea. This response requires release of ACh from tuft cells to stimulate neighboring ciliated epithelial cells via muscarinic AChRs (mAChRs) to increase their frequency of beating. Additionally, autocrine ACh signaling can both enhance tuft cell intracellular calcium levels like it does in taste cells,[44] as well as suppress it,[42] suggesting that ACh may regulate the release of other factors from tuft cells. Although ACh is perhaps the best-characterized tuft cell effector molecule, no function has been described for ACh from intestinal tuft cells. Given its functions elsewhere, we might expect tuft cell ACh to rapidly regulate an epithelial process or else signal to neurons.

1.5 Acetylcholine in the intestine

ACh is the primary neurotransmitter of the parasympathetic nervous system, known for causing contraction of smooth muscle, dilation of blood vessels, increased bodily secretion, and slowed heart rate.[45] These functions, colloquially summarized as “rest and digest”, are particularly important in the intestine. ACh from neurons induce the contraction of smooth muscles that surround the intestine to produce peristaltic forces that help move and digest food. Additionally, ACh signals on intestinal epithelial cells (IECs) to induce fluid secretion into the intestinal lumen to aid in digestion and

uptake of nutrients by enhancing the solubility of digested food. ACh binds to mAChRs on the basolateral membrane of IECs, driving increased Ca^{2+} signaling which activates Ca^{2+}-dependent Cl- channels (CaCCs), or in some cases the cystic fibrosis transmembrane conductance regulator (CFTR), to actively pump chloride (Cl^-) and bicarbonate (HCO_3^-) ions into the lumen.[46,47] Positively charged sodium ions (Na^+) passively follow the active transport of the negatively charged ions and together the increased osmolarity of the lumenal contents draws H_2O molecules from the tissue into the lumen via paracellular pathways, resulting in net fluid secretion. ACh-induced fluid secretion is transient but can be stimulated repeatedly.

By definition, mucosal membranes require a mucus layer and this in turn requires proper hydration to be an effective barrier against the microbiota and environmental agents.[48] Specifically, ACh-driven fluid secretion promotes epithelial barrier defense by aiding in the proper unfurling of mucin glycoproteins secreted by goblet cells.[49,50] Additionally, some goblet cells release mucus in response to ACh[50–52]—the two are typically linked. Mutations in CFTR, as in the case of patients with cystic fibrosis, cause defects in intestinal fluid secretion and mucus hydration, leading to viscous mucus, intestinal obstruction, and bacterial overgrowth.[50,53] Thus, ACh-driven fluid secretion promotes barrier defense.

Less is known about how ACh-induced fluid secretion is affected by enteric infection, in particular intestinal helminths and ensuing Type 2 epithelial remodeling. Increased mucus production from the increased numbers of goblet cells combined with increased intestinal contractility, both driven by IL-13, comprise the “weep and sweep” mechanism required for clearing helminths from the SI.[5] Just as ACh-elicited intestinal

smooth muscle contractions become more intense during helminth infection,[54] it seems logical that fluid secretion would also increase to support the increased mucus production from goblet cells. Indeed, it has always been assumed that fluid secretion is important for physically flushing helminths away from the villi and out of the intestine. Tuft cells are a potential source of more ACh to enhance this fluid secretion. The fact that various helminths encode secreted AChEs, presumably to degrade host-derived ACh, has furthered the notion that ACh plays an important role in the Type 2 response and helminth clearance.[55–57]

Neurons have long been considered the primary source of ACh in the intestine, but recent reports identifying a variety of non-neuronal sources of ACh have added to this paradigm. One study implicated epithelial cells as a non-neuronal source of ACh in the colon,[58] and others have demonstrated that many immune cells found in the intestine in high numbers, including ILC2s, CD4+ T cells, and B cells, express ChAT upon activation and can produce ACh.[59–62] ACh is a molecule with many effects and many sources as well.

1.6 Ussing chamber

Our understanding of the movement of ions across epithelial tissues—the basis for fluid secretion—has benefited immensely from the electrophysiology device known as the Ussing chamber.[63] Initially developed by Hans Ussing in the early 1900s to study fluid secretion from frog skin, the Ussing chamber approach has offered a window into the workings of tissues like the intestine and airways that would otherwise be difficult to study *in vivo*.

The device consists of two chambers filled with physiologic buffer that are separated by a piece of tissue taken *ex vivo* from an animal or an epithelial monolayer grown *in vitro*. For the intestine, the intestinal tube is fileted open so that it lays flat with villi on one side and the muscle and serosa on the other. The tissue is then mounted between the chambers such that villi and the lumenal side of the epithelial cells faces one chamber and the serosal or basolateral side faces the other chamber. This creates a polarized system where the tissue, but in essence just the epithelium with its tight junctions, is the barrier preventing free movement and equilibration of ions between the two chambers. One pair of electrodes located on either side of the tissue measures the voltage difference generated by the tissue, while another pair of electrodes located in each chamber injects current to keep the voltage difference across the tissue clamped to zero. The intestinal epithelium can then be stimulated by ACh, or its stabilized analogue CCh, and as Cl^- ions flow from the basolateral buffer through the tissue, into the epithelial cells and finally out into the lumenal buffer, the voltage electrodes record a net-negative shift in the voltage of the lumenal chamber. To offset the greater negative charge the current-delivering electrodes inject more current into the basolateral chamber: this is the “short-circuit current”, or Isc, that is measured to quantify ion flux and fluid secretion.

1.7 Dissertation objective and significance

Helminth infection remains a massive global health burden that necessitates continued research into the fundamental biology of the arm of the immune system known as Type 2 immunity. Recent advances in our understanding of the initiation of

Type 2 immunity by SI tuft cells have laid the groundwork for further dissection of both basic tuft cell biology as well as how they contribute to effective anti-helminth immunity. The goal of my dissertation is two-fold: first, expand our understanding of SI tuft cell effector functions by studying the function of tuft cell-derived ACh, and second, to relate this function to the problem of helminth infection. This research holds promise to inform both our treatment of helminth infection as well as allergic diseases.

SI tuft cells secrete IL-25 and leukotrienes to activate ILC2s to initiate the Type 2 response to intestinal helminths, but little else is known about the biology of SI tuft cells. What other functions do they perform with their many effector molecules? ACh is a potent neurotransmitter that has previously been demonstrated to be produced by tuft cells in barrier tissues such as the airways and urethra. In the SI, ACh produced by enteric neurons is one of the primary inducers of fluid secretion via signaling on epithelial cells. Here we have identified tuft cells as another source of ACh capable of inducing lumenal fluid secretion from epithelial cells. In response to sensing of the metabolite succinate via SUCNR1 or non-specific activation of TRPM5, SI tuft cells secreted ACh, which signaled on neighboring epithelial cells via mAChRs to induce a rapid and transient, chloride-dependent secretory response. Notably, tuft-induced fluid secretion did not require neuronal involvement or any other previously described tuft cell effector molecules. Additionally, we found that tuft-derived ACh regulated epithelial fluid secretion in other mucosal tissues including the trachea and colon. This fluid secretion represents a rapid effector response that can be engaged homeostatically to hydrate the mucosal barrier and flush stimuli away from the tissue and is consistent with the

function of tuft cells in driving rapid avoidance/expelling behaviors in other tissues. These findings will be discussed in depth in Chapter 2.

The result of the Type 2 immune response in the SI is often summarized under the catchy moniker of “weep and sweep”. Indeed, IL-13-dependent increases in mucus production from goblet cells and intestinal contractility by smooth muscle cells have been shown to contribute to helminth clearance. Fluid secretion—the other half of the “weep” response—has also been assumed to be important but has not been directly implicated in worm clearance. The recent discovery that tuft cell hyperplasia occurs during Type 2 remodeling presents an intriguing question: why make more tuft cells? They must perform another function besides initial sensing of parasites, otherwise why make so many more of them? Here we show that the number of ACh-producing tuft cells increases during Type 2 remodeling, resulting in greater fluid secretion responses that coincide with peak tuft cell numbers and helminth clearance. Indeed, tuft-derived ACh was required for efficient helminth clearance, likely due to the enhanced fluid secretion, since it did not induce intestinal contractions (i.e. the “sweep”) or otherwise contribute to Type 2 activation via the tuft-ILC2 circuit. Conversely, tuft-dependent fluid secretion had no effect on protist abundance or localization. Thus, we have described the first ILC2-independent effector function for SI tuft cells, linked increased fluid secretion to tuft cell hyperplasia, and shown that tuft-derived ACh contributes to helminth clearance. These findings will be discussed in depth in Chapter 3.

1.8 Figures

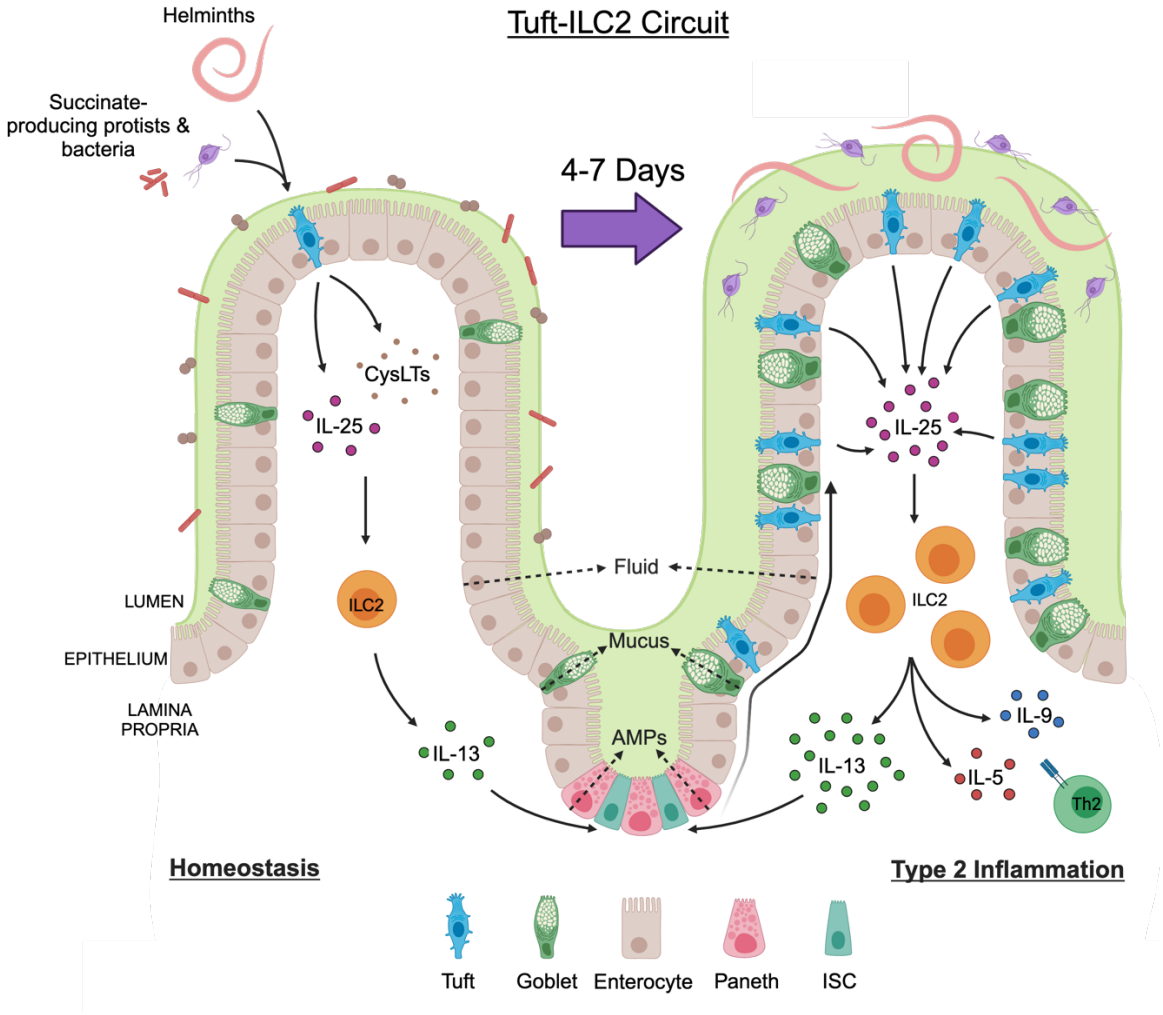

Figure 1: Tuft-ILC2 circuit. Small intestinal tuft cells detect the presence of helminths as well as the metabolite succinate produced by *Tritrichomonas* sp. protists and certain bacteria and signal to ILC2s to initiate intestinal Type 2 epithelial remodeling in a process known as the tuft-ILC2 circuit. Tuft cells secrete IL-25 as well as cysteinyl leukotrienes (CysLTs), which activate lamina propria resident ILC2s to produce IL-5 and IL-13. Among many other functions including inducing eosinophilia and smooth muscle hypertrophy, IL-13 signals on the intestinal stem cell (ISC) compartment to bias the differentiation of epithelial cells towards the goblet cell and tuft cell fate. As the epithelium rapidly renews (4-7 days) the cellular composition changes, with increased numbers of mucus-producing goblet cells and especially tuft cells, which increase nearly 10-fold. In a process known as “weep and sweep”, the mucus produced by goblet cells, combined with secretion of fluid from enterocytes and anti-microbial peptides (AMPs) from Paneth and goblet cells pushes the helminths away from the villi and increased smooth muscle contractility pushes them out of the intestine. Created with BioRender.com.

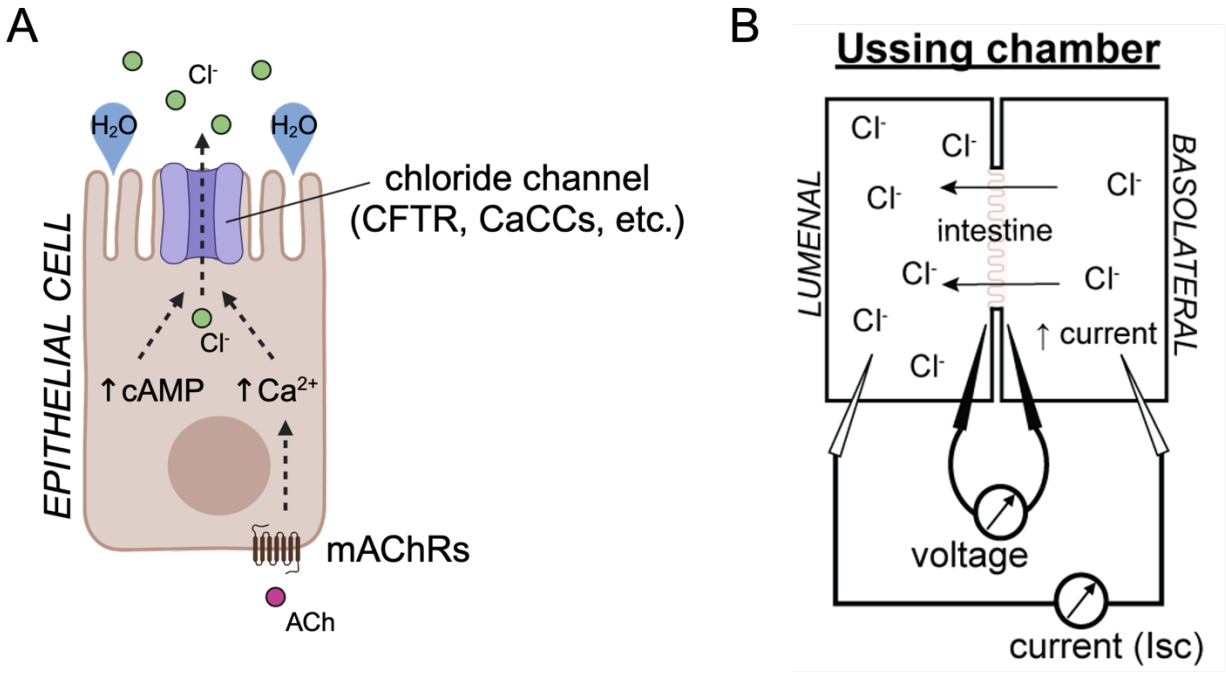

Figure 2: Epithelial fluid secretion and the Ussing chamber. (**A**) Epithelial fluid secretion occurs via increases in either intracellular cyclic adenosine monophosphate (cAMP) or calcium (Ca^{2+}) that cause secretion of chloride ions (Cl^-) from the cell into the lumenal space. Numerous factors, known as secretogogues, are capable of inducing cAMP or Ca^{2+} flux. Acetylcholine (ACh) is a major driver of Ca^{2+}-dependent fluid secretion but can induce cAMP-dependent fluid secretion as well. ACh signals through muscarinic ACh receptors (mAChRs) expressed on the basolateral membrane of epithelial cells, activating G proteins that mobilize Ca^{2+} or cAMP to activate Ca^{2+}-dependent chloride (Cl^-) channels (CaCCs) or cystic fibrosis transmembrane conductance regulator (CFTR), respectively, to secrete Cl^-. The movement of negatively charged Cl^- ions into the lumen pulls positively charged sodium ions (Na^+) along, and together the increased osmolarity attracts H_2O molecules from the tissue into the lumen. (**B**) The physical movement of electrical charge from one side of the epithelium to the other is the basis for detecting fluid secretion *ex vivo* using a device called the Ussing chamber. A piece of epithelial tissue (i.e. small intestine) is fileted open so that it lies flat and mounted on an slider inserted between two chambers filled with physiologic buffer. The epithelium, held together by tight junctions, forms a barrier to ions moving between the two chambers such that at baseline there is a constant transepithelial voltage measured by a pair of electrodes on either side of the tissue. Via a technique called voltage-clamping, another set of electrodes periodically inject current into the basolateral chamber to offset the transepithelial voltage back to zero. This current is known as the short-circuit current, or Isc. Upon basolateral stimulation of the tissue by ACh, chloride ions are secreted into the lumenal chamber, making the transepithelial voltage more negative. The Isc increases to offset the transepithelial voltage and we measure the change in Isc from the baseline to the peak of the response as the delta Isc (ΔIsc). Created with BioRender.com.

CHAPTER 2

Tuft cell-derived acetylcholine regulates epithelial fluid secretion

This chapter is adapted from the following publication:

Billipp TE, Fung C, Webeck LM, Sargent DB, Gologorsky MB, McDaniel MM, Kasal DN, McGinty JW, Barrow KA, Rich LM, Barilli A, Sabat M, Debley JS, Myers R, Howitt MR, von Moltke J. Tuft cell-derived acetylcholine regulates epithelial fluid secretion and helminth clearance. *Immunity* (In Review).

2.1 Introduction

The physiologic function and immune defense of mucosal tissues require fluid secretion, and epithelial cells employ multiple independent mechanisms to regulate this process. For example, cyclic AMP (cAMP) induces apical chloride (Cl^-) secretion from epithelial cells through cystic fibrosis transmembrane conductance regulator (CFTR).[64–67] The resulting ionic gradient draws Na^+ and then water out of the tissue and into the lumen, where it hydrates mucus and can contribute to epithelial "flushing".[68,69] Loss-of-function mutations in CFTR cause cystic fibrosis, a disease characterized by viscous mucus, reduced lung function, and bacterial overgrowth.[64] Epithelial Cl^-/water secretion can also occur via calcium-dependent ion channels, with muscarinic acetylcholine receptors (mAChR) in the basolateral membrane often inducing the necessary intracellular calcium flux.[68] Acetylcholine (ACh) is a canonical neurotransmitter synthesized by the enzyme choline acetyltransferase (*Chat*). Neurons innervating mucosal barriers can induce ACh-dependent fluid secretion, but non-neuronal sources of ACh have now been widely reported in other contexts.[47,58,69–71]

Among epithelial cells, tuft cells are the dominant source of ACh.[43,72] Found across mucosal tissues, they are a lineage of chemosensory cells that monitor the lumenal microenvironment and release effectors to regulate the mucosa. *Chat* expression is part of a transcriptional signature shared by all murine tuft cells[26,32] and ChAT protein has been detected in human tuft cells in the intestine and airways.[73,74] The function of tuft cell-derived ACh has also been studied in several tissues. For example, tuft cells in the nasal epithelium sense bitter and bacteria-derived ligands[38] and secrete ACh, which signals on neurons to induce neurogenic inflammation.[40]

Tracheal tuft cells activate nicotinic ACh receptors (nAChRs) to cause a brief cessation in breathing[39] and mAChRs on neighboring epithelial cells to increase ciliary beat frequency[43,44] in response to similar ligands. Likewise, tuft cells in the urethra use ACh to activate neurons and regulate urine release.[75,42] However, the function of tuft cell-derived ACh in the intestine is unknown, nor has a link between tuft cells and fluid secretion been tested.

We show that in response to sensing of succinate or direct activation of TRPM5, SI tuft cells secrete ACh to induce epithelial fluid secretion in the intestine and airways, independently of neurons. Unlike other tissues where nearly 100% of tuft cells express *Chat*, the frequency of *Chat*+ SI tuft cells occurred in a gradient from the proximal to distal SI, increasing from approximately 40% to 80% of tuft cells. Succinate-induced fluid secretion was restricted to the distal SI where *Chat*+ frequency and SUCNR1 expression was highest. Consistent with their high expression of *Sucnr1,* tuft cells in the trachea also responded to succinate by inducing ACh-dependent fluid secretion. In the proximal SI and colon tuft cell activation via the TRPM5 agonist Class 8 induced fluid secretion but the exact ligands sensed by tuft cells in these tissues remain to be determined. Oral administration of Class 8 induced fluid secretion *in vivo* as measured by fecal water content. This work identifies a function for tuft-derived ACh in the SI that is distinct from both prior reports of tuft-derived ACh in other tissues and prior functions of SI tuft cells in activating ILC2s. By coupling chemosensing to rapid epithelial fluid secretion, tuft cells coordinate an epithelium-intrinsic effector unit that can flush offending agents away from the tissue.

2.2 Results

SI tuft cells express Chat in a proximal to distal gradient

Neuronal *Chat* is important for intestinal function, but the role of *Chat* in intestinal tuft cells has not been studied. To assess *Chat* expression by tuft cells in the SI at single cell resolution, we employed *Chat-GFP* transgenic reporter mice. Immunolabeling for GFP colocalized with the tuft cell marker DCLK1 in both the proximal SI (pSI; first 5-10 cm) and distal SI (dSI; last 5-10 cm) (Fig. 1A). By flow cytometry, >99% of GFP+ epithelial cells stained for the tuft cell-specific *Il25-RFP* reporter (Fig. 1B). However, not all tuft cells were GFP+ (Fig. S1A), and we observed a gradient in the frequency of GFP+ tuft cells that increased from 40% of all tuft cells in the pSI to 80% in the dSI (Fig. 1C-D). The discovery of GFP-negative tuft cells was unexpected, as the *Chat* reporter marks nearly 100% of tuft cells in other tissues.[43] To validate our findings, we crossed *Chat*-Cre mice, in which Cre is expressed from the endogenous *Chat* locus, to *Rosa26::STOP$^{fl/fl}$::CAG-tdTomato* (Ai9) mice for lineage tracing. Using CD24 and Siglec-F to identify tuft cells, we again observed both reporter-positive and -negative tuft cells, with an increased frequency of reporter-positive tuft cells in the distal compared to the proximal SI (Fig. S1B).

Given the binary nature of *Chat-GFP* expression in SI tuft cells, we hypothesized that *Chat* might mark transcriptionally distinct tuft cell subsets. We therefore sorted GFP+ and GFP- tuft cells, performed bulk RNA sequencing, and identified differentially expressed genes (DEGs) (Fig. S1C, Table S1, Data File S1). Surprisingly, despite the binary nature of GFP expression, *Chat* was downregulated only 2.8-fold (FDR = .0009) in GFP- cells, suggesting translation is regulated via untranslated regions of the

endogenous *Chat* transcript that are retained in the transgene (Fig. S1C). More broadly, even with a lenient fold-change (FC) cutoff of 2 (FDR <.01), there were only 105 DEGs. None of the downregulated genes were part of the SI tuft cell signature,[76] but *Sucnr1* (FC = 3.3, FDR = .0007) and the downstream G alpha subunit *Gnat3* (FC = 4.9, FDR = .0001) were upregulated in GFP+ cells (Fig S1C, Table S1). Comparing *Chat*+ tuft cells to previously reported intestinal tuft cell subsets "Tuft-1" and "Tuft-2",[72] we found greater enrichment for Tuft-2 genes (Fig. S1D), but the best match was with a dSI tuft cell signature we generated by sorting tuft cells from the proximal and distal 5 cm of unmanipulated intestines (Fig. S1D-E, Table S2, Data File S2). This signature similarly includes *Sucnr1* and *Gnat3,* and we hypothesize that transcriptional differences between GFP+ and GFP- cells resulted mostly from a distal bias among sorted GFP+ cells, consistent with the gradient we observed (Fig. 1D).

We also considered the possibility that *Chat*- cells were an immature stage before *Chat*+ cells, but while GFP+ cells predominated in the villi and GFP- cells in the crypts, there were still GFP+ cells in the crypts (Fig. S1F) and GFP- cells at the villus tips (Fig. S1G), making a developmental relationship unlikely. Both IL4ra-dependent and IL4ra-independent tuft cells have been identified in the SI,[77] but we found many *Chat-GFP*+ tuft cells in the SI of *Il4ra*$^{-/-}$ mice, suggesting *Chat* expression is not exclusive to IL-13-induced tuft cells (Fig. S1H). The mechanisms regulating *Chat* expression in tuft cells therefore remain unknown.

ACh from tuft cells induces fluid secretion from the SI epithelium

ACh rapidly induces fluid, mucus, and antimicrobial peptide secretion when it binds muscarinic ACh receptors (mAChRs) on SI epithelial cells.[47,51,78,79] Classically,

enteric neurons are considered the primary source of ACh that regulates SI secretion,[46,47,80] but we hypothesized that tuft cells could link lumenal chemosensing to epithelial secretion via basolateral release of ACh.

To make sensitive, real-time measurements of SI epithelial electrophysiology, we employed Ussing chambers,[63] which have been used to measure ACh-induced epithelial ion flux.[81] Two chambers containing physiologic buffer are separated by a piece of SI epithelium and the voltage across the epithelium is clamped. When negatively charged ions (e.g. Cl^-) are secreted into the lumenal chamber, current is injected into the basolateral chamber to restore the voltage (Fig. 2A). This "short-circuit" current, or Isc, is directly proportional to ion flux.[63]

To test whether tuft cells regulate ion flux, we mounted SI tissue from unmanipulated mice in the Ussing chamber and stimulated with Na_2-succinate (succinate), since it is the best-defined ligand for SI tuft cells.[31–33] When we stimulated the lumenal side of the SI tissue with 10 mM succinate, we recorded a rapid increase in the Isc that lasted several minutes before returning close to baseline (Fig. 2B). We quantified this response by measuring the change in Isc from the baseline before stimulation to its peak, known as the delta Isc (ΔIsc; see Fig. 2B inset). To control for the addition of sodium, we tested NaCl at an equimolar concentration of sodium (20 mM). NaCl was sufficient to increase the Isc, but the response was significantly smaller than the succinate response and failed to return to baseline. The succinate response, on the other hand, had similar kinetics to the response elicited by the ACh mimic carbachol (CCh), given basolaterally to maximally stimulate mAChRs (Fig. 2B). The succinate response was greatly diminished in SI from *Sucnr1*$^{-/-}$ mice,

though a residual, likely sodium-dependent increase remained (Fig. S2A). To avoid the sodium response, we used the synthetic SUCNR1 agonist cis-epoxysuccinic acid (cESA),[82] which stimulated an Isc response comparable to succinate, but that was entirely *Sucnr1*-dependent (Fig. S2A). We used cESA in place of succinate for most of the subsequent Ussing experiments.

To further characterize the succinate/cESA Isc response, we began by testing the role of epithelial polarity. cESA induced ion flux when given lumenally, but not basolaterally, consistent with lumenal restriction of SUCNR1 in tuft cells (Fig. S2B). Conversely, CCh stimulated ion flux when given basolaterally, but not lumenally, consistent with basolateral restriction of mAChRs on intestinal epithelial cells (IECs).[47] Since the Isc represents net ion flux across the epithelium, the increased Isc response to succinate could be due to either increased lumenal secretion of negatively charged anions (e.g. Cl^-, $HCO3^-$) or increased absorption of positively charged cations (e.g. Na^+, K^+) from the lumen.[47] To test the contribution of Cl^- ions selectively, we replaced Cl^- with gluconate, which cannot cross the epithelium,[63,83] and found that both the cESA and CCh responses were abrogated (Fig. 2C). Bumetanide, an inhibitor of the basolateral chloride transporter NKCC1 that is required for sustained Cl^- secretion,[64] likewise decreased the response to cESA (Fig. S2C).

Since enteric neurons are both a major source of ACh and major regulators of fluid secretion in the intestine, we investigated the possibility that SI tuft cells activate enteric neurons. Studies of *Chat*+ tuft cells in the airways have emphasized their close contact with neurons and provided evidence that signaling can occur from tuft cells to neurons, often via release of ACh.[40,39] We therefore looked for similar tuft-neuronal

connections by microscopy using the *Chat-GFP* reporter, which marks cholinergic intestinal neurons as well as tuft cells. We found some instances where a GFP+ tuft cell was approached by a GFP+ neuron, but we never saw neurons extend into the epithelium and contact tuft cells, as they do in the airways (Fig. S2D). *Chat*+ neurons represent only a subset of total intestinal neurons,[84] yet staining for the pan-neuronal marker BIII tubulin (TUJ1) revealed no additional neuronal contacts (Fig. S2E), suggesting that neuronal contacts with tuft cells, much less “synapses”, are uncommon in the SI.

Recognizing that signaling can occur without direct contact, we experimentally tested the requirement for neurons in the succinate response. First, we disrupted neuronal integrity by physically “stripping” the submucosa off the back of the epithelium to eliminate most of the submucosal and all of the myenteric neuronal plexuses.[63] Alternatively, we used tetrodotoxin (TTX) to inhibit neuronal action potentials in intact SI tissue.[47] Neither treatment reduced the cESA or CCh responses; in the stripped tissue the CCh response was instead increased, likely due to enhanced diffusion (Fig. 2D). Altogether, our data show that succinate/cESA binds to SUCNR1 expressed apically on epithelial cells and induces chloride-dependent fluid secretion, independently of enteric neurons or submucosal tissue.

To confirm that tuft cells were the cells that sensed succinate/cESA to initiate the secretion response, we stimulated dSI from tuft cell-deficient *Pou2f3*$^{-/-}$, and chemosensing-deficient *Trpm5*$^{-/-}$ mice. As with SI tissue from *Sucnr1*$^{-/-}$ mice, tissues from these mice failed to respond to cESA (Fig. 2E). Importantly, the CCh response was intact in all knockout mice, demonstrating that the tissue’s capacity for ACh-dependent

fluid secretion was unaltered. To test whether ACh was involved in the cESA response, we pretreated the dSI with the pan-mAChR inhibitor atropine and found that this completely blocked the cESA and CCh responses (Fig. 2F). Deletion of *Chat* from IECs using *Chat$^{fl/fl}$;Vil1-Cre(Tg+)* mice also abrogated the cESA response (Fig. 2G). Although tuft cells are the only *Chat*-expressing IECs, we also deleted *Chat* in tuft cells specifically using *Chat$^{fl/fl}$;Pou2f3$^{Cre-ERT2/+}$* mice, and confirmed that tuft cell-derived ACh production was required for cESA-induced fluid secretion (Fig. 2H).

Other tuft cell effectors (e.g. LTC_4 or PGD_2) have been implicated in acute responses and tuft cells themselves express the receptor for IL-25,[32,85,86] but we excluded the involvement of IL-25 and LTC_4 in ion flux using dSI from *Il25$^{-/-}$* and *Alox5$^{fl/fl}$;Vil1-Cre1000(Tg+)* mice, respectively (Fig. S2F,G). Pretreatment with the COX inhibitor ibuprofen to block PGD_2 synthesis also did not affect the cESA response (Fig. S2H). Furthermore, PGD_2, which has not been previously linked with fluid secretion but has been reported to induce mucus secretion from goblet cells (GCs) in the colon,[85] did not induce ion flux in the dSI (or the colon) when administered basolaterally (Fig. S2I). We also investigated the possibility that tuft cells were signaling to neighboring cells via gap junctions.[87] The gap junction inhibitor carbenoxolone partially blocked cAMP-driven fluid secretion induced by IBMX + forskolin, but had no effect on cESA or CCh responses (Fig. S2J). Thus, we have demonstrated that tuft cells in the dSI sense lumenal succinate/cESA and release ACh basolaterally, which stimulates mAChR-dependent Cl^- ion secretion (Fig. 2I). The response is epithelium-intrinsic and does not involve enteric neurons.

A TRPM5 agonist induces tuft- and ACh-dependent fluid secretion in the pSI and dSI

In characterizing the succinate response, we found that the pSI did not respond to succinate stimulation (Fig. 2J). This finding is consistent with greater succinate receptor (*Sucnr1*) expression in tuft cells from the dSI compared to the pSI (Table S2),[33] and may also reflect the reduced frequency of *Chat*+ tuft cells in the pSI (Fig. 1D). Since the pSI was responsive to CCh, we reasoned that pSI tuft cells could induce fluid secretion if properly stimulated. We first tested several putative tuft cell ligands. Worm excretory and secretory products from *Nippostrongylus brasiliensis* (*Nb*), known as NES, failed to stimulate ion flux whether made from infective L3 larvae or adult worms (data not shown). The bacterial metabolite N-C11-G did not induce ion flux either (Fig. S2K). Next, we tried a chemogenetic approach with Gq- or Gi-coupled receptors that respond only to synthetic ligands (DREADDs)[88] using constitutive (*Il25-Cre*) or inducible (*Pou2f3*$^{Cre\text{-}ERT2/+}$) for tuft cell-specific expression. Although tuft cells expressed the HA tag included in the DREADD constructs, stimulation with Compound 21[89] was insufficient to drive a fluid secretion response in the pSI or dSI (Fig. S2L-O). Perhaps G proteins required for DREADD function are not available in tuft cells or the signals induced downstream of DREADD activation are not sufficient to induce ACh release.

Finally, we decided to stimulate TRPM5 directly, since all tuft cell chemosensing pathways identified to date converge on TRPM5. We acquired a TRPM5 agonist compound called Class 8 (C8),[90,91] and found that it induced ion flux in both the pSI and dSI when administered lumenally or basolaterally, with a trend toward higher basolateral responses (Fig. 2K, S2P-Q). The C8 response was similar to cESA- or CCh-induced ion

flux, and was TRPM5-dependent in the pSI and dSI (Fig. 2K-L, S2R). The C8 response was also tuft cell- and ACh-dependent in both locations (Fig. 2L-M). In the pSI, C8 induced a slow TRPM5-independent increase in Isc (Fig. 2K), but this off-target effect could be eliminated by lowering the dose of C8 (Fig. S2S). We conclude that in response to direct TRPM5 activation, tuft cells in the pSI and dSI can release ACh to induce fluid secretion from the intestinal epithelium.

Tuft cell-mediated fluid secretion occurs across mucosal tissues and is detectable in vivo

We previously found that *Sucnr1* expression is even higher in tracheal tuft cells than those of the SI,[32] so to test if tuft cells regulate fluid secretion at multiple mucosal barriers, we stimulated tracheal tissue in the Ussing chamber with succinate. As in the dSI, we found that this induced a rapid increase in the Isc that was *Pou2f3*-, *Sucnr1*-, and *Trpm5*-dependent (Fig. 3A-B). In addition, the response was mAChR-dependent (Fig. 3C). By comparison, the cecum and colon, where tuft cells express *Sucnr1* at low levels,[32] responded only weakly to succinate stimulation and in a tuft-independent manner (Fig. S3A). Colonic tissue did respond to TRPM5 agonism with C8, with a larger response in the proximal colon (pCol) than the distal colon (dCol) (Fig. 3D-E). The reported tuft ligand N-C11-G[85] did not stimulate fluid secretion from the dSI or dCol (Fig. S3B), and also failed to elicit tuft-dependent leukotriene production from intestinal epithelial monolayers (Fig. S3C). Therefore, tuft cell control of epithelial fluid secretion is a common effector function across barrier tissues.

The Ussing chamber measures ion flux but cannot measure water movement directly. We therefore wanted to test if activating tuft cells *in vivo* could induce fluid secretion into the intestine. We dosed mice with C8 or vehicle in the morning and then measured the wet weight of fecal pellets 3 hours later. In mice given vehicle, the fecal water content declined, likely due to reduced water intake during the day. C8 treatment prevented this decline, indicating sustained fluid secretion (Fig. 3F). Importantly, this fluid secretion was dependent on epithelial *Chat* (Fig. 3G, S3D). Thus, activation of tuft cells along the intestinal tract induces ACh-dependent ion flux that drives fluid secretion into the intestinal lumen.

2.3 Discussion

This study identifies an epithelium-intrinsic response unit that couples tuft cell chemosensing to epithelial fluid secretion via the release of ACh from tuft cells. This effector function is common to tuft cells in multiple tissues and is executed within seconds of activation.

Some details of tuft cell-regulated fluid secretion remain unresolved. For example, we do not understand the regulation of *Chat* in SI tuft cells. It is unclear why only a subset of SI tuft cells are *Chat*+, why there is a proximal to distal gradient of *Chat*+ tuft cells, and why the frequency of *Chat*+ tuft cells decreases during Type 2 inflammation (although the total number increases due to tuft cell hyperplasia). Furthermore, most tuft cells do not express *Slc5a7*, which encodes CHT1, the transporter that neurons use to import choline for ACh synthesis, nor *Slc18a3*, which encodes VAChT, a transporter that loads ACh into secretory vesicles in neurons.[92]

Lastly, it remains to be seen whether tuft cell-derived ACh also induces bicarbonate secretion, as this often occurs together with chloride release and further supports the unfolding of extracellular mucus.[50]

We have also not identified the precise ACh receptor(s) that mediate(s) the fluid secretion response, although inhibition by atropine implicates a muscarinic rather than nicotinic receptor. *Chrm1* and *Chrm3* are the only detectable muscarinic receptor transcripts in unmanipulated SI epithelium[32,72] and *Nb* clearance is delayed in *Chrm3*$^{-/-}$ mice.[93] Induction of Type 2 cytokines is also impaired in these *Chrm3*$^{-/-}$ mice, so conditional *Chrm* alleles will be needed to identify in which cells the receptors are required and for which aspects of Type 2 immunity. It also remains unclear which IECs ACh signals on and whether they are located in the villi (mostly comprised of absorptive enterocytes) or in the crypts (as older research has postulated).

Although we have focused on the SI in this study, we propose tuft cells link chemosensing to fluid secretion in all tissues. Indeed, with the exception of tuft-ILC2 circuit activation, all other known tuft cell effector functions occur instantaneously and seem to mediate evasion (e.g. breathing cessation)[38,39] and expulsion (e.g. mucociliary sweep) of microbes and other agonists.[43,44] Fluid secretion fits this paradigm. The mucosal barrier must be constantly hydrated and fluid secretion can provide a flushing effect. Based on the ligands tuft cells sense in different tissues, such mechanisms could be important to clear allergens from the upper airways or bacteria from the trachea and urethra. Tuft cell sensing may also reduce baseline fluid secretion, as one recent study suggested.[94] The ligands and function of tuft cells in the colon are only just being elucidated,[85] but we predict that tuft cell-regulated fluid secretion would help maintain a

healthy mucosal barrier here too. Tuft cell frequency is generally decreased in patients with active inflammatory bowel disease,[95,96] consistent with a role for tuft cells in preventing bacterial infiltration. Conversely, increased tuft cell frequency was detected in colonic biopsies from patients with diarrhea-predominant irritable bowel syndrome, a largely non-inflammatory condition of unknown origin.[97]

Why tuft cells sense succinate in either the SI or, as we have now demonstrated, the trachea, remains unclear. Perhaps tuft cell-mediated fluid secretion, together with IL-13-induced anti-microbial peptides and mucus production, acts more locally to keep microbes away from the epithelium.[98] Succinate levels have also been shown to increase in contexts of bacterial dysbiosis, and inducing tuft cell hyperplasia with succinate treatment reduces inflammation in a model of ileitis.[95] As for the trachea, aberrant release of cellular succinate into the airways, which occurs in some patients with cystic fibrosis, can promote colonization and biofilm formation by the pathosymbiont *Pseudomonas aeruginosa.*[99] Induction of CFTR-dependent fluid secretion by prostaglandin E_2 released from airway tuft cells has also been suggested.[100] Thus, tracheal tuft cells may induce fluid secretion to flush away succinate and other soluble molecules and to deter bacterial accumulation.

Therapeutically, benefit may be achieved by tuning tuft cell effector functions up or down, depending on the context and need. For example, tuft cell-induced fluid secretion may prove useful in treating cystic fibrosis patients in whom CFTR-dependent fluid secretion is impaired, while certain patients suffering from diarrhea might benefit from reduced tuft cell function. Future study should investigate the involvement of tuft cell-induced fluid secretion in human disease.

2.4 Figures

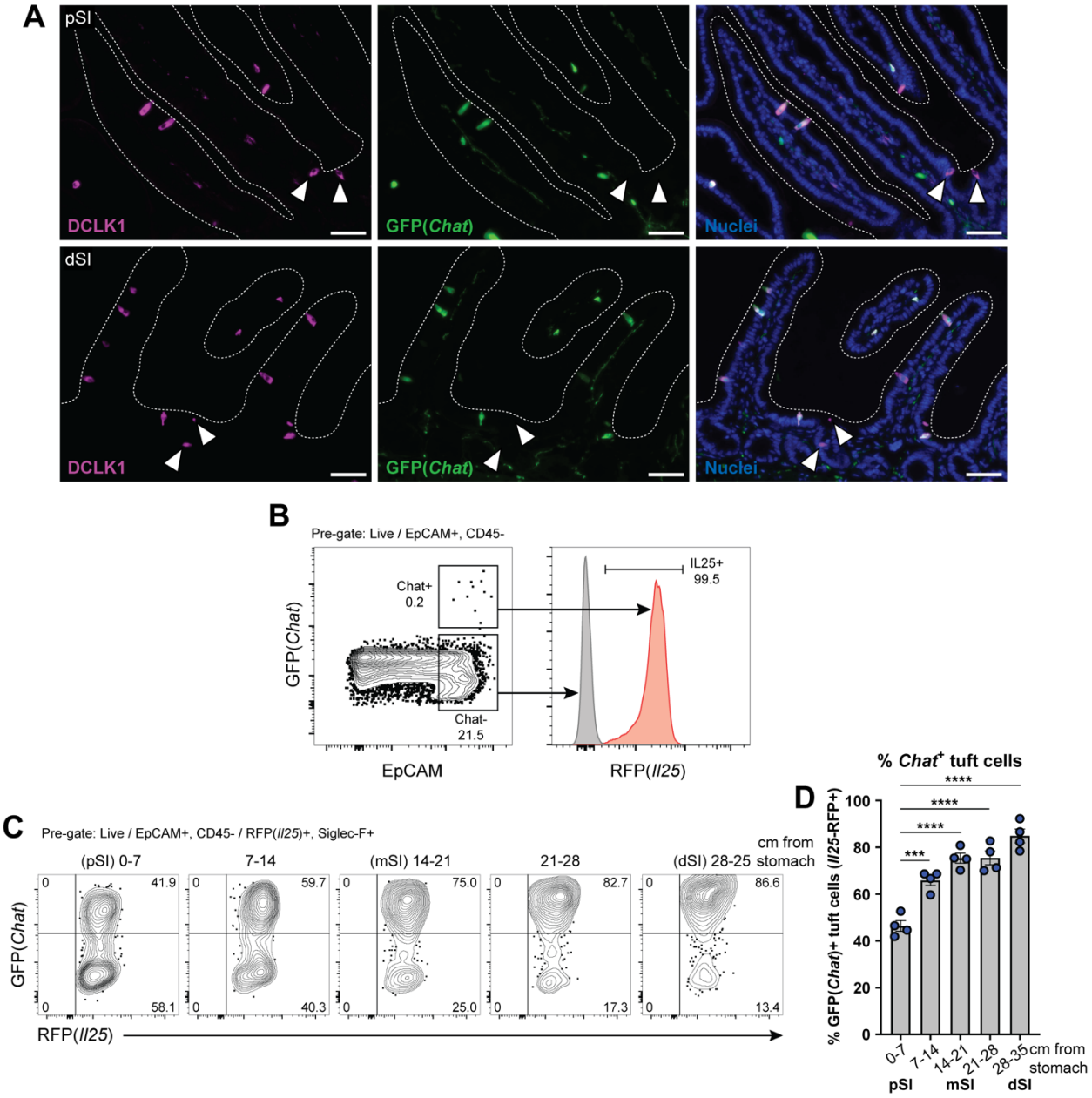

Figure 1: SI tuft cells express *Chat* in a proximal to distal gradient. (**A**) Representative images of GFP(*Chat*) expression (green) by DCLK1+ tuft cells (magenta) in the proximal SI (pSI) and distal SI (dSI) by immunofluorescence. White arrows indicate GFP(*Chat*)- tuft cells. Nuclei stained with DAPI (blue). Scale bars: 50 μm (**B**) GFP+ epithelial cells (EpCAM+) are RFP(*Il25*)+ tuft cells. (**C** and **D**) (C) Representative flow cytometry and (D) quantification of the percentage of GFP+ tuft cells by sequential 7 cm section across the length of the SI. In D, each symbol represents an individual mouse (columns represent different tissues from same mouse) from three pooled experiments. *p < 0.05, **p < 0.01, ***p < 0.001 by one way ANOVA with Tukey's multiple comparisons test (D). mSI, medial SI. Graphs depict mean +/- SEM. Also see Figure S1.

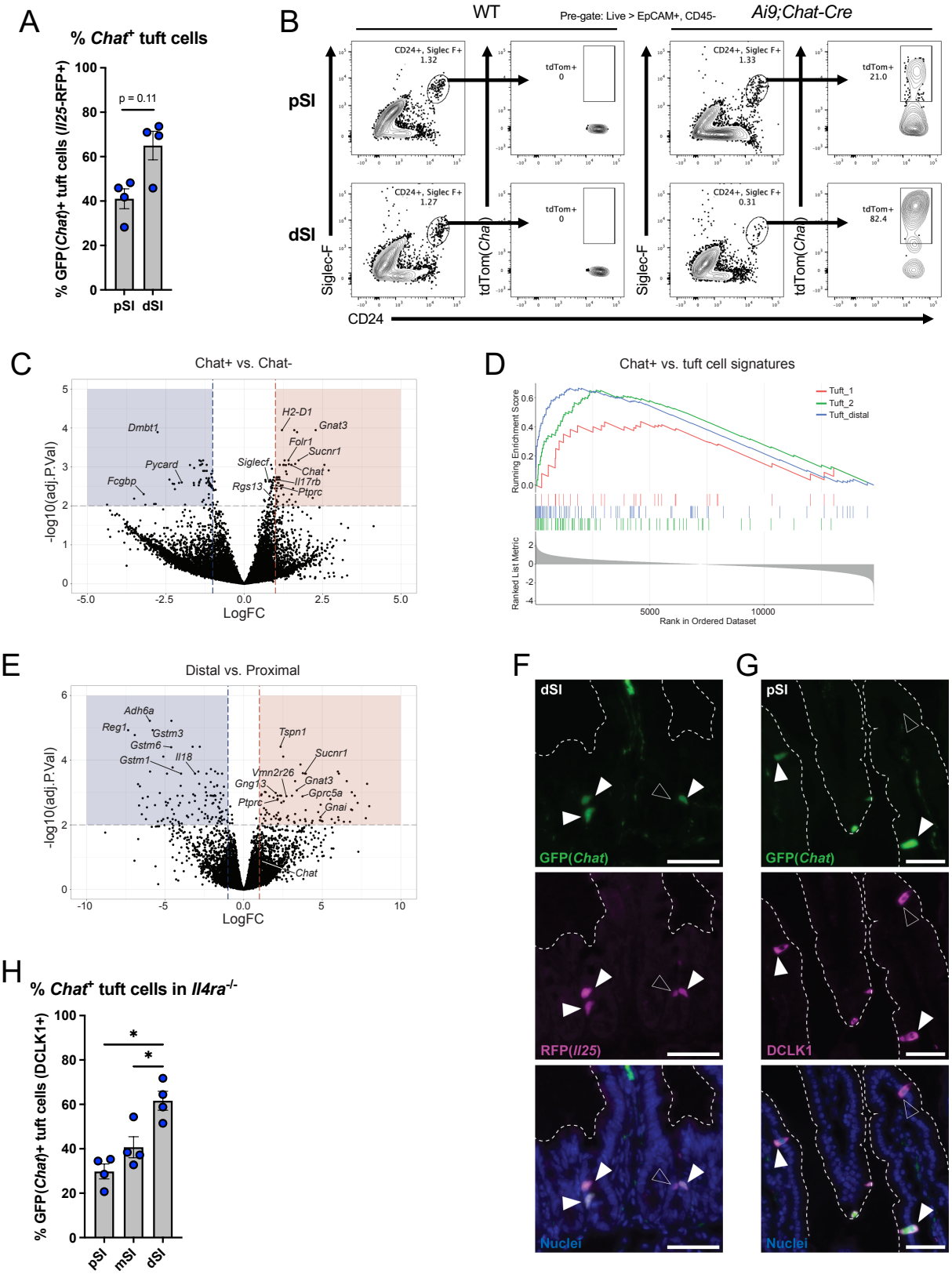
A
% Chat+ tuft cells
% GFP(Chat)+ tuft cells (Il25-RFP+)
p = 0.11
pSI
dSI
B
WT
Pre-gate: Live > EpCAM+, CD45-
Ai9;Chat-Cre
pSI
dSI
CD24+, Siglec F+
1.32
tdTom+
0
1.33
21.0
1.27
82.4
0.31
Siglec-F
tdTom(Cha
CD24
C
Chat+ vs. Chat-
-log10(adj.P.Val)
LogFC
Dmbt1
Pycard
Fcgbp
H2-D1
Gnat3
Folr1
Sucnr1
Siglecf
Chat
Il17rb
Rgs13
Ptprc
D
Chat+ vs. tuft cell signatures
Running Enrichment Score
Tuft_1
Tuft_2
Tuft_distal
Ranked List Metric
Rank in Ordered Dataset
E
Distal vs. Proximal
Adh6a
Reg1
Gstm3
Gstm6
Gstm1
Il18
Tspn1
Sucnr1
Vmn2r26
Gng13
Gnat3
Gprc5a
Ptprc
Gnai
Chat
F
G
dSI
pSI
GFP(Chat)
RFP(Il25)
DCLK1
Nuclei
H
% Chat+ tuft cells in Il4ra-/-
% GFP(Chat)+ tuft cells (DCLK1+)
pSI
mSI
dSI

Supplemental Figure 1: (**A**) Quantification of GFP+ tuft cells (RFP+) from pSI and dSI of *Chat-GFP*;*Il25*$^{RFP/+}$ mice by immunofluorescence (IF). (**B**) Representative flow cytometry of traced tdTom+ tuft cells (CD24+, Siglec-F+) from pSI and dSI of wild-type (WT) and *Ai9;Chat-Cre* mice. (**C**) Volcano plot showing log2FC of genes expressed in *Chat*+ tuft cells (n=4) versus *Chat*- tuft cells (n=3) sorted from whole SI of *Chat-GFP*;*Il25*$^{RFP/+}$ mice. (**D**) Gene set enrichment analysis comparing *Chat*+ tuft cell gene expression to Tuft-1 and Tuft-2 consensus gene signatures and the dSI tuft cell signature from (**E**) Volcano plot showing log2FC of genes expressed in tuft cells sorted from the dSI (n=4) versus tuft cells sorted from the pSI (n=4) of B6 mice. (**F**) Representative immunofluorescence image showing GFP+ (green) tuft cells (RFP+, magenta) in the SI crypt (solid white arrows), next to one GFP- tuft cell (open white arrow). Nuclei stained with DAPI (blue). Scale bars: 50 μm. (**G**) Representative immunofluorescence image showing a GFP- (green) tuft cell (DCLK1+, magenta) at the villus tip (open white arrow), past other GFP+ tuft cells (solid white arrows). Nuclei stained with DAPI (blue). Scale bars: 50 μm. (**H**) Quantification of GFP(*Chat*)+ tuft cells (DCLK1+) from denoted tissues of *Il4ra*$^{-/-}$*;Chat-GFP* mice by immunofluorescence. In the graphs, each symbol represents an individual mouse (columns represent different tissues from same mouse) from two pooled experiments. *$p < 0.05$, **$p < 0.01$, ***$p < 0.001$ by Mann-Whitney test (A) or one way ANOVA with Tukey's multiple comparisons test (G). mSI, medial SI. Graphs depict mean +/- SEM.

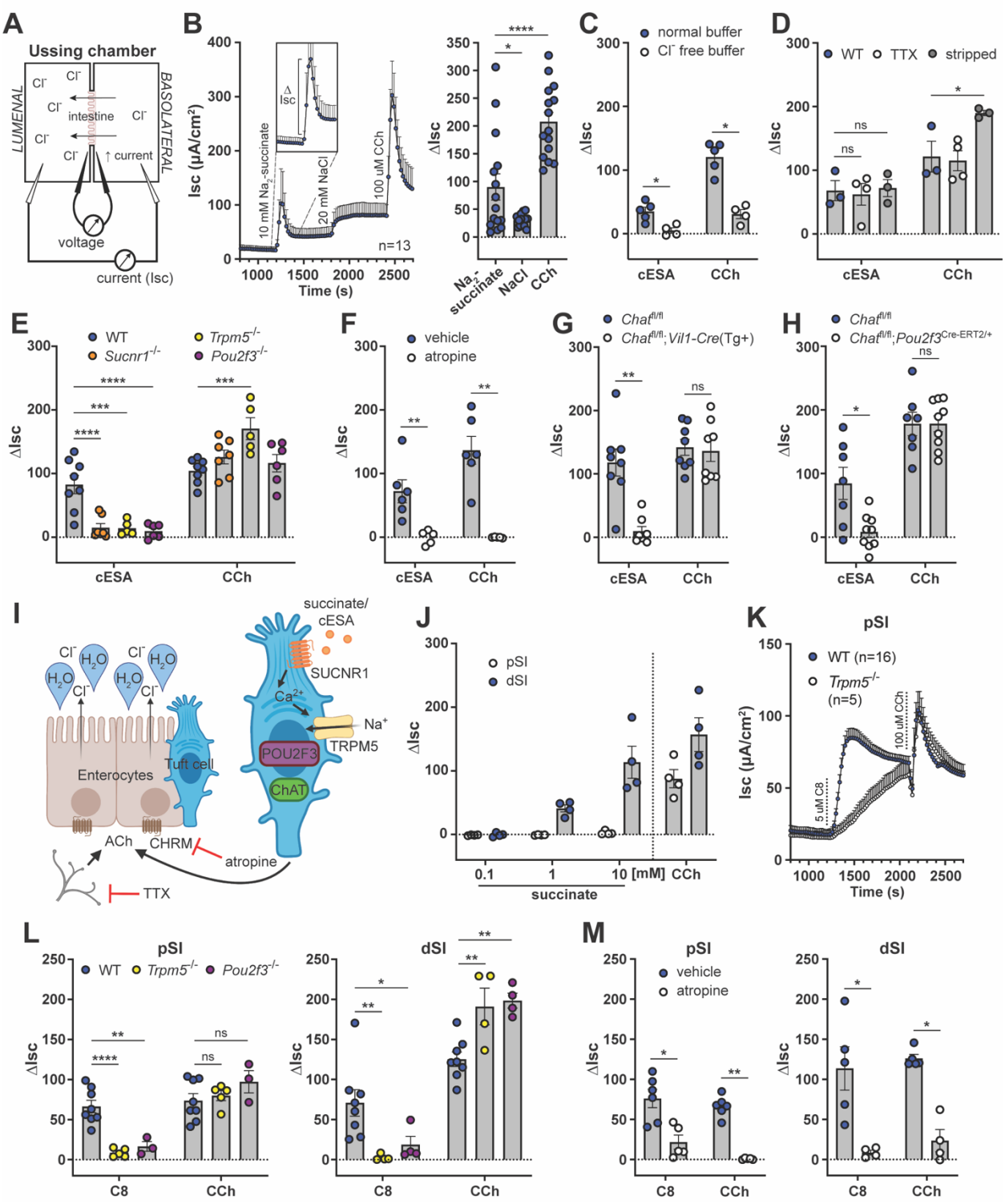

Figure 2: Tuft cell-derived ACh induces epithelial fluid secretion. (**A**) Ussing chamber schematic. (**B**) Average Isc traces and quantification of the delta Isc (ΔIsc, see inset and bar graph) of WT dSI tissue stimulated as indicated (10 mM Na_2-succinate and 20 mM NaCl, lumenal; 100 μM CCh, basolateral). (**C**) ΔIsc values of WT dSI in presence of normal chloride- (Cl^-) containing buffer or buffer selectively lacking

Cl^-, stimulated as indicated (10 mM cESA, lumenal). (**D**) ΔIsc values of WT intact dSI compared to stripped dSI and dSI pretreated 15 min with TTX (1 μM, basolateral), stimulated as indicated. (**E**) ΔIsc values of dSI from mice of indicated genotypes stimulated as indicated. (**F**) ΔIsc values of WT dSI compared to dSI pretreated 15 min with pan-CHRM inhibitor atropine (10 μM, basolateral), stimulated as indicated. (**G** and **H**) ΔIsc values of dSI with (G) epithelial cell- (*Vil1-Cre*) and (H) tuft cell-specific (*Pou2f3*$^{ERT2\text{-}Cre/+}$) *Chat* deletion, stimulated as indicated. (**I**) Model of tuft cell chemosensing of succinate driving ACh-dependent fluid secretion independent of neurons. (**J**) ΔIsc values of WT pSI and dSI stimulated as indicated. (**K**) Average Isc traces of pSI from WT or *Trpm5*$^{-/-}$ mice stimulated as indicated (5 μM C8, basolateral). (**L** and **M**) ΔIsc values of WT tissues compared to (L) tissues from indicated genotypes or (M) tissues pretreated 15 min with atropine (10 μM, basolateral), stimulated as indicated. In the graphs, each symbol represents an individual mouse (one tissue or average of two) pooled from two or more experiments. Groups represent sequential stimulations of the same tissue. *p < 0.05, **p < 0.01, ***p < 0.001, ****p < 0.001 by RM one way ANOVA with Tukey's multiple comparisons test (B), two way ANOVA with Dunnett's multiple comparisons test (D, E, L), multiple Mann-Whitney tests with Holm Sídák's multiple comparisons test (C, F, G, H, M). ns, not significant. Graphs depict mean +/- SEM. Also see Figure S2. Created with BioRender.com.

Fig. S2: Related to Fig. 2

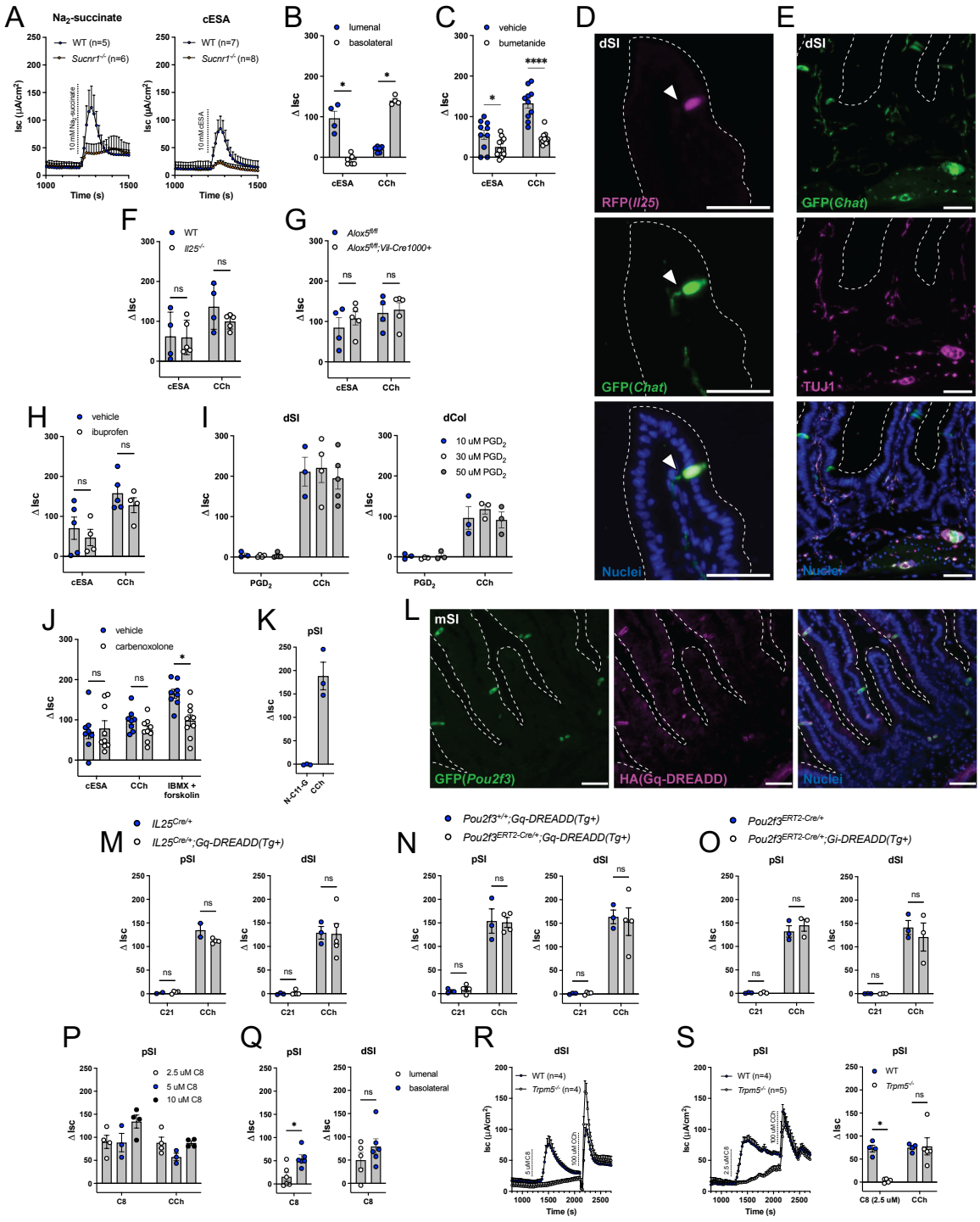

Supplemental Figure 2: (**A**) Average Isc traces of dSI from WT or *Sucnr1*$^{-/-}$ mice stimulated as indicate (Na_2-succinate and cESA, lumenal). (**B**) ΔIsc values of WT dSI stimulated as indicated. (**C**) ΔIsc values of WT dSI pretreated 15 min with vehicle or bumetanide (100 μM, basolateral), stimulated as indicated (10

mM cESA lumenal; 100 μM CCh, basolateral). (**D**) Representative immunofluorescence image of a GFP+ (green) neuronal process (indicated by solid white arrow) approaching a GFP+/RFP+ (magenta) tuft cell from the dSI of *Chat-GFP*;*Il25*$^{RFP/+}$ mice. Nuclei stained with DAPI (blue). Scale bars: 50 μm. (**E**) Representative immunofluorescence image of GFP+ (green) neurons co-stained for BIII tubulin (TUJ1, magenta) in the dSI. Nuclei stained with DAPI (blue). Scale bars: 50 μm. (**F**, **G**, and **H**) (F and G) ΔIsc values of dSI from indicated genotypes or (H) WT dSI compared to dSI pretreated 15 min with ibuprofen (10 μM, bilateral), stimulated as indicated. (**I**) ΔIsc values of WT tissues stimulated as indicated (PGD_2, basolateral). (**J**) ΔIsc values for WT dSI compared to dSI pretreated 15 min with carbenoxolone (1 mM, lumenal), stimulated as indicated (100 μM IBMX + 10 μM forskolin, bilateral). (**K**) ΔIsc values of WT pSI stimulated as indicated (100 μM N-C11-G, lumenal). (**L**) Representative immunofluorescence image of GFP+ (green) tuft cells expressing HA+ Gq-DREADDs (magenta) in the crypts and villi of the medial SI (mSI). Nuclei stained with DAPI (blue). Scale bars: 50 μm. (**M**, **N**, and **O**) (M) ΔIsc values of indicated tissues from unmanipulated mice or (N and O) indicated tissues from mice 7 days after start of tamoxifen chow, stimulated as indicated (1 μM C21, bilateral). (**P**) ΔIsc values of WT pSI stimulated as indicated (C8, bilateral). (**Q**) ΔIsc values of WT tissues from pSI and dSI stimulated as indicated. (**R**) Average Isc traces of dSI stimulated as indicated (5 μM C8, basolateral). (**S**) Average Isc traces and ΔIsc values of pSI stimulated as indicated (2.5 μM C8, basolateral). In the graphs, each symbol represents an individual mouse (one tissue or average of two) pooled from two or more experiments. Groups represent sequential stimulations of the same tissue. In (C) paired vehicle and bumetanide-treated tissues are from the same mouse. *$p < 0.05$, **$p < 0.01$, ***$p < 0.001$, ****$p < 0.001$ by multiple Mann-Whitney tests with Holm Sídák's multiple comparisons test (B, F-H, J, M-O, S), Wilcoxon matched-pairs signed rank test with Holm Sídák's multiple comparisons test (C), or Mann-Whitney test (Q). ns, not significant. Graphs depict mean +/- SEM.

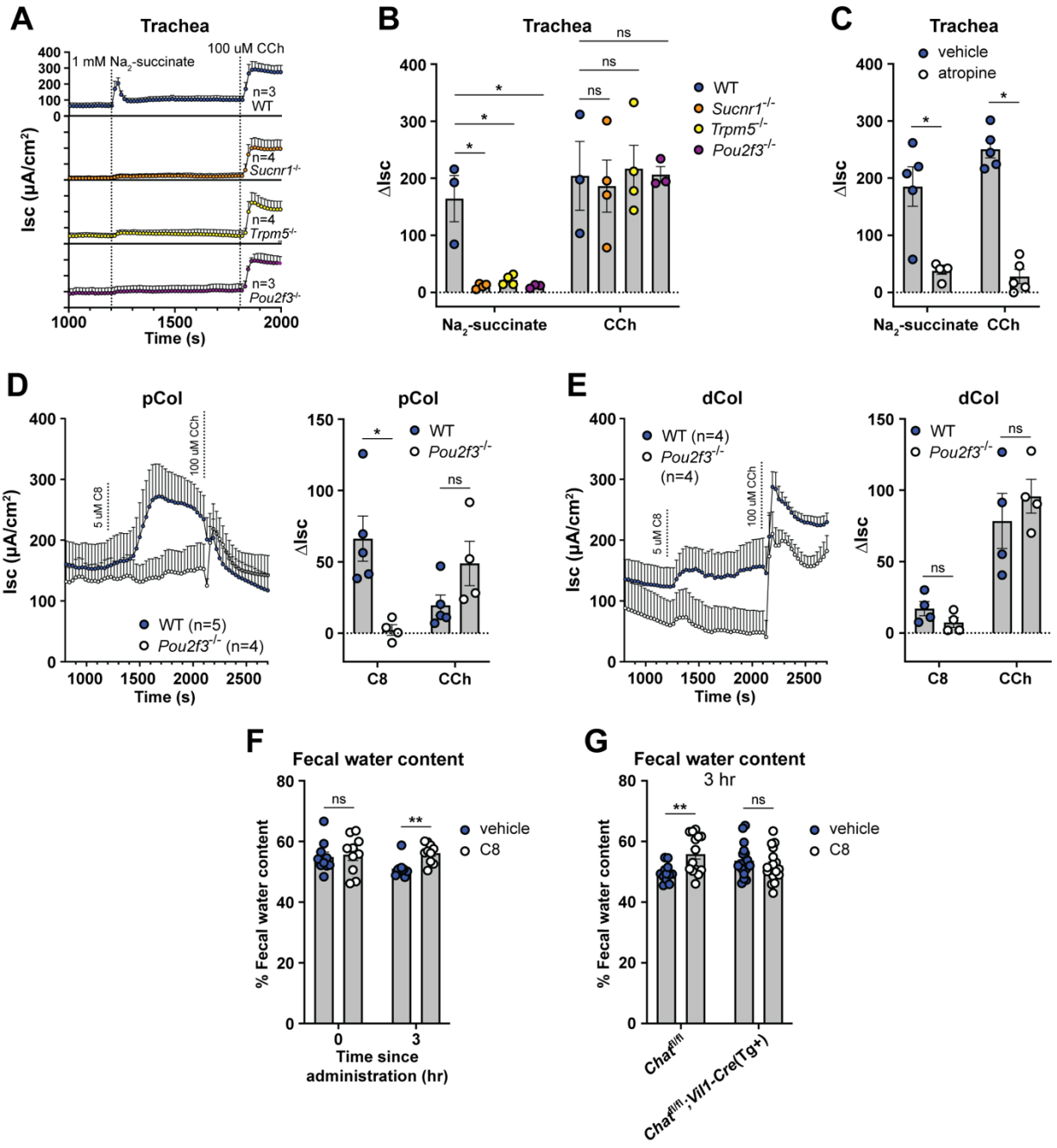

Figure 3: ***Tuft cell-mediated fluid secretion occurs across mucosal tissues and is detectable in vivo.*** (**A** and **B**) (A) Average Isc traces and (B) ΔIsc values of trachea from mice of indicated genotypes stimulated as indicated (1 mM Na_2-succinate, lumenal; 100 µM CCh, basolateral). (**C**) ΔIsc values of WT trachea compared to trachea pretreated 15 min with atropine (10 µM, basolateral), stimulated as indicated. (**D** and **E**) Average Isc traces and ΔIsc values of WT and *Pou2f3*$^{-/-}$ tissues stimulated as indicated (5 µM C8, basolateral). (**F** and **G**) Quantification of water content of fecal pellets collected from (A) WT or (B) *Chat-fl;Vil1-Cre(Tg+)* mice treated orally with vehicle or C8 (30 mg/kg) for the indicated durations. In the graphs, each symbol represents an individual mouse (one tissue or average of two)

pooled from two or more experiments. Groups represent sequential stimulations or timepoints of the same tissue or animal. *p < 0.05, **p < 0.01, ***p < 0.001, ****p < 0.001 by, two way ANOVA with Tukey's multiple comparisons test (B), or multiple Mann-Whitney tests with Holm Sídák's multiple comparisons test (C-G). ns, not significant. Graphs depict mean +/- SEM. Also see Figure S3.

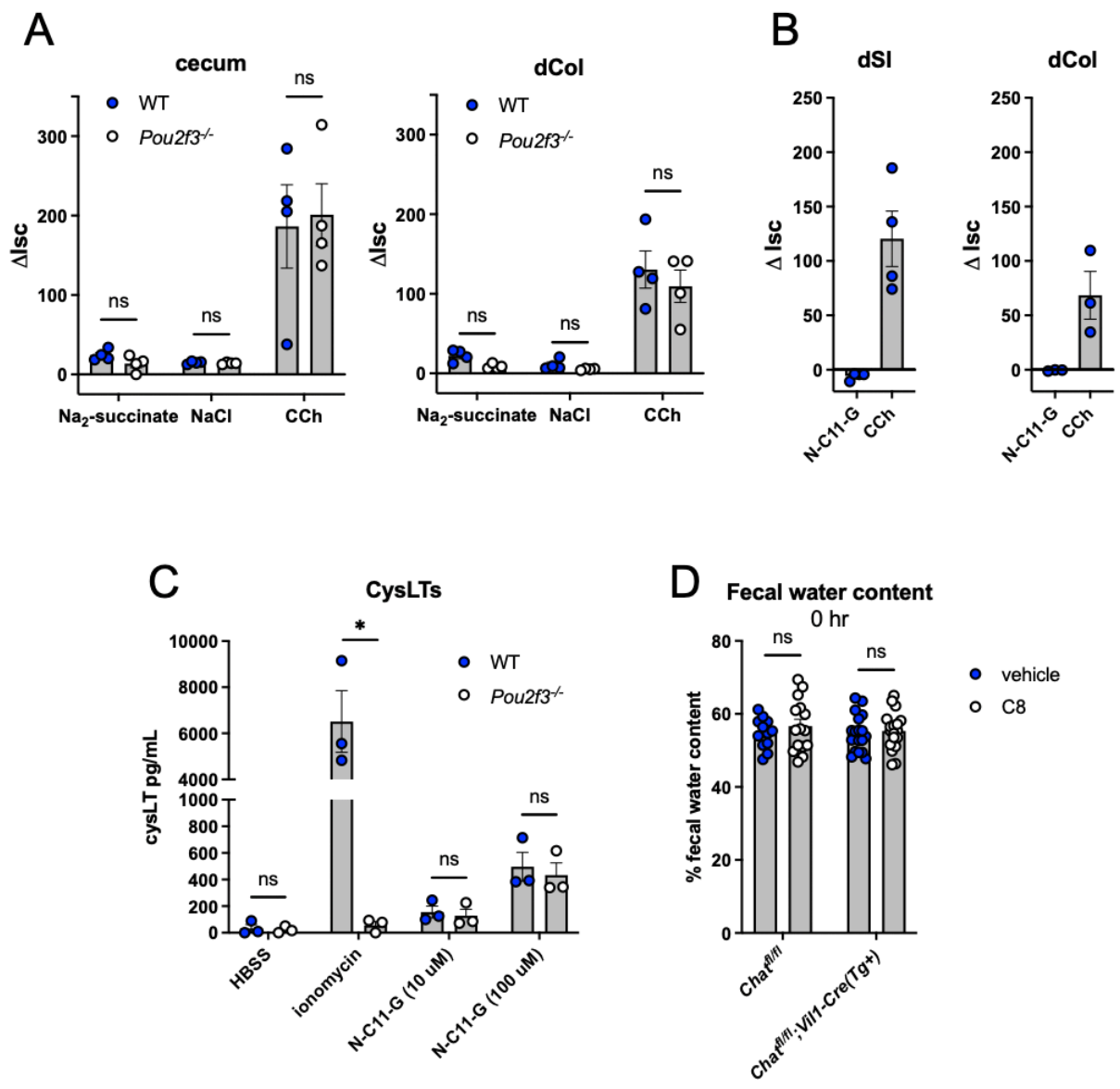

Supplemental Figure 3: (**A**) ΔIsc values of WT and *Pou2f3*$^{-/-}$ tissues stimulated as indicated (10 mM Na_2-succinate and 20 mM NaCl, lumenal; 100 μM CCh, basolateral). (**B**) ΔIsc values of WT tissues stimulated as indicated (100 μM N-C11-G, lumenal). (**C**) Cysteinyl leukotriene (CysLTs) production from WT and *Pou2f3*$^{-/-}$ SI epithelial monolayers stimulated as indicated. (**D**) Quantification of water content of fecal pellets collected from indicated mice immediately after oral treatment with C8 (30 mg/kg). In the graphs, each symbol represents an individual mouse pooled from two or more experiments. In (A-B) groups represent sequential stimulations of the same tissue and in (C) groups represent individual monolayers. *p < 0.05, **p < 0.01, ***p < 0.001, ****p < 0.001 by multiple Mann-Whitney tests with Holm Sídák's multiple comparisons test (A, D), or multiple unpaired t tests with Holm Sídák's multiple comparisons test (C). ns, not significant. Graphs depict mean +/- SEM.

CHAPTER 3

Tuft cell-derived acetylcholine regulates helminth clearance

This chapter is adapted from the following publication:

Billipp TE, Fung C, Webeck LM, Sargent DB, Gologorsky MB, McDaniel MM, Kasal DN, McGinty JW, Barrow KA, Rich LM, Barilli A, Sabat M, Debley JS, Myers R, Howitt MR, von Moltke J. Tuft cell-derived acetylcholine regulates epithelial fluid secretion and helminth clearance. *Immunity* (In Review).

3.1 Introduction

Small intestinal (SI) tuft cells play a critical role in the initiation of "Type 2" immune responses to helminth infection and colonization by *Tritrichomonas sp.* protists.[20,29,18] Tuft cells express SUCNR1, the receptor for extracellular succinate, which *Tritrichomonas sp.* and the microbiota secrete as a metabolite.[31–33] SUCNR1 signaling causes intracellular Ca^{2+} flux that opens the cation channel TRPM5. The resulting Na^{+} influx depolarizes the tuft cell and likely regulates secretion of most tuft cell effector molecules.[101,102] *Sucnr1*$^{-/-}$ mice fail to detect *Tritrichomonas sp.* colonization, but the immune response to helminth infection is unaffected.[32,31] Nonetheless, sensing of both helminths and protists is severely attenuated in *Trpm5*$^{-/-}$ mice or *Pou2f3*$^{-/-}$ mice that lack tuft cells entirely.[18,20,32]

Once activated by lumenal signals, tuft cells produce IL-25 and, in some cases, leukotriene C4 (LTC_4) to activate resident group 2 innate lymphoid cells (ILC2s) in the underlying *lamina propria* (LP).[29,30] ILC2s secrete canonical Type 2 cytokines, including IL-13, that collectively recruit Type 2 immune cells and coordinate intestinal remodeling. Among its many targets, IL-13 produced by ILC2s signals on undifferentiated epithelial cells to bias differentiation towards mucus-producing goblet cells and tuft cells.[20,29,103,104] Given the 3-5 day turnover of the intestinal epithelium, this feed-forward process, known as the tuft-ILC2 circuit, results in dramatic hyperplasia of both goblet cells and tuft cells, the latter of which increase 10-fold.[20,29,18]

The Type 2 effector functions that clear worms from the intestine,[5,105] collectively referred to as "weep and sweep," require the coordination of multiple signals. In addition to increasing the number of tuft and goblet cells, IL-13 upregulates production of mucus

and anti-helminthic/microbial peptides in the epithelium,[106,65,107] increases fluid secretion,[108] and increases expression of mAChRs on smooth muscle,[66,67,54] but actual secretion ("weep") and muscle contraction ("sweep") generally require additional signals. ACh is one molecule that can acutely activate both weep and sweep,[54] and mAChRs are required for helminth clearance.[93,109] Conversely, helminths secrete ACh esterases (AChE), likely in an attempt to inhibit weep and sweep responses.[55,56,57] The sources of ACh in Type 2 immunity, however, are not defined.

By sensing lumenal signals and activating ILC2s, tuft cells serve as sentinels for intestinal Type 2 immunity, but the fact that many more tuft cells are generated after the agonist has been detected suggests an additional effector function for these cells. Here we describe such an effector function, which is independent of ILC2s. We show that in response to sensing of succinate or direct activation of TRPM5, tuft cells secrete ACh to induce epithelial fluid secretion in the intestine and airways. During Type 2 SI remodeling, *Chat*+ tuft cells increase in number, enhancing the fluid secretion response. Upon helminth infection, mice with *Chat*-deficient tuft cells experience delayed helminth clearance despite normal tuft-ILC2 circuit activation. We conclude that tuft cell-derived ACh regulates epithelial fluid secretion, and that this effector function can contribute to Type 2 immune responses during helminth infection.

3.2 Results

Tuft cell-derived ACh is not required for ILC2 activation

Having defined ACh-dependent fluid secretion as a tuft cell effector function in unmanipulated mice, we next considered the role of tuft cell-derived ACh during Type 2

immunity. Consistent with previous reports in the airways,[110] we found that tamoxifen partially suppressed Type 2 responses in the intestine. For example, treating protist-colonized *Chat*$^{fl/fl}$*;Pou2f3*$^{Cre\text{-}Ert2/+}$ mice with tamoxifen for one week reduced tuft cell counts by nearly half in both WT and Cre+ mice (Fig. S4A). The effect of tamoxifen was less noticeable during helminth infection, perhaps because this induces more Type 2 inflammation (Fig. S4B). Nonetheless, given these non-specific effects of tamoxifen, we focused on identifying *Chat*-dependent effects by analyzing *Chat*-sufficient and *Chat*-deficient mice that had all been treated with tamoxifen.

Previously characterized SI tuft cell effector molecules (e.g. IL-25 and LTC_4) have primarily been shown to regulate ILC2 activation.[29,30] Also, recent studies have reported that ILC2s express *Chat* following activation and that ACh can potentiate their production of cytokines and proliferation, perhaps via autocrine signaling[59,60]. We therefore asked if tuft cell-derived ACh was signaling to ILC2s in addition to inducing fluid secretion. We began by testing if ACh could enhance ILC2 activation using an *in vitro* model of acute (6-hour) ILC2 stimulation.[30] Pairing ACh with IL-25 to mimic the results of tuft cell activation, we failed to detect any ACh-dependent ILC2 activation as measured by IL-13 reporter expression and secretion of IL-13 and IL-5 (Fig. S4C-D). By contrast, LTC_4 greatly enhanced ILC2 activation when given with IL-25, as expected. We conclude that ACh does not induce cytokine expression in ILC2s sorted from unmanipulated mice and is therefore unlikely to contribute to their initial activation.

To test if tuft cell-derived ACh was involved in ILC2 activation *in vivo* and at later timepoints, we generated *Chat*$^{fl/fl}$*;Pou2f3*$^{ERT2\text{-}Cre/+}$ mice that also expressed an IL-13 reporter (Smart13). We treated these mice with tamoxifen, infected with *Nb*, and

assessed early ILC2 activation in the LP 4 days post infection (dpi), about 2 days after the worms arrive in the intestine. We found no difference in ILC2 activation or expansion (Fig. 4A, S4E). Since *Chat* has been detected in activated but not resting ILC2s, we also tested if tuft cell-derived ACh regulated ILC2s later during infection. Given the difficulty of isolating viable cells from Type 2 inflamed SI, we assessed ILC2s in the mesenteric lymph nodes at 5 and 7 dpi. Again, we saw equivalent activation and expansion of ILC2s between *Chat*-sufficient and -deficient mice (Fig. 4B, S4F). We conclude that tuft cell-derived ACh does not contribute to ILC2 activation during helminth infection of the SI.

Tuft cell-derived ACh is not required for Type 2 intestinal remodeling

An effective immune response to helminths requires intestinal remodeling, such as hyperplasia of tuft cells and mucus-producing GCs and lengthening of the SI.[33,111] IL-13 is critical for this process, but ACh might also contribute. For example, ACh has been implicated in direct modulation of epithelial cell differentiation,[112,113] and could also impact tissue remodeling via other AChR-expressing cells, such as neurons.[84]

Using tuft cell frequency, goblet cell frequency, and intestinal length as markers of SI remodeling, we found little or no defect 7 days after *Nb* infection of mice with either constitutive (*Vil1-Cre(Tg+)*) or acute (*Vil1-Cre-Ert2(Tg+)*) deletion of *Chat* in IECs (Fig. 4C-E). The same was true both 5 and 7 days after *Nb* infection when we used *Pou2f3-Cre-ERT2* for tuft cell-specific *Chat* deletion (Fig. 4F-H). Since tuft cell circuits are distinct in the pSI and dSI,[32,30] we also tested Type 2 remodeling in the dSI 4 and 7 days after starting treatment with succinate-supplemented drinking water. As before,

there was little effect of either constitutive or inducible IEC *Chat* deletion (Fig. 4I-K; S4G). Likewise, *Chat*$^{fl/fl}$*;Vil1-Cre(Tg+)* mice vertically colonized with protists had no defect in tuft cell hyperplasia or SI length at homeostasis or following one week of additional succinate drinking water treatment (Fig. 4L, S4H). Acute loss of *Chat* in protist-colonized *Chat*$^{fl/fl}$*;Vil1-Cre-ERT2(Tg+)* mice also had no effect on tuft cell hyperplasia 5 days later (Fig. S4I). In sum, Type 2 remodeling is broadly intact in the absence of tuft cell ACh. We did observe small but significant decreases in tuft cell hyperplasia or SI lengthening in some assays, but this effect was inconsistent and minimal compared to loss of other tuft cell effector molecules (e.g. IL-25 and LTC_4).[29,30]

Tuft cell hyperplasia results in enhanced ACh-dependent fluid secretion

The ability of tuft cells to induce fluid secretion in the steady state led us to ask how it would change during Type 2 inflammation, when tuft cell numbers can increase 10-fold and fluid secretion might support worm clearance as part of the canonical weep and sweep response. First, we asked whether the number and frequency of *Chat*+ tuft cells changed with Type 2 inflammation. While the frequency of *Chat*+ tuft cells decreased (Fig. S5A), this was more than compensated for by the hyperplasia, such that the total number of *Chat*+ tuft cells per millimeter crypt/villus was increased in the pSI and especially the dSI 7 days after either succinate-treatment or *Nb*-infection (Fig. 5A).

Next, we infected mice with *Nb* to induce tuft cell hyperplasia and quantified the fluid secretion response to succinate in the pSI and dSI across the course of infection. Although pSI tuft cells do not respond to succinate at steady state, we wondered if those that emerge during infection might be responsive. The pSI did not become

responsive to succinate (or cESA) over the course of infection, but the dSI succinate response increased by day 7, when tuft cell numbers peaked (Fig. 5B, S5B-C). The increased response to succinate was less than the ~3-fold increase of *Chat*+ tuft cells that we observed on D7 of *Nb* infection, likely because the epithelium's total capacity to respond to ACh/CCh was reduced by Type 2 inflammation, as previously reported (Fig. 5B).[114] This effect could be quantified by measuring the ratio of succinate-induced ΔIsc to CCh-induced ΔIsc (Fig. 5C), highlighting how hyperplasia allows tuft cells to capture a greater proportion of the total epithelial ACh response. We confirmed that the increased succinate response on day 7 still required epithelium-derived ACh (Fig. 5D, S5D) and did not occur without *Sucnr1* (Fig. S5E). Enhanced succinate/cESA-induced fluid secretion was also observed if tuft cell hyperplasia was established with oral succinate or *Tritrichomonas* colonization (Fig. 5E). We found that tuft cell hyperplasia induced by *Nb* infection also increased C8-dependent fluid secretion in both the pSI and dSI, and that this required epithelial *Chat* (Fig. 5F-G, S5F-K).

To further test the hypothesis that increased numbers of tuft cells drive increased succinate-induced fluid secretion during Type 2 remodeling, we turned to Balb/c mice. Unmanipulated Balb/c mice are nearly tuft cell-deficient in the dSI, but activation of ILC2s with exogenous IL-25 increases tuft cell numbers (Fig. S5L).[76] Accordingly, unmanipulated Balb/c dSI did not respond to cESA in the Ussing chamber, but responsiveness was induced by rIL-25 treatment, indicating that increased numbers of ACh-producing tuft cells were needed (Fig. S5M).

Lastly, to test if *in vivo* fluid secretion was enhanced during Type 2 remodeling, we measured the fecal water content of protist-colonized mice. Compared to

uncolonized mice, mice colonized with the succinate-producing protist *T. musculis* had increased fecal water content by 14 and 20 days after colonization (Fig. 5H). This suggested that tuft cells were repeatedly responding to protist-derived succinate and inducing fluid secretion. Thus, the increased number of *Chat*+ tuft cells induced during SI Type 2 inflammation drives increased ACh-dependent fluid secretion despite an overall desensitization of the tissue to ACh.

Tuft cell ACh regulates helminth clearance but not protist colonization

There is little evidence to suggest that tuft cell sensing of *Tritrichomonas sp.* and the resulting Type 2 immune response in the SI alter the total abundance of protists,[18] but we wondered if tuft cell induced fluid secretion might instead regulate protist localization along the length of the SI, with the goal of containing protists to the dSI and cecum. We therefore assessed the abundance of protists across the pSI, dSI, and cecum of vertically-colonized *Chat$^{fl/fl}$;Vil1-Cre* mice (Fig. S6A), hypothesizing an increase of protists in the pSI of *Chat*-deficient mice. Constitutive deletion of *Chat* in tuft cells had no effect on protist abundance or localization across the SI or cecum (Fig. S6B). Treating protist-colonized mice with succinate to amplify Type 2 immunity also did not uncover a phenotype (Fig. S6B), and acute deletion of *Chat* for 5 days likewise failed to alter protist abundance or localization (Fig. S6C). Thus, the physiologic function of protist sensing by tuft cells remains unclear.

On the other hand, the requirement for tuft cell sensing and downstream Type 2 immunity for clearing helminths from the SI is well established.[20,32,77] To test if tuft cell ACh contributes to helminth clearance, despite not impacting ILC2 activation or tissue remodeling, we assessed worm burden in mice lacking epithelial *Chat* at 7 dpi, a

timepoint when WT mice begin to clear worms from the SI. Indeed, both constitutive and acute deletion of epithelial *Chat* led to an increased SI worm burden (Fig. 6A). Tuft-specific *Chat* deletion using *Pou2f3-Cre-Ert2* led to the same clearance delay 7 dpi (Fig. 6B). Worm burdens were equivalent in CRE-positive and -negative mice 5 dpi, suggesting normal colonization of the SI by *Nb* arriving from the lung. The delayed clearance was also not due to the loss of one *Pou2f3* allele in $Chat^{fl/fl};Pou2f3^{Cre\text{-}ERT2/+}$ mice as they cleared worms normally when not treated with tamoxifen (Fig. S6D). In order to allow initiation of type 2 remodeling to proceed normally and delete tuft cell ACh only during worm clearance, we waited until 5 dpi to administer a single dose of tamoxifen to $Chat^{fl/fl};Vil1\text{-}Cre\text{-}ERT2$ mice. Consistent with our earlier observation that tamoxifen suppresses intestinal Type 2 immunity, worm clearance in WT mice was delayed to day 8, but we again found a *Chat*-dependent delay in worm clearance despite normal intestinal remodeling. (Fig. 6C, Fig. S6E-F). Thus, we propose that tuft cell-derived ACh contributes to worm clearance by the induction of epithelial fluid secretion.

3.3 Discussion

This study identifies an epithelium-intrinsic response unit that couples tuft cell chemosensing to epithelial fluid secretion via the release of ACh from tuft cells. This effector function is common to tuft cells in multiple tissues and is executed within seconds of activation. In the SI, tuft cell-derived ACh is required for timely clearance of helminth infection, but unlike all previously identified tuft cell effector functions, tuft cell-derived ACh does not impact ILC2 activation nor downstream intestinal remodeling.

Instead, it appears that tuft cell ACh provides an acute signal that contributes to the weep and sweep responses that push worms out of the intestine. The magnitude of tuft cell-dependent fluid secretion correlates with the number of *Chat*+ tuft cells, suggesting one possible function for the tuft cell hyperplasia that occurs even after initial sensing of the helminth has been achieved.

While tuft cell-derived ACh was not required for ILC2 activation during helminth infection and intestinal remodeling was largely intact, there were slight yet significant defects in tuft cell numbers or SI length at some timepoints analyzed. Prior literature has shown that deletion of *Chrm3* from the SI epithelium causes an *increase* in tuft cell numbers at baseline but a *decrease* in tuft cells following irradiation.[112] Perhaps epithelial ACh signaling has damage-induced functions that overlap with helminth-induced intestinal remodeling. Regulation of intestinal epithelial differentiation by tuft cell-derived ACh bears further study.

Lastly, ACh-regulated smooth muscle contraction is critical for SI helminth clearance[67,103] and tuft cells have been linked to smooth muscle function in other tissues.[42,86] The short extracellular half-life of ACh combined with the distance between epithelial tuft cells and smooth muscles that surround the SI make direct signaling unlikely. Nonetheless, while we did not see evidence of direct contact between tuft cells and enteric neurons, they have been previously reported in the SI[26,115,116] and thus we cannot rule out the possibility that tuft cell ACh regulates smooth muscle contraction via the enteric nervous system.

During Type 2 inflammation in the SI, the maximal fluid secretion induced by ACh is dramatically reduced,[114] possibly to prevent excessive fluid loss or diarrhea during

chronic helminth infection. At the same time, the number of *Chat*+ tuft cells increases, such that tuft cell-regulated fluid secretion is maintained or even enhanced compared to baseline. This re-wiring of ACh-regulated fluid secretion may represent a regulatory mechanism that minimizes fluid loss due to endogenous signals while maintaining the ability to respond to lumen-restricted agonists such as helminths via tuft cell sensing. In that regard, tuft cells also have an advantage over mast cells and neurons, which can induce enhanced fluid secretion during Type 2 inflammation via release of histamine and/or prostaglandin E_2,[114] but can only respond to ligands that penetrate the mucosal barrier. Relatedly, it remains unclear whether the acetylcholinesterases secreted by helminths can penetrate the mucosal barrier to target ACh in the tissue, or whether helminths are only able to counter the effects of ACh during tissue-dwelling phases of their lifecycle.

Further study should test the relevance of tuft cell-induced fluid secretion in other intestinal helminth infections. Supplementing fluid secretion using Class 8 tuft cell activation, AChE inhibitors, or specific mAChR agonists may also speed the clearance of worms during *N. brasiliensis* infection. These studies could then inform the treatment of human infection.

3.4 Figures

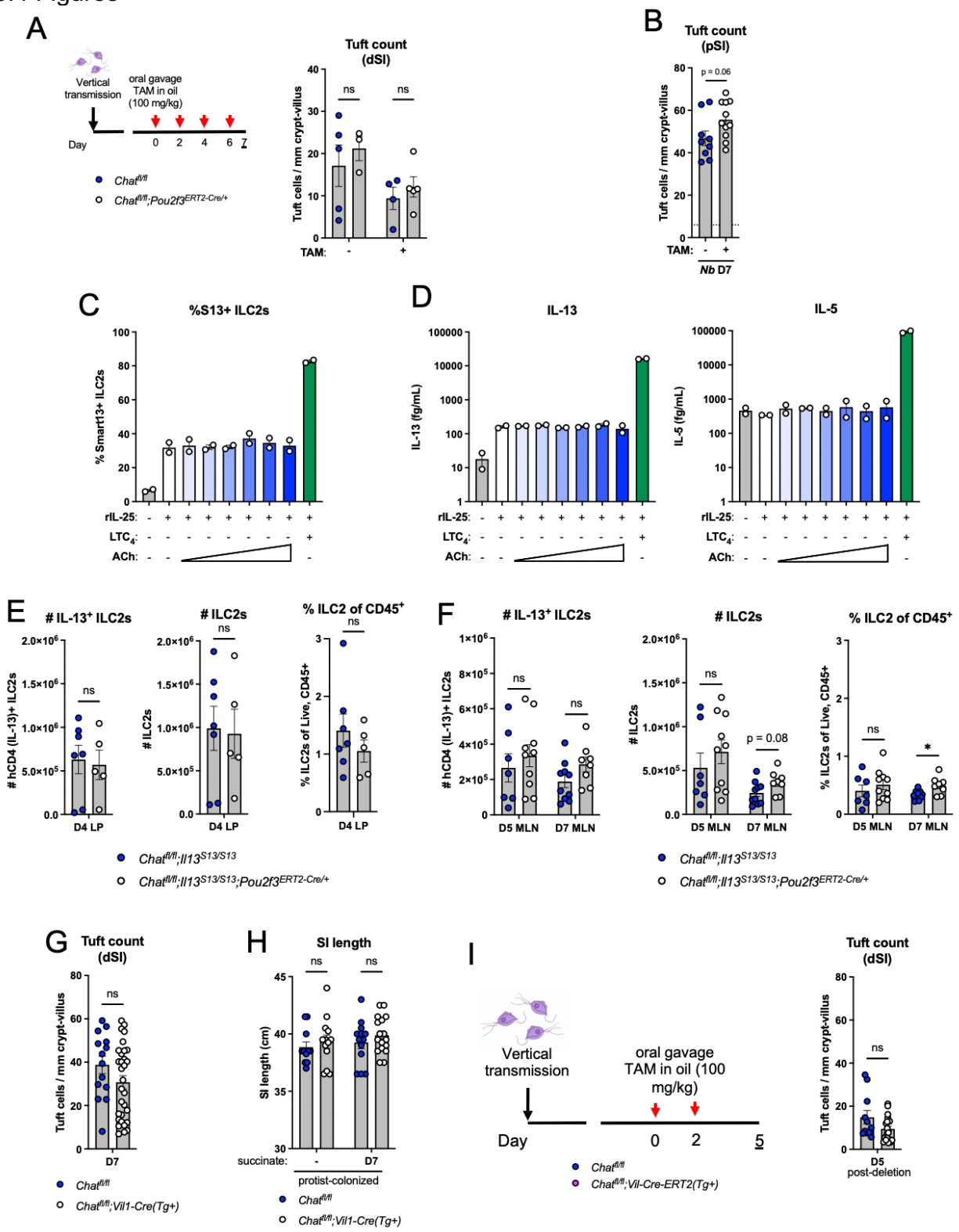

Supplemental Figure 4: (**A**) Schematic of tamoxifen (TAM) treatment of protist-colonized *Chat-fl; Pou2f3*$^{ERT2\text{-}Cre/+}$ mice and quantification of dSI tuft counts by immunofluorescence at D7 after start of

treatment. (**B**) Quantification of pSI tuft counts by immunofluorescence of WT mice treated with or without tamoxifen and infected with *Nb* for 7 days. (**C** and **D**) (C) Flow cytometric quantification of percent hCD4+ (IL-13+) SILP ILC2s and (D) IL-13 and IL-5 concentration in their supernatant after 6 hr *in vitro* culture with the indicated conditions (0.1 ng/mL rIL-25, serial 10-fold dilutions of ACh from 10 mM to 0.1 μM, 1 nM LTC_4). (**E** and **F**) Quantification of number of hCD4+ (IL-13+) ILC2s, total ILC2s, and percent ILC2s at the indicated timepoints, tissues, and genotypes. (**G**) Quantification of dSI tuft counts by immunofluorescence from indicated mice treated with 150 mM succinate drinking water for 7 days. (**H**) SI length from indicated mice vertically-colonized with *T. rainier* protists with or without 7 days of additional 150 mM succinate drinking water treatment. (**I**) Schematic of acute deletion of *Chat* from vertically *T. musculis* (*Tm*) -colonized mice and quantification of dSI tuft counts by immunofluorescence 5 days after start of treatment. In the (A-B, E-I), each symbol represents an individual mouse from two or more pooled experiments. In (C and D) each symbol represents a technical replicate of cells sorted from pooled mice. *p < 0.05, **p < 0.01, ***p < 0.001, ****p < 0.001 by multiple Mann-Whitney tests with Holm Sídák's multiple comparisons test (A, F, H) or Mann-Whitney test (B, E, G, I). ns, not significant. Graphs depict mean +/- SEM.

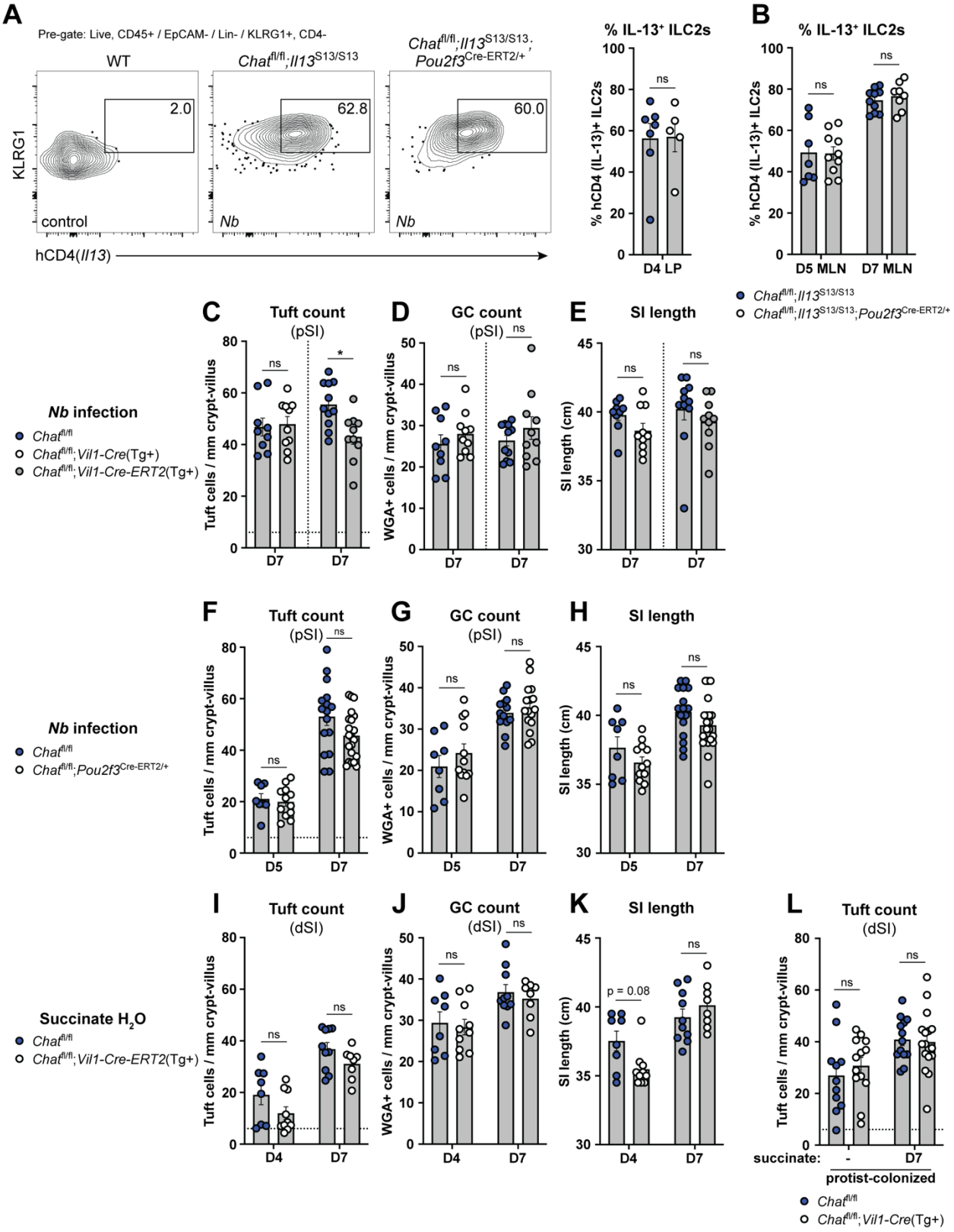

Figure 4: Tuft cell-derived ACh is not required for ILC2 activation or intestinal remodeling. (**A** and **B**) (A) Representative flow cytometry and quantification of percent hCD4^{+} (IL-13^{+}) ILC2s (Lin^{-}, CD45^{+},

KLRG1^{+}, CD4^{-}) in the SI LP and (B) mesenteric lymph nodes (MLN) at the indicated *Nb* infection timepoints. (**C**, **D**, and **E**) (C) Quantification of pSI tuft cells (DCLK1+) and (D) goblet cells (WGA+) by immunofluorescence and (E) total SI length from the indicated mice at D7 of *Nb* infection. (**F**, **G**, and **H**) Same analysis as in C-E in the indicated mice at the indicated *Nb* infection timepoints. (**I**, **J**, and **K**) Same analysis as in C-E in the indicated mice at the indicated timepoints of 150 mM succinate drinking water treatment. (**L**) Quantification of tuft cells (DCLK1+) by immunofluorescence from indicated mice vertically-colonized with *T. rainier* protists with or without 7 days of additional 150 mM succinate drinking water treatment. In the graphs, each symbol represents an individual mouse from two or more pooled experiments. For graphs of tuft cell counts, horizontal dashed line signifies baseline tuft cell count in unmanipulated mice. *$p < 0.05$, **$p < 0.01$, ***$p < 0.001$, ****$p < 0.001$ by Mann Whitney test (A) or multiple Mann-Whitney tests with Holm Sídák's multiple comparisons test (B-L). ns, not significant. Graphs depict mean +/- SEM. Also see Fig. S4.

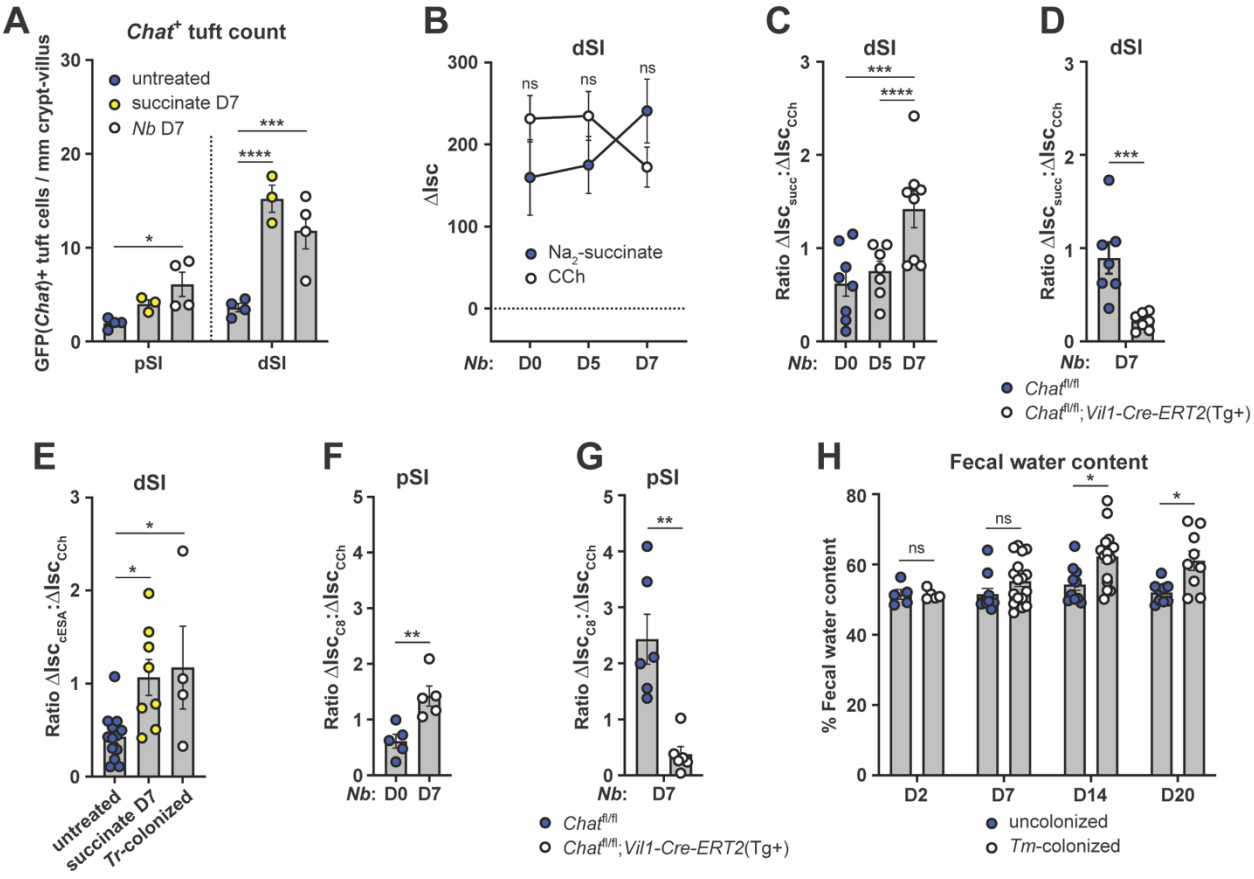

Figure 5: Tuft cell hyperplasia results in enhanced ACh-dependent fluid secretion. (**A**) Quantification of GFP(*Chat*)+ tuft cells (*Il25*-RFP+) from the pSI and dSI of WT mice untreated, treated with 150 mM Na_2-succinate drinking water (succinate), or infected with *N. brasiliensis* (*Nb*) for 7 days. (**B**) ΔIsc values of dSI from WT mice infected with *Nb* for the indicated number of days and stimulated as indicated (10 mM succinate, lumenal; 100 μM CCh, basolateral). (**C**) Ratio of succinate ΔIsc values to CCh ΔIsc values of dSI from (B). (**D**) Ratio of succinate ΔIsc values to CCh ΔIsc values of dSI of indicated mice 7 days after *Nb* infection. (**E**) Ratio of cESA ΔIsc values to CCh ΔIsc values of dSI from WT mice treated with succinate (as in A) or vertically colonized with *T. rainier* (*Tr*) protists. (**F** and **G**) Ratio of C8 ΔIsc values to CCh ΔIsc values of pSI from (F) WT or (G) mice of indicated genotypes mice at indicated timepoints after *Nb* infection. (**H**) Quantification of water content of fecal pellets collected at indicated timepoints post *T. musculis* (*Tm*) colonization of WT mice. In the graphs, each symbol represents an individual mouse pooled from two or more experiments. *p < 0.05, **p < 0.01, ***p < 0.001, ****p < 0.001 by two way ANOVA with Dunnett's multiple comparisons test (A), Mann-Whitney test (B, D, F-G), one way ANOVA (C, E), or multiple Mann-Whitney tests with Holm Sídák's multiple comparisons test (H). ns, not significant. Graphs depict mean +/- SEM. Also see Fig. S5.

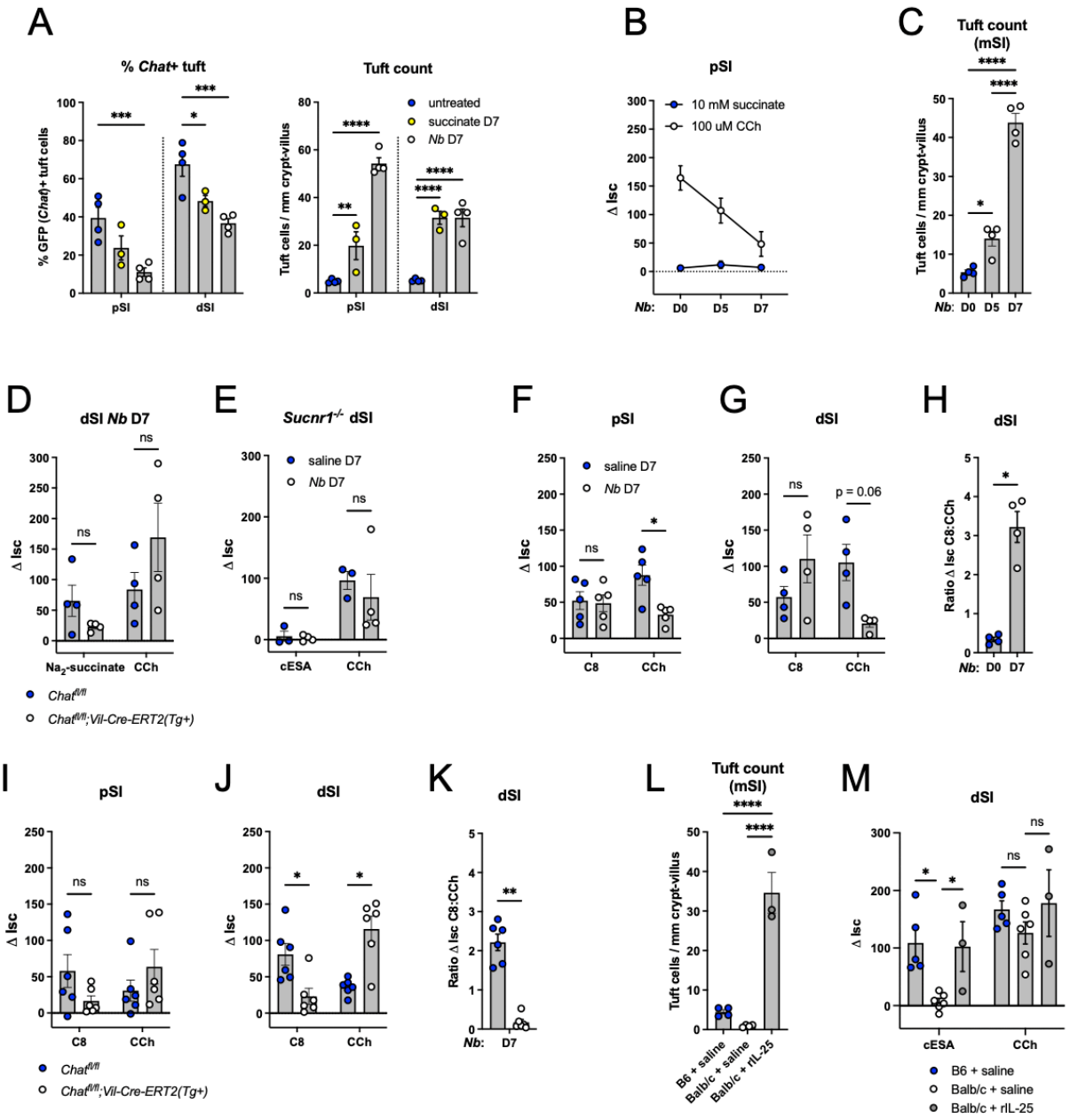

Supplemental Figure 5: (**A**) Quantification of percent GFP(*Chat*)+ tuft cells and RFP(*Il25*)+ tuft cells from the pSI and dSI of WT mice untreated, treated with 150 mM Na_2-succinate drinking water (succinate), or infected with *N. brasiliensis* (*Nb*) for the duration indicated. (**B**) ΔIsc values of pSI from WT mice infected with *Nb* for the indicated number of days and stimulated as indicated (10 mM succinate, lumenal; 100 μM CCh, basolateral). (**C**) Quantification of tuft cells (DCLK1+) by immunofluorescence from medial SI (mSI) of mice in (B). (**D**) ΔIsc values of dSI from mice of indicated genotypes infected with *Nb* for 7 days and stimulated as indicated. (**E**) ΔIsc values of *Sucnr1*$^{-/-}$ dSI with or without 7 day *Nb* infection, stimulated as indicated. (**F-G**) ΔIsc values of (F) pSI and (G) dSI from WT mice with or without 7 day *Nb* infection, stimulated as indicated. (**H**) Ratio of C8 ΔIsc values to CCh ΔIsc values in (G). (**I** and **J**) ΔIsc values of (I)

pSI and (J) dSI from mice of indicated genotype infected with *Nb* for 7 days, stimulated as indicated. (**K**) Ratio of C8 ΔIsc values to CCh ΔIsc values from (J). (**L**) Quantification of tuft cells (DCLK1+) by immunofluorescence in the mSI of mice of indicated genotypes treated as indicated. (**M**) ΔIsc values of dSI from mice in (L) stimulated as indicated. In the graphs, each symbol represents an individual mouse (one tissue or average of two) from two or more pooled experiments. *p < 0.05, **p < 0.01, ***p < 0.001, ****p < 0.001 by two way ANOVA with Dunnett's multiple comparisons test (A) two way ANOVA with Tukey's multiple comparisons test (M), Mann-Whitney test (B, H, K), one way ANOVA with Tukey's multiple comparisons test (C, L), or multiple Mann-Whitney tests with Holm Sídák's multiple comparisons test (D-G, I-J). ns, not significant. Graphs depict mean +/- SEM.

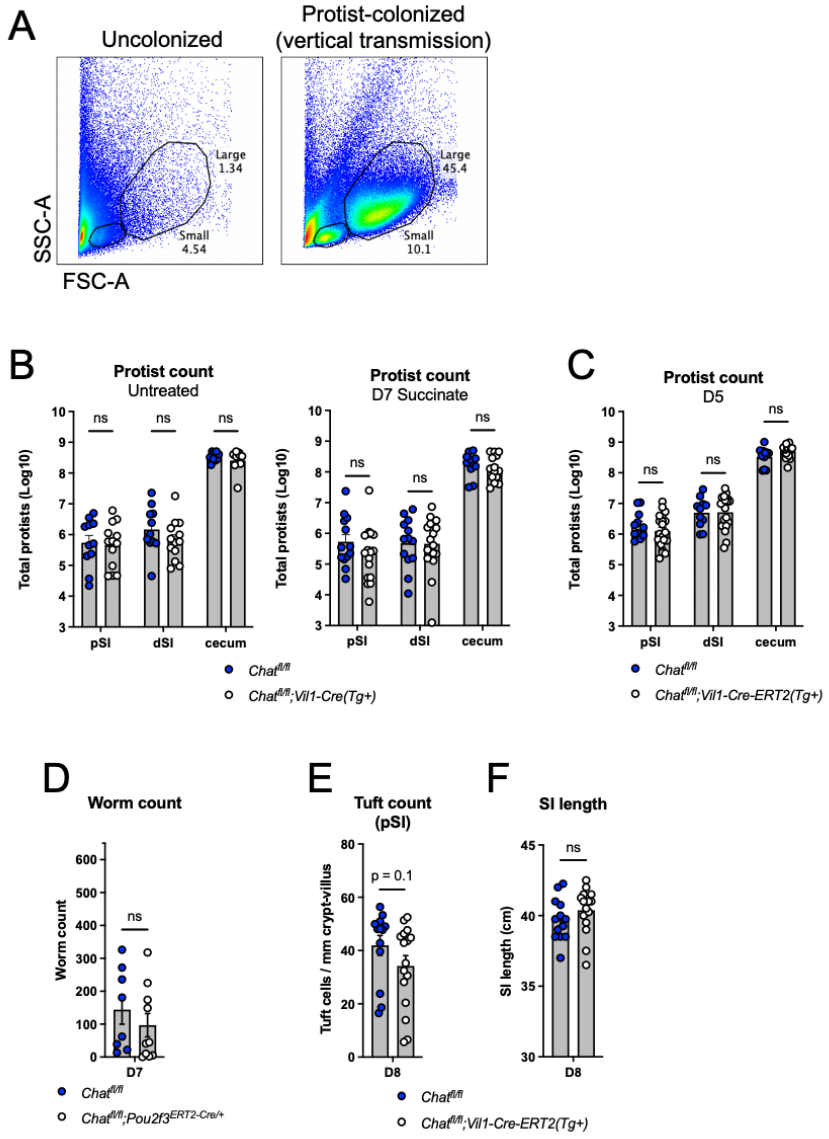

Supplemental Figure 6: (**A**) Representative flow cytometry of cecal contents from uncolonized and protist-colonized mice showing gating of protists by size. The "Large" gate contains *Tritrichomonas sp.* protists. (**B**) Quantification of total protists by flow cytometry in indicated tissues of vertically-colonized mice of indicated genotypes left untreated or given 150 mM Na_2-succinate in drinking water for 7 days. (**C**) Quantification of total protists by flow cytometry in indicated tissues of vertically-colonized mice of indicated genotypes administered tamoxifen 5 days prior to analysis. (**D**) Quantification of total SI *Nb* in mice of indicated genotype infected with *Nb* for 7 days without tamoxifen administration. (**E** and **F**) (E) Quantification of tuft cells (DCLK1+) by immunofluorescence and (F) total SI length 8 days post *Nb* infection of mice of indicated genotype given a single dose of tamoxifen (125 mg/kg) on day 5. In the graphs, each symbol represents an individual mouse (one tissue or average of two) from two or more pooled experiments. *p < 0.05, **p < 0.01, ***p < 0.001, ****p < 0.001 by multiple Mann-Whitney tests with

Holm Sídák's multiple comparisons test (B-C) or Mann-Whitney test (D-F). ns, not significant. Graphs depict mean +/- SEM.

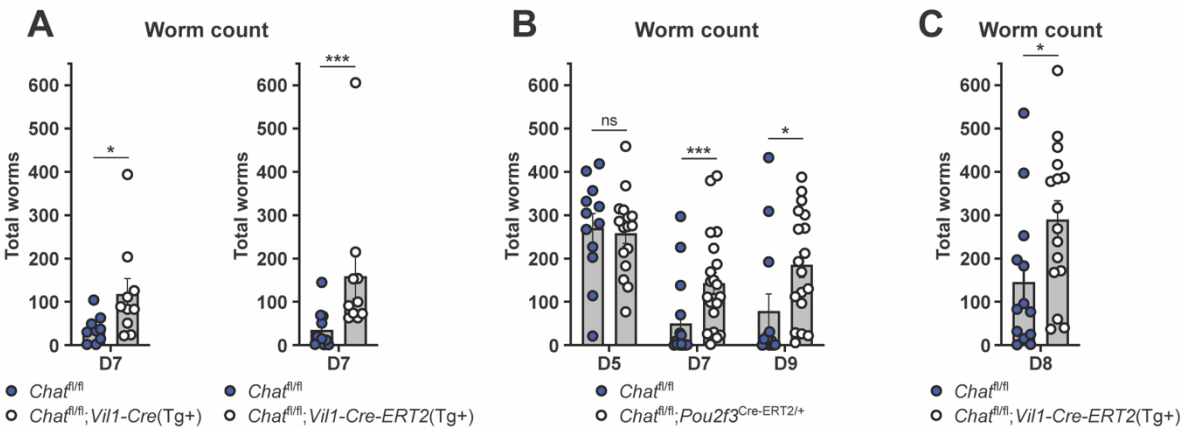

Figure 6: Tuft cell-derived ACh contributes to helminth clearance. (**A** and **B**) Quantification of total SI *Nb* in mice of indicated genotypes at (A) 7 or (B) indicated days post infection. (**C**) Quantification of total SI *Nb* 8 days post infection in mice of indicated genotypes given single dose of tamoxifen on D5. In the graphs, each symbol represents an individual mouse pooled from two or more experiments. *p < 0.05, **p < 0.01, ***p < 0.001, ****p < 0.001 by Mann-Whitney test (A, C), or multiple Mann-Whitney tests with Holm Sídák's multiple comparisons test (B). ns, not significant. Graphs depict mean +/- SEM. Also see Fig. S6.

CHAPTER 4
Materials and methods

Study Design

All experiments were performed using randomly assigned mice without investigator blinding. No data were excluded, except from Ussing chambers when mounted tissues failed to respond to stimulation by a positive control (e.g. CCh). All data points reflect biological replicates, except for *in vitro* ILC2 stimulations and epithelial monolayer experiments where each data point is a technical replicate. Data were pooled from multiple experiments unless otherwise noted. The number of independent experiments is included in the figure legends.

Experimental Animals

Mice aged 6 weeks and older were used for all experiments. Mice were age-matched within each experiment. Pooled results include both male and female mice of varying ages unless otherwise indicated. Mouse strains used in this study are listed in Table S3. Acute deletion of conditional alleles in mice was achieved by oral gavage with tamoxifen dissolved in corn oil (100 mg/kg). *Chat$^{fl/fl}$;Vil1-Cre-ERT2(Tg+)* mice were administered tamoxifen on day -4 and 0 of infection with *N. brasiliensis* and on day -6 and -4 of treatment with 150 mM succinate drinking water, or as noted in the text. *Chat$^{fl/fl}$;Pou2f3$^{Cre-ERT2/+}$* mice were administered tamoxifen every other day starting on day -4 of *N. brasiliensis* infection or as noted in the text. *DREADD(Tg+); Pou2f3$^{Cre-ERT2/+}$* mice were administered tamoxifen chow for 7 days prior to Ussing experiments. All mice (CRE+ and CRE-) received tamoxifen treatment. All mice were maintained in specific pathogen-free conditions at the University of Washington or Stanford University and

were confirmed to be free of *Tritrichomonas sp.* by microscopy and qPCR, unless specifically colonized for experimental purposes. All procedures were conducted within University of Washington or Stanford University (Class 8 gavage) IACUC guidelines under approved protocols.

Measuring epithelial ion flux with Ussing chambers

Ussing chamber protocols were informed by Clarke et al.[63]

Tissue mounting: Mice 7-12 weeks of age were euthanized by CO_2 and segments of the intestine (SI, cecum, colon) were harvested and flushed with cold Krebs Buffered Ringer's solution + mannitol (10 mM D-mannitol, 115 mM NaCl, 2.4 mM K_2HPO_4, 0.4 mM KH_2PO_4, 25 mM $NaHCO_3$, 1.2 mM $CaCl_2$ dihydrate, 1.2 $MgCl_2$ hexahydrate; pH 7.25-7.4). Intestines (first 5 cm of pSI and last 5 cm of dSI) were fileted open along the mesenteric line, trimmed and mounted to the pins of an Ussing chamber cassette with aperture of 0.3 cm^2 (Physiologic Instruments, Reno, USA), avoiding Peyer's patches. For some experiments the SI was pinned to a Sylgard-coated plate with the serosal side up and the muscle layer scored with a scalpel and "stripped" away using forceps under a dissection scope. The resulting epithelium-submucosa tissue was mounted in a cassette as normal. For trachea preparations, the entire trachea was harvested, surrounding tissue (esophagus) removed, and cut open lengthwise along the anterior side (away from esophagus) for mounting in a 2 mm^2 aperture cassette (Physiologic Instruments, Reno, USA). Cassettes containing tissues were mounted in Ussing chambers (Physiologic Instruments, Reno, USA) and the lumenal chambers filled with 5

mL of KBR + mannitol and the basolateral chambers filled with 5 mL of KBR + glucose (10 mM D-glucose, 115 mM NaCl, 2.4 mM K_2HPO_4, 0.4 mM KH_2PO_4, 25 mM $NaHCO_3$, 1.2 mM $CaCl_2$ dihydrate, 1.2 $MgCl_2$ hexahydrate; pH 7.25-7.4). The chambers were warmed to 37C and bubbled with carbogen (95% O_2, 5% CO_2) for the duration of the experiment. For Cl^- replacement experiments, Cl^- free KBR was used, in which gluconate is substituted for Cl- (115 mM D-gluconic acid sodium salt, 2.4 mM K_2HPO_4, 0.4 mM KH_2PO_4, 25 mM $NaHCO_3$, 4 mM calcium D-gluconate monohydrate, 1.2 mM magnesium D-gluconate hydrate; pH 7.25-7.4).

Measuring the short circuit current (Isc): Automatic voltage clamping was performed by MultiChannel Voltage-Current Clamp (Physiologic Instruments, Reno, USA). Voltage differences between electrodes and fluid resistance of the buffer were compensated prior to insertion of the tissue cassette. Isc was measured by voltage clamp every 1 second and recorded using Acquire & Analyze software (Physiologic Instruments, Reno, USA) and normalized to tissue area. After a 20 min equilibration period, tissues were stimulated lumenally with Na_2-succinate (1, 10 mM) or cis-epoxysuccinic acid (10 mM), basolaterally with 5 μM Class 8, or bilaterally with 1 μM Compound 21. For succinate/cESA stimulation, subsequent stimulations were administered every 10 min; for Class 8 the interval was increased to 15 min due to the slower kinetics of the response. Subsequent stimulations included lumenal 20 mM NaCl, basolateral 100 μM CCh, and bilateral cocktail of 100 μM 3-Isobutyl-1-methylxanthine (IBMX) + 10 μM forskolin. Chemical inhibitors were administered 5 min after start of equilibration period (15 min before first stimulation): basolateral 100 μM bumetanide, bilateral 10 μM

ibuprofen, basolateral 10 μM atropine, basolateral 1 μM tetrodotoxin, and lumenal 1 mM carbenoxolone. ΔIsc values were calculated as the difference between the Isc measurement at the peak of the stim response and the Isc measurement taken right before adding the agonist. For tissues that did not respond to the agonist (e.g., knockout mouse intestines, tissues treated with inhibitors) and therefore had no peak response, the Isc value was taken at the same timepoint as the peak Isc value for the corresponding WT or control tissue.

Measuring fecal water content

Mice were orally gavaged with vehicle (0.5% methylcellulose + 1% Tween 20) or 30 mg/kg Class 8, and fecal samples (2+ pellets) were taken at 0 and 3 hours post gavage. For protist-colonized experiments, B6 mice were colonized with *T. musculis* protists and fecal samples collected at 2, 7,14, and 20 days post colonization. Fecal samples were dried at 60C overnight and % water content calculated as (1-(dry weight/wet weight))*100.

Monolayer culture and cysteinyl leukotriene ELISA

Proximal small intestine was isolated and villi were gently scraped off with a glass coverslip. Tissue was incubated for 30 minutes at 4° with 2mM EDTA to release epithelial crypts, then washed twice with cold PBS and filtered through a 70 um strainer. Crypts were resuspended in complete monolayer media (DMEM/F12 supplemented with 2mM glutamine, 100U/mL penicillin, 100mg/mL streptomycin, 10mM HEPES, N2 supplement, B27 supplement, R-spondin (10% supernatants from R-spondin secreting

cells), Noggin (10% supernatant from Noggin secreting cells), 500mM N-acetylcysteine, 50ug/mL mEGF, and 10 μM Y27632). Plates were coated with 2% Matrigel in cold DMEM/F12 and incubated at 37° for at least 30 minutes. Media was aspirated from the plate, and 1000 crypts were plated per well of a 48-well plate. Crypts were incubated overnight, and non-adherent cells were aspirated the next day. Test stimuli diluted in HBSS containing $Ca^{2+/}Mg^{2+}$ were added to monolayers and stimulated at 37° for 30 minutes. Supernatants were collected and used for the Cysteinyl Leukotriene Express ELISA kit (Cayman Chemical) according to manufacturer's protocol.

Succinate and cytokine treatment

For succinate experiments mice were given 150mM sodium succinate hexahydrate (Thermo) ad libitum in drinking water for the indicated amount of time. Recombinant murine IL-25 (500 ng; R&D) was given for 3 consecutive days intraperitoneally in 200 μL PBS.

Helminth infections and analysis

N. brasiliensis larvae were raised and maintained as previously described.[117]

Mice were infected subcutaneously with 500 *N. brasiliensis* L3. At sacrifice, the entire SI was fileted open and total worms counted under a stereomicroscope.

Protist colonization and analysis

Breeding pairs were colonized with *Tritrichomonas musculis* or *T. rainier* as previously described.[118] Pups from colonized breeding pairs were analyzed. Protist numbers were

quantified by flow cytometry as described by Chudnovskiy et al.[36] Briefly, 10 cm of pSI and dSI were flushed into a 15 mL conical with 10 mL RT PBS using a gavage needle. Cecal contents were harvested into 15 mL conical, weighed, and then 10 mL RT PBS added. Samples were let sit for 30 min at RT, vortexed, and then passed through a 70 μm filter. Protists were washed, stained with DAPI, then count beads added and data collected on a FACSCanto II (BD Biosciences). Protist numbers per gram of cecal content was calculated.

Intestinal tissue fixation and staining

Intestinal tissues were flushed with PBS and fixed in 4% paraformaldehyde for 3-4 hours at 4°C, washed with PBS, and incubated in 30% (w/v) sucrose overnight at 4°C. Samples were then coiled into “Swiss rolls”, embedded in Optimal Cutting Temperature Compound (Tissue-Tek) and sectioned at 8 μm on a CM1950 cryostat (Leica). Immunofluorescent staining was performed in PBS with 1% BSA at room temperature as follows: 1 hr 10% donkey serum with 1:1000 Fc Block, 1 hr (or O/N at 4°C) primary antibody, 5 min wash, 45 min secondary donkey antibody and/or WGA-488, 5 min wash, and mounted with Vectashield plus DAPI (Vector Laboratories). Images were acquired with an Axio Observer A1 (Zeiss) microscope with a 10X or 20X A Plan objective. Tuft cell frequency was calculated using ImageJ software to manually quantify DCLK1$^+$ cells per millimeter of crypt-villus axis. Goblet cell frequency was calculated using ImageJ software to manually quantify total WGA+ cells in the villus (crypts were excluded because WGA also labels Paneth cells) per millimeter of crypt villus axis. For

each replicate, four 10x images of the Swiss roll were analyzed and at least 25 total villi counted.

Single-cell tissue preparation for flow cytometry

For single cell epithelial preparations from SI, tissues were flushed with PBS, Peyer's patches removed, opened longitudinally, and rinsed with PBS. Tissue was cut into small pieces, shaken vigorously for 20 seconds in 30 mL cold HBSS (Ca^{+2}/Mg^{+2}-free) with 1 mM HEPES, drained, and then incubated rocking at 37°C for 10 min in 15 mL HBSS (Ca^{+2}/Mg^{+2}-free) supplemented with 3 mM EDTA and 1 mM HEPES. Tissues were vortexed thoroughly and released epithelial cells passed through a 70 μm filter. This process was repeated for a total of 3 rounds. Supernatants were pooled and washed with HBSS (Ca^{+2}/Mg^{+2}-free) with 1 mM HEPES before staining for flow cytometry.

For lamina propria (LP) preparations from uninfected mice, SI was processed as above to remove the epithelial fraction. Tissues were then incubated shaking at 37°C for 30 minutes in 10 mL RPMI 1640 supplemented with 20% FCS, 1 mM HEPES, 0.05 mg/ml DNase I (Sigma Aldrich), and 1 mg/mL Collagenase A (Sigma Aldrich). Tissues were vortexed and cells were passed through a 100 μm filter, then a 40 μm filter, washing with cold HBSS (Ca^{2+}/Mg^{2+}-free) with 1 mM HEPES. Cells were washed and stained for flow cytometry.

For LP preparations from *N. brasiliensis*-infected mice (D4), mice were anaesthetized with 5% avertin. The peritoneal cavity was opened, the SI nicked at the junction with the stomach and transected at the cecum and flushed with 20 mL of 37°C HBSS (Ca^{2+}/Mg^{2+}-free) plus 1 mM HEPES. Then the mice were perfused through the

heart with 30 mL of 37°C HBSS (Ca^{2+}/Mg^{2+}-free) with 30 mM EDTA and 1 mM HEPES. Three minutes after perfusion was completed, the first 10 cm of the proximal SI was harvested, Peyer's patches removed, opened longitudinally, and cut into small pieces and shaken vigorously for 20 seconds in 30 mL cold HBSS (Ca^{2+}/Mg^{2+}-free) with 1 mM HEPES, then drained. Tissues were then digested and processed as above in uninfected mice.

For mesenteric lymph node (MLN) preparations, SI-draining MLN were harvested into RPMI + 5% FBS on ice, mashed through a 70 μm filter, the filter washed with RPMI + 5% FBS, and cells washed and stained for flow cytometry.

Flow cytometry and cell sorting

Single cell suspensions from tissues were prepared as described above. For flow cytometry, SI epithelium and MLN samples were stained in DPBS (Ca^{2+}/Mg^{2+}-free) with 3% FCS and LP samples were stained in PBS (Ca^{2+}/Mg^{2+}-free) with 3% FCS, 2 mM EDTA, and 0.02 mg/mL DNase I with antibodies to surface markers for 30 min at 4°C, followed by DAPI (Roche) for dead cell exclusion. When cell counts were needed, counting beads (Spherotech) were added prior to running flow cytometry. Samples were run on a FACSCanto II or LSRII (BD Biosciences) and analyzed with FlowJo 10.8.1. Samples were FSC-A/SSC-A gated to exclude debris, FSC-A/FSC-H gated to select single cells, and gated to exclude dead cells. For cell sorting, single cell suspensions were prepared and stained as described and sorted on an Aria III (BD Biosciences).

ILC2 Stimulation Assay

Entire SILP from several mice were pooled and ILC2s (EpCAM-, $CD45^+$, Lin(CD3, CD4, CD5, CD8, CD11b, CD19, NK1.1, $FcER1)^-$, $KLRG1^+$) sorted as described. Sorted cells were plated at 5000 cells per well in a 96-well plate and incubated at 37°C overnight in 10 ng/ml IL-7 (R&D Systems) and basal media composed of high glucose DMEM supplemented with non-essential amino acids, 10% FBS, 100 U/mL penicillin, 100mg/mL streptomycin, 10mM HEPES, 1mM sodium pyruvate, 100μM 2-mercaptoethanol, and 2mM L-glutamine. The next morning, media was replaced and cells were stimulated with the indicated agonist. After a six-hour stimulation, supernatant was collected and the cells were washed and stained with 1 uL/well of PE-conjugated anti-human CD4 for 20 min at 4°C. Cells were washed, resuspended in DAPI and analyzed on a CantoRUO (BD Biosciences). Cytokine levels in supernatants were measured using Enhanced Sensitivity Flex Sets (BD Biosciences) for mouse IL-5 and IL-13 according to the manufacturer's protocol. Data was collected on an LSRII (BD Biosciences).

RNA Sequencing and Analysis

150-200 tuft cells were sorted directly into lysis buffer from the SMART-Seq v4 Ultra Low Input RNA Kit (Takara) and cDNA generated following manufacturer's instructions. Cells were sorted from four individual mice for each experiment. Sequencing libraries were generated using the Nextera XT library preparation kit with multiplexing primers, according to manufacturer's protocol (Illumina), and library quality assessed using Tapestation (Agilent). High throughput sequencing was performed on NextSeq 2000 (Illumina), sequencing dual-indexed and paired-end 59 base pair reads. All samples

were in the same run with a target depth of 5 million reads. Base calls were processed to FASTQs on BaseSpace (Illumina), and a base call quality-trimming step was applied to remove low-confidence base calls from the ends of reads. The FASTQs were aligned to the GRCm38 mouse reference genome, using STAR v.2.4.2a and gene counts were generated using htseq-count. Further analysis of the data was performed using the DIY.Transcriptomics (diytranscriptomics.com) pipeline, with experiment-specific modifications. Samples were filtered to exclude genes with counts per million = 0 in 4 or more samples and genes annotated as pseudogenes. Finally, samples were normalized to each other. To identify differentially expressed genes, precision weights were first applied to each gene based on its mean-variance relationship using VOOM,[119] then data was normalized using the TMM method[120] in EdgeR.[121] Linear modeling and bayesian stats were employed via Limma[122] to find genes that were up- or down-regulated by 2-fold (Log2FC = 1) or more, with a false-discovery rate (FDR) of 0.01. The code and results for these analyses are included as Data File S1 and S2.

Statistical Analysis

Statistical analysis was performed as noted in figure legends using Prism 9 (GraphPad) software. Graphs show mean +/- SEM.

Table S3

Reagent or Resource	**Source**	**Identifier**
B6.Cg-Tg(RP23-268L19-EGFP)2Mik/J (Chat-GFP)	Jackson Laboratory	JAX #007902
B6.*Il25*$^{Flare25/Flare25}$ (Il25-RFP)	R. Locksley (PMID: 26675736)	NA
B6.*Il13*$^{Smart13/Smart13}$ (Smart13)	R. Locksley (PMID: 22138715)	NA
C57BL/6N-Pou2f3<tm1(KOMP)Vlcg>/Tcp (*Pou2f3*$^{-/-}$)	Canadian Mouse Mutant Repository	CMMR #ABDF

B6.129P2-Trpm5^{tm1Dgen}/J (*Trpm5$^{-/-}$*)	Jackson Laboratory	JAX #005848
B6.*Sucnr1$^{-/-}$*	In-house (PMID: 30021144)	NA
B6.*Il25$^{-/-}$*	A. McKenzie (PMID: 16606668)	NA
B6;129-Chat^{tm1Jrs}/J (*Chat$^{fl/fl}$*)	Jackson Laboratory	JAX #016920
B6.Cg-Tg(Vil1-cre)997Gum/J	Jackson Laboratory	JAX #004586
B6.Cg-Tg(Vil1-cre)1000Gum/J (Vil1-Cre1000)	Jackson Laboratory	JAX #021504
B6.Cg-Tg(Vil1-cre/ERT2)23Syr/J (*Vil1-Cre-Ert2*)	Jackson Laboratory	JAX #020282
B6(129S4)-*Pou2f3$^{tm1.1(cre/ERT2)Imt}$*/J (Pou2f3-Cre-Ert2)	Jackson Laboratory	JAX #037511
B6.129S-Chattm1(cre)Lowl/MwarJ (*Chat-Cre*)	Jackson Laboratory	JAX #031661
B6.*Il25-Cre*	R. Locksley (PMID: 35245089)	NA
B6.Cg-*Gt(ROSA)26Sor$^{tm9(CAG-tdTomato)Hze}$*/J (Ai9)	Jackson Laboratory	JAX #007909
B6N;129-Tg(CAG-CHRM3*,-mCitrine)1Ute/J (Gq-DREADD)	Jackson Laboratory	JAX #026220
B6.129-*Gt(ROSA)26Sor$^{tm1(CAG-CHRM4*,-mCitrine)Ute}$*/J (Gi-DREADD)	Jackson Laboratory	JAX #026219
B6.*Alox5$^{fl/fl}$*	In-house (PMID: 32160525)	NA
B6.*Il4ra$^{-/-}$*	F. Brombacher (PMID: 15142530)	NA

Table S4

Reagent or Resource	**Dilution Factor**	**Source**	**Identifier**
Rabbit α-DCLK1	1:1000	Abcam	Cat#ab31704
Rabbit α-TUJ1 (Beta-III tubulin)	1:500	Abcam	Cat#ab18207
Goat α-GFP	1:500	Novus Bio	Cat#NB100-1770
Rabbit α-dsRed	1:500	Clontech	Cat#632496
Rabbit α-HA, clone 16B12	1:1000	Biolegend	Cat#901516

WGA-488	1:150	Thermo	Cat#W11261
Donkey α-Rabbit IgG AF594	1:1000	Thermo	Cat#A-21207
Donkey α-Goat IgG AF488	1:500	Thermo	Cat#A-11055
CD16 / CD32, clone 2.4G2	1:1000	Tonbo	Cat# 70-0161-M001
CD3 PerCP-Cy5.5, clone 145-2C11	1:100	Biolegend	Cat#100328
CD3 BV421, clone 145-2C11	1:400	Biolegend	Cat#100335
CD4 BV711, clone RM4-5	1:250	Biolegend	Cat#100549
CD4 eF450, clone RM4-5	1:200	eBioscience	Cat# 48-0042-80
hCD4 PE, clone RPA-T4	1:50	Biolegend	Cat#300508
CD5 PerCP-Cy5.5, clone 53-7.3	1:500	Biolegend	Cat#100624
CD5 eF450, clone 53-7.3	1:400	Biolegend	Cat#100607
CD8 PerCP-Cy5.5, clone 53-6.7	1:200	Biolegend	Cat#100724
CD8 BV421, clone 53-6.7	1:400	Biolegend	Cat#100737
CD11b AF700, clone M1/70	1:250	Biolegend	Cat#101222
CD11b BV421, clone M1/70	1:400	Biolegend	Cat# 101235
CD19 PerCP-Cy5.5, clone 6D5	1:250	Biolegend	Cat#115533
CD19 BV421, clone 6D5	1:400	Biolegend	Cat# 115537
CD24 PE, clone M1/69	1:300	Biolegend	Cat#101807
CD24 PerCP-Cy5.5, clone M1/69	1:300	Biolegend	Cat#101824
CD45 BV605, clone 30F11	1:300	Biolegend	Cat#103155
CD45 BV650, clone 30F11	1:500	Biolegend	Cat#103151
EpCAM PE-Dazzle, clone G8.8	1:300	Biolegend	Cat#118235
EpCAM AF488, clone G8.8	1:300	Biolegend	Cat#118210
EpCAM PE-Cy7, clone G8.8	1:300	Biolegend	Cat#118215

FcER1 BV421, clone Mar-1	1:400	Biolegend	Cat#334623
IL17RB APC, clone 9B10	1:100	Biolegend	Cat#146307
KLRG1 PE-Cy7, clone 2F1	1:250	Biolegend	Cat#138416
NK1.1 PerCP-Cy5.5, clone PK136	1:100	Biolegend	Cat#108728
NK1.1 BV421, clone PK136	1:200	Biolegend	Cat#108731
Siglec-F APC-Cy7, clone E50-2440	1:100	BD	Cat#565527
Siglec-F AF647, clone E50-2440	1:100	BD	Cat# 562680
Thy1.2 (CD90.2) BV605, clone 53-2.1	1:500	Biolegend	Cat#140318

CHAPTER 5
Summary and future directions

5.1 Summary

Fluid secretion is essential to epithelial barrier function and defense across mucosal sites from the intestines to the airways. Most epithelial cells are tasked with basic functions regulating host physiology such as absorbing nutrients or exchanging gasses. Tuft cells are a rare epithelial cell subset with chemosensory capabilities that allow them to act as sentinels and signal to both the epithelium and cells of the underlying tissue to coordinate a variety of physiological and immune responses to noxious compounds, bacteria, protists, and helminths. In this study, we describe how tuft cells secrete acetylcholine (ACh) to induce fluid secretion from neighboring epithelial cells. Tuft cells in the distal small intestine (SI) sensed the metabolite succinate produced by commensal protists and certain bacteria, while tuft cells in the proximal SI, colon, and trachea could be activated using the chemosensory ion channel TRPM5 agonist, Class 8, to induce fluid secretion. Fluid secretion as measured with an Ussing chamber required chloride ions and was transient, representing a short burst of fluid secretion to flush the stimuli away from the epithelium. Tuft cell activation via oral Class 8 induced sufficient fluid secretion *in vivo* to be detected in the feces. While rapid fluid secretion is consistent with the sort of immediate, deterrent-style ACh-dependent responses employed by tuft cells in the airways and urogenital tract, our finding represents a novel function for SI tuft cells, which have previously only been linked to the activation of ILC2s. Additionally, this response did not require involvement of sensory or enteric neurons.

We thoroughly tested whether tuft-derived ACh played a role in ILC2 activation or Type 2 epithelial remodeling but found little to no contribution across an array of tuft cell activators, from succinate drinking water to protists and helminths. Yet as IL-13-driven epithelial remodeling progressed during helminth infection and the number of *Chat*+ tuft cells increased, so did the fluid secretion response. The peak of tuft-induced fluid secretion coincided with peak goblet cell hyperplasia and smooth muscle contractility, likely complementing the “weep and sweep” that flushes helminths out of the SI. In support of this, genetic deletion of tuft-derived ACh delayed clearance of the helminth *N. brasiliensis* by several days. Deletion of tuft-derived ACh just prior to normal helminth clearance recapitulated early deletion, and we ruled out the possibility that tuft cell activation induced intestinal contractility. The fact that worms were ultimately cleared reflects the redundancy of immune defense mechanisms and the fact that the efficacy of mucus secretion and intestinal contractility are likely enhanced by, but not entirely dependent upon fluid secretion. Loss of tuft-derived ACh had no effect on the abundance or localization of succinate-producing protists for reasons that require further study but are consistent with limited effect of the overall Type 2 response on protists. Tuft-derived ACh is therefore an important component of “weep and sweep”, the critical threshold of fluid, mucus, and intestinal contractility needed to clear worms from the intestine. The ongoing secretion of ACh by tuft cells during Type 2 responses presents a potential reason for tuft hyperplasia that is independent from simply regulating ILC2s. The significance of tuft-induced fluid secretion in other mucosal tissues remains to be worked out but interesting connections to potential pathogens and clinical phenotypes abound.

5.2 Future directions

Regulation of *Chat* and ACh in tuft cells

The mechanism by which tuft cells secrete ACh remains a mystery as most tuft cells do not express the canonical genes found in cholinergic neurons for packaging ACh into vesicles (*Slc18a3*/VAChT) or recycling ACh's degradation product choline (*Slc5a7*/CHT1).[92] This fact is shared with some but not all other non-neuronal *Chat*-expressing cells, suggesting perhaps a common mechanism. Expression of *Slc18a3* does increase during helminth infection, suggesting a more conventional mechanism of vesicle secretion, but tuft cells are capable of releasing ACh at homeostasis. Tuft cells express several members of the OCT family of organic cation transporters that have been reported to allow release of ACh, as well as members of the CTL family of transporters thought to uptake choline, the building block of ACh.[123,124] High resolution imaging studies have identified extensive tubulo-vesicular networks in the apical, but not basolateral, portion of tuft cells, the significance of which is not known.[125,126] Ideally, immortalized tuft cells would allow for deeper mechanistic studies, but in the meantime other non-neuronal *Chat*-expressing cells like CD4+ T cells might prove useful in uncovering a shared, non-neuronal mechanism of ACh release.

The proximal-distal regulation of *Chat* expression in SI tuft cells is likewise intriguing. The reduced frequency of ACh-competent tuft cells in the proximal SI might reflect the greater emphasis on nutrient absorption in that tissue, while in the distal SI epithelial secretion of mucus, anti-microbial peptides, and fluid might be more important to contain higher microbial burdens emanating from the cecum and colon. As the phenomenon of diarrhea shows us, too much fluid secretion can be deleterious.

Perhaps this is why as tuft cell numbers increased during Type 2 remodeling the overall frequency of *Chat*+ tuft cells diminished, resulting in a smaller-than-expected increase in *Chat*+ tuft cells. The proximal and distal SI also became less sensitive to ACh during the course of infection, consistent with prior studies in Balb/c mice showing that sensitivity to ACh is reduced in an *Il4ra*-dependent manner following infection with a variety of helminths.[114] While this downregulation could theoretically reduce the risk of life-threatening diarrhea in cases of chronic helminth infection, it is not clear if fluid secretion is actually diminished *in vivo* as this would seem to contradict the concept of "weep and sweep"*.* The drop might instead reflect the limitations of the Ussing chamber, which cannot distinguish reduced acute secretion from increased baseline ion flux due to increased epithelial permeability. Studies measuring the movement of water using deuterated H_2O in the Ussing chamber could help unravel this question.

Future studies should also test if tuft-derived ACh and fluid secretion are important in other models of helminth infection, such as *H. polygyrus* or *Trichuris muris*. Since primary *H. polygyrus* infection results in chronic parasitization, fluid secretion might not contribute to overt clearance as with *N. brasiliensis,* but instead impair the initial burrowing into the tissue or localization within the SI.[127] Though *H. polygyrus* is capable of chronic colonization their numbers do diminish slowly over time—perhaps there is a role for tuft-induced fluid secretion.

Helminth-derived AChE and apical ACh secretion

Like *N. brasiliensis*, *H. polygyrus* worms secrete soluble AChE during the intestinal phase of infection. Numerous studies have shown that these enzymes

possess potent ACh-degrading activity *in vitro*[55–57] and administration of one recombinant AChE *in vivo* was able to alter the outcome of airway inflammation, indicating broad, systemic effects.[128] We can therefore assume that helminths are capable of antagonizing host ACh signaling broadly and might target tuft cell-derived ACh to prevent fluid secretion. The fact that loss of epithelial *Chat* results in impaired worm clearance suggests that their efforts are only partially successful, but future studies should test if genetic knockdown or knockout of helminth AChE genes can speed up worm clearance from the host. Genetic knockdown or knockout of helminth genes is made difficult by their complex lifecycles, but recent advances have been made using RNAi in *N. brasiliensis*[129] or CRISPR with *N. brasiliensis*[130] and *Strongyloides stercoralis,* a human-adapted helminth similar to *N. brasiliensis.*[131]

One of several hypotheses as to why intestinal helminths produce AChEs posits that host-derived ACh can bind to nAChRs located on the helminth body segments causing spastic paralysis by a mechanism similar to the anti-helminthic drug pyrantel pamoate.[132] Helminths might therefore be protecting themselves from paralysis and fighting to maintain the ability to migrate against the ongoing “weep and sweep”. ACh from tuft cells is clearly secreted basolaterally since epithelial mAChRs that drive fluid secretion are only sensitive to basolateral stimulation, but it is possible that tuft-derived ACh is also secreted lumenally as one study in the airways suggested.[43] Further study is needed to measure whether ACh levels in the lumen increase during helminth infection in a tuft-derived ACh-dependent manner. The collaborative effect of increasing fluid secretion while also paralyzing the worm could be substantial and enhance the effect of either alone.

Function of fluid secretion in trachea and colon

More work is needed to explore the significance fluid secretion induced by succinate in the trachea and Class 8 in the proximal colon. Sensing of succinate in a bacterial context is a promising avenue for the trachea, given the fact that excess succinate in the airway promotes *Pseudomonas aeruginosa* colonization and biofilm formation.[99] Fluid secretion might be triggered when succinate concentration reaches a sufficiently high level to support bacterial growth, in order to dilute out the succinate again. This concept shares some similarity with the report showing that human sinonasal tuft cells sense airway glucose levels as an indicator of bacterial growth, with low levels indicating high bacterial load and triggering release of antimicrobial peptides.[87] Fluid secretion would certainly also complement mucocilliary clearance in the cases of tuft cell sensing of formylated peptides produced by bacteria.[43,133] Overall this would be consistent with the theme of airway tuft cells detecting bacterial products—or the conditions conducive to bacterial growth—and inducing rapid avoidance and clearance responses.

The function of tuft-induced fluid secretion in the colon is less clear. Colonic tuft cells have not been yet implicated in Type 2 immunity to helminths, likely due to the general restriction of helminths to the SI. Protists are found from the distal SI to the cecum and colon, but succinate does not induce fluid secretion in the cecum or colon. Work needs to be done to identify receptor-ligand pairs for colonic tuft cells. There is some data showing that ILC2s play a role in protection from colonic infection with the protozoan parasite *Entamoeba histolytica*, but the role of tuft cells in the response has not been tested.[134] *E. histolytica* is known for inducing diarrhea, so perhaps colonic tuft

cells induce some of that fluid secretion, which could be enhanced for parasite clearance or blocked to avoid dehydration and/or shock.

Human relevance of tuft-induced fluid secretion and therapeutic utilization of tuft activation in other tissues

The human relevance of tuft-driven fluid secretion is a crucial subject for further research. Both activation and suppression of tuft-induced fluid secretion could prove useful in the clinic. Patients with cystic fibrosis might benefit from inducing tuft-dependent fluid secretion, while patients with microbially-induced diarrhea could potentially benefit from suppressing the pathway. Tuft cells are the only *Chat*-expressing epithelial cell in human intestine[73] so human intestinal biopsies could be easily stimulated in the Ussing chamber using TRPM5 agonist Class 8.[135]

Beyond ACh and fluid secretion, future work should also investigate if intratracheal succinate administration can drive Type 2 immune activation in the trachea, since tracheal tuft cells express *Il25* and make cysteinyl leukotrienes in response to airway allergen exposure.[136] Similar studies with Class 8 in the colon would also be informative as to the potential role for colonic tuft cells in Type 2 immunity. Activation of a Type 2 response in the colon via tuft cells might combat the effects of pathological Type 1/17 inflammation seen with models of colitis and colon cancer, similar to the success of oral succinate treatment in a model of ileitis/inflammatory bowel disease (IBD).[95]

Other potential targets of tuft-derived ACh

Goblet cells and mucus secretion

We have focused on tuft cell ACh signaling on enterocytes to drive fluid secretion, but ACh receptors are expressed by many cells, including other types of intestinal epithelial cells. Goblet cells undergo compound exocytosis of mucus in response to ACh,[51,78,48] and the formation of goblet-associated antigen passages (GAPs) has also been linked to ACh signaling.[137,138] Additionally, tuft cell ACh was recently reported to induce mucus secretion from cholangiocytes in the gallbladder.[86] We therefore extensively tested the hypothesis that ACh from SI tuft cells signals on villus goblet cells to induce mucus secretion and GAP formation, but we could not find any evidence that this occurs *in vivo* (data not shown). A recent study demonstrating that muscarinic receptor expression is restricted to GCs at the base of SI crypts, and that only these cells respond acutely to CCh,[52] may explain why we did not detect tuft cell-dependent regulation of GC mucus secretion. While it remains possible that ACh from SI crypt tuft cells regulates secretion by GCs (and Paneth cells), we generally found fewer *Chat*+ tuft cells in the crypts than in the villi, and chemosensing pathways are likely not yet functional in immature crypt tuft cells. Perhaps in the colon tuft cell ACh regulates the function of sentinel GCs at crypt openings.[139]

Tuft-neuronal signaling

Despite finding little evidence that neurons consistently and specifically form synapses with tuft cells like they do with enteroendocrine cells,[140] it remains possible that signaling occurs from tuft cells to neurons via ACh. Indeed, we have observed notable examples of *Chat*+ neuronal processes approaching *Chat*+ tuft cells very closely in pSI and dSI tissue sections and one study found that 60% of SI tuft cells were

in “close contact” with a neuronal fiber, defined as less than 2 um apart.[116] While the constant migration of tuft cells out of the crypt and up the villi might pose a problem for sustained neuronal connections, there is some precedent for it as enteroendocrine cells manage to maintain synapse-like neuropod connections to neurons, though they live much longer than tuft cells.[140,141] Beyond imaging and colocalization studies, functional studies testing the ability of tuft cells to signal to neurons are needed to address this persistent question. Retrograde neuronal tracing from tuft cells to neurons might be feasible if a suitable virus can be pseudotyped to specifically infect tuft cells, whether by Cre-driven expression of an orthotopic receptor in tuft cells[142] or viral expression of a tuft-specific ligand, such as norovirus capsid protein.[143] The constant turnover of the SI epithelium presents a challenge for this approach, once again. Calcium imaging of intestinal neurons following tuft cell activation with succinate or Class 8 may be more tractable. Other markers of recent neuronal firing such as cFos may also be of use. The possibility of neuronal signaling to tuft cells, which express receptors for numerous neurotransmitters, also bears further inquiry.

Tuft-enteroendocrine signaling

Another observation made during long hours looking for tuft-neuronal contacts on the microscope is that *Chat*+, DCLK1+ tuft cells occasionally sit next to *Chat*+ DCLK1- cells. We have not been able to identify these cells, but one study observed that ~5% of DCLK1+ tuft cells make close contact with one of several subsets of enteroendocrine cells marked by staining for the peptide hormones CCK, PYY, and GLP-1.[116] Perhaps tuft cells regulate nutrient absorption or satiety indirectly through ACh signaling to enteroendocrine cells.[141] This could work in concert with the broader regulation of host

metabolism by Type 2 immunity or simply serve as a rapid effector response to prevent further ingestion of undesirable dietary components.

Chat+ epithelial cells and adaptive immunity

The SI can be roughly divided into villus-crypt tissue that specializes in nutrient absorption and gut-associated lymphoid tissue (GALT) that specializes in adaptive immune responses to luminal antigens.[144] While we have demonstrated a role for ChAT+ tuft cells in the villi, the function of ChAT+ tuft cells in the follicle-associated epithelium (FAE) of GALT remains entirely unknown. While imaging *Chat*-GFP mice we noticed a high density of *Chat*+ epithelial cells in the FAE overlying the domes of both Peyer's patches (PPs) and isolated lymphoid follicles (ILFs). A subset of these cells stained for DCLK1, marking them as tuft cells, but most did not. Canonically, microfold, or M, cells are the primary cell in the FAE.[145] Staining for the marker GP2 failed to mark most of the *Chat*+, DCLK1- cells but RNA sequencing of these cells confirmed their identity as M cells. *Chat*+ M cells have been noted before,[146] but the function of ACh from these cells, or from tuft cells located in the FAE, has not been investigated.

Peyer's patches (PPs) are the primary site of exposure of the immune system to antigens from the diet, commensal microbiome, and pathogens.[144] Antigen delivery is facilitated by M cells[145] as well as a network of stromal cell conduits that deliver lumenal fluid into the B and T cell-rich interfollicular region of the PP.[147] The flow of lumenal fluid into PPs is driven by fluid absorption across the epithelium and can be stopped by treatment with laxatives or inhibition of the ion channels that generate the osmotic gradient for fluid absorption. Since we know that ChAT+ tuft cells can induce fluid secretion, we hypothesize that tuft cell stimulation would increase luminal Cl^-, Na^+, and

H2O, increasing the osmotic gradient across the FAE resulting in greater fluid and thus antigen uptake into the PP. Antigen availability effects the quality of T cell help and B cell affinity maturation.[147] Additionally, the DCs, B cells, and T cells found in the PP express nicotinic ACh receptors[148] and may be directly regulated by tuft cell-derived ACh. The effect of ACh on intestinal immune cells is poorly understood, although ACh is known to have anti-inflammatory effects on macrophages[149] and increase plasma cell differentiation in the spleen.[150] We therefore hypothesize that ACh produced by ChAT+ cells in the FAE regulates adaptive immune responses in PPs.

ACh also induces the contraction of lymphatic vessels, known as lacteals, found in the intestinal villi.[151] One lacteal—lymphatic endothelial cells surrounded by smooth muscle—runs the length of each villus in relatively close proximity to the basolateral membrane of epithelial cells. Tuft cell-derived ACh may therefore signal on lacteals to affect the rate at which lymphatic fluid drains to lymphoid tissues, with effects on antigen presentation and adaptive immunity. Clearly there is much to left to learn about tuft-derived ACh!

REFERENCES

1. Hotez, P.J., Brindley, P.J., Bethony, J.M., King, C.H., Pearce, E.J., and Jacobson, J. (2008). Helminth infections: the great neglected tropical diseases. J Clin Invest *118*, 1311–1321. 10.1172/JCI34261.

2. Dobson, A., Lafferty, K.D., Kuris, A.M., Hechinger, R.F., and Jetz, W. (2008). Homage to Linnaeus: How many parasites? How many hosts? Proc Natl Acad Sci U S A *105*, 11482–11489. 10.1073/pnas.0803232105.

3. Cox, F.E.G. (2002). History of Human Parasitology. Clin Microbiol Rev *15*, 595–612. 10.1128/CMR.15.4.595-612.2002.

4. Maizels, R.M., and Yazdanbakhsh, M. (2003). Immune Regulation by helminth parasites: cellular and molecular mechanisms. Nat Rev Immunol *3*, 733–744. 10.1038/nri1183.

5. Grencis, R.K. (2015). Immunity to Helminths: Resistance, Regulation, and Susceptibility to Gastrointestinal Nematodes. Annual Review of Immunology *33*, 201–225. 10.1146/annurev-immunol-032713-120218.

6. Harris, N.L., and Loke, P. (2017). Recent Advances in Type-2-Cell-Mediated Immunity: Insights from Helminth Infection. Immunity *47*, 1024–1036. 10.1016/j.immuni.2017.11.015.

7. McSorley, H.J., and Maizels, R.M. (2012). Helminth Infections and Host Immune Regulation. Clin Microbiol Rev *25*, 585–608. 10.1128/CMR.05040-11.

8. Yazdanbakhsh, M., and Matricardi, P.M. (2004). Parasites and the hygiene hypothesis. Clinic Rev Allerg Immunol *26*, 15–23. 10.1385/CRIAI:26:1:15.

9. Bach, J.-F. (2002). The Effect of Infections on Susceptibility to Autoimmune and Allergic Diseases. N Engl J Med *347*, 911–920. 10.1056/NEJMra020100.

10. Akdis, C.A., Akdis, M., Boyd, S.D., Sampath, V., Galli, S.J., and Nadeau, K.C. (2023). Allergy: Mechanistic insights into new methods of prevention and therapy. Science Translational Medicine *15*, eadd2563. 10.1126/scitranslmed.add2563.

11. Colonna, M. (2018). Innate Lymphoid Cells: Diversity, Plasticity, and Unique Functions in Immunity. Immunity *48*, 1104–1117. 10.1016/j.immuni.2018.05.013.

12. Moro, K., Yamada, T., Tanabe, M., Takeuchi, T., Ikawa, T., Kawamoto, H., Furusawa, J., Ohtani, M., Fujii, H., and Koyasu, S. (2010). Innate production of TH2 cytokines by adipose tissue-associated c-Kit+Sca-1+ lymphoid cells. Nature *463*, 540–544. 10.1038/nature08636.

13. Neill, D.R., Wong, S.H., Bellosi, A., Flynn, R.J., Daly, M., Langford, T.K.A., Bucks, C., Kane, C.M., Fallon, P.G., Pannell, R., et al. (2010). Nuocytes represent a new innate effector leukocyte that mediates type-2 immunity. Nature *464*, 1367–1370. 10.1038/nature08900.

14. Price, A.E., Liang, H.-E., Sullivan, B.M., Reinhardt, R.L., Eisley, C.J., Erle, D.J., and Locksley, R.M. (2010). Systemically dispersed innate IL-13–expressing cells in type 2 immunity. Proceedings of the National Academy of Sciences *107*, 11489–11494. 10.1073/pnas.1003988107.

15. Shih, H.-Y., Sciumè, G., Mikami, Y., Guo, L., Sun, H.-W., Brooks, S.R., Urban, J.F., Davis, F.P., Kanno, Y., and O'Shea, J.J. (2016). Developmental Acquisition of Regulomes Underlies Innate Lymphoid Cell Functionality. Cell *165*, 1120–1133. 10.1016/j.cell.2016.04.029.

16. Van Dyken, S.J., Nussbaum, J.C., Lee, J., Molofsky, A.B., Liang, H.-E., Pollack, J.L., Gate, R.E., Haliburton, G.E., Ye, C.J., Marson, A., et al. (2016). A tissue checkpoint regulates type 2 immunity. Nat Immunol *17*, 1381–1387. 10.1038/ni.3582.

17. McGinty, J.W., and von Moltke, J. (2020). A three course menu for ILC and bystander T cell activation. Current Opinion in Immunology *62*, 15–21. 10.1016/j.coi.2019.11.005.

18. Howitt, M.R., Lavoie, S., Michaud, M., Blum, A.M., Tran, S.V., Weinstock, J.V., Gallini, C.A., Redding, K., Margolskee, R.F., Osborne, L.C., et al. (2016). Tuft cells, taste-chemosensory cells, orchestrate parasite type 2 immunity in the gut. Science *351*, 1329–1333. 10.1126/science.aaf1648.

19. von Moltke, J., Ji, M., Liang, H.-E., and Locksley, R.M. (2016). Tuft-cell-derived IL-25 regulates an intestinal ILC2–epithelial response circuit. Nature *529*, 221–225. 10.1038/nature16161.

20. Gerbe, F., Sidot, E., Smyth, D.J., Ohmoto, M., Matsumoto, I., Dardalhon, V., Cesses, P., Garnier, L., Pouzolles, M., Brulin, B., et al. (2016). Intestinal epithelial tuft cells initiate type 2 mucosal immunity to helminth parasites. Nature *529*, 226–230. 10.1038/nature16527.

21. Rhodin, J., and Dalhamn, T. (1956). Electron microscopy of the tracheal ciliated mucosa in rat. Zeitschrift für Zellforschung *44*, 345–412. 10.1007/BF00345847.

22. Jarvi, O., and Keyrilainen, O. (1956). On the cellular structures of the epithelial invasions in the glandular stomach of mice caused by intramural application of 20-methylcholantren. Acta Pathol Microbiol Scand Suppl *39*, 72–73.

23. OHMOTO, M., YAMAGUCHI, T., YAMASHITA, J., BACHMANOV, A.A., HIROTA, J., and MATSUMOTO, I. (2013). Pou2f3/Skn-1a Is Necessary for the Generation or Differentiation of Solitary Chemosensory Cells in the Anterior Nasal Cavity. Bioscience, Biotechnology, and Biochemistry *77*, 2154–2156. 10.1271/bbb.130454.

24. Yamashita, J., Ohmoto, M., Yamaguchi, T., Matsumoto, I., and Hirota, J. (2017). Skn-1a/Pou2f3 functions as a master regulator to generate Trpm5-expressing chemosensory cells in mice. PLoS ONE *12*, e0189340. 10.1371/journal.pone.0189340.

25. Höfer, D., Püschel, B., and Drenckhahn, D. (1996). Taste receptor-like cells in the rat gut identified by expression of alpha-gustducin. Proceedings of the National Academy of Sciences *93*, 6631–6634. 10.1073/pnas.93.13.6631.

26. Bezençon, C., Fürholz, A., Raymond, F., Mansourian, R., Métairon, S., Le Coutre, J., and Damak, S. (2008). Murine intestinal cells expressing Trpm5 are mostly brush cells and express markers of neuronal and inflammatory cells. J Comp Neurol *509*, 514–525. 10.1002/cne.21768.

27. Kinnamon, S.C., and Finger, T.E. (2019). Recent advances in taste transduction and signaling. F1000Res *8*, 2117. 10.12688/f1000research.21099.1.

28. Schneider, C., O'Leary, C.E., and Locksley, R.M. (2019). Regulation of immune responses by tuft cells. Nat Rev Immunol *19*, 584–593. 10.1038/s41577-019-0176-x.

29. von Moltke, J., Ji, M., Liang, H.-E., and Locksley, R.M. (2016). Tuft-cell-derived IL-25 regulates an intestinal ILC2-epithelial response circuit. Nature *529*, 221–225. 10.1038/nature16161.

30. McGinty, J.W., Ting, H.-A., Billipp, T.E., Nadjsombati, M.S., Khan, D.M., Barrett, N.A., Liang, H.-E., Matsumoto, I., and von Moltke, J. (2020). Tuft-Cell-Derived Leukotrienes Drive Rapid Anti-helminth Immunity in the Small Intestine but Are Dispensable for Anti-protist Immunity. Immunity *52*, 528-541.e7. 10.1016/j.immuni.2020.02.005.

31. Lei, W., Ren, W., Ohmoto, M., Urban, J.F., Matsumoto, I., Margolskee, R.F., and Jiang, P. (2018). Activation of intestinal tuft cell-expressed Sucnr1 triggers type 2 immunity in the mouse small intestine. Proc Natl Acad Sci U S A *115*, 5552–5557. 10.1073/pnas.1720758115.

32. Nadjsombati, M.S., McGinty, J.W., Lyons-Cohen, M.R., Jaffe, J.B., DiPeso, L., Schneider, C., Miller, C.N., Pollack, J.L., Nagana Gowda, G.A., Fontana, M.F., et al. (2018). Detection of Succinate by Intestinal Tuft Cells Triggers a Type 2 Innate Immune Circuit. Immunity *49*, 33-41.e7. 10.1016/j.immuni.2018.06.016.

33. Schneider, C., O'Leary, C.E., von Moltke, J., Liang, H.-E., Ang, Q.Y., Turnbaugh, P.J., Radhakrishnan, S., Pellizzon, M., Ma, A., and Locksley, R.M. (2018). A Metabolite-Triggered Tuft Cell-ILC2 Circuit Drives Small Intestinal Remodeling. Cell *174*, 271-284.e14. 10.1016/j.cell.2018.05.014.

34. Rubic, T., Lametschwandtner, G., Jost, S., Hinteregger, S., Kund, J., Carballido-Perrig, N., Schwärzler, C., Junt, T., Voshol, H., Meingassner, J.G., et al. (2008).

Triggering the succinate receptor GPR91 on dendritic cells enhances immunity. Nat Immunol *9*, 1261–1269. 10.1038/ni.1657.

35. Escalante, N.K., Lemire, P., Cruz Tleugabulova, M., Prescott, D., Mortha, A., Streutker, C.J., Girardin, S.E., Philpott, D.J., and Mallevaey, T. (2016). The common mouse protozoa Tritrichomonas muris alters mucosal T cell homeostasis and colitis susceptibility. J Exp Med *213*, 2841–2850. 10.1084/jem.20161776.

36. Chudnovskiy, A., Mortha, A., Kana, V., Kennard, A., Ramirez, J.D., Rahman, A., Remark, R., Mogno, I., Ng, R., Gnjatic, S., et al. (2016). Host-Protozoan Interactions Protect from Mucosal Infections through Activation of the Inflammasome. Cell *167*, 444-456.e14. 10.1016/j.cell.2016.08.076.

37. Billipp, T.E., Nadjsombati, M.S., and von Moltke, J. (2021). Tuning tuft cells: new ligands and effector functions reveal tissue-specific function. Current Opinion in Immunology *68*, 98–106. 10.1016/j.coi.2020.09.006.

38. Tizzano, M., Gulbransen, B.D., Vandenbeuch, A., Clapp, T.R., Herman, J.P., Sibhatu, H.M., Churchill, M.E.A., Silver, W.L., Kinnamon, S.C., and Finger, T.E. (2010). Nasal chemosensory cells use bitter taste signaling to detect irritants and bacterial signals. Proc Natl Acad Sci U S A *107*, 3210–3215. 10.1073/pnas.0911934107.

39. Krasteva, G., Canning, B.J., Hartmann, P., Veres, T.Z., Papadakis, T., Mühlfeld, C., Schliecker, K., Tallini, Y.N., Braun, A., Hackstein, H., et al. (2011). Cholinergic chemosensory cells in the trachea regulate breathing. Proc Natl Acad Sci U S A *108*, 9478–9483. 10.1073/pnas.1019418108.

40. Saunders, C.J., Christensen, M., Finger, T.E., and Tizzano, M. (2014). Cholinergic neurotransmission links solitary chemosensory cells to nasal inflammation. Proc Natl Acad Sci U S A *111*, 6075–6080. 10.1073/pnas.1402251111.

41. Florsheim, E.B., Sullivan, Z.A., Khoury-Hanold, W., and Medzhitov, R. (2021). Food allergy as a biological food quality control system. Cell *184*, 1440–1454. 10.1016/j.cell.2020.12.007.

42. Deckmann, K., Filipski, K., Krasteva-Christ, G., Fronius, M., Althaus, M., Rafiq, A., Papadakis, T., Renno, L., Jurastow, I., Wessels, L., et al. (2014). Bitter triggers acetylcholine release from polymodal urethral chemosensory cells and bladder reflexes. Proc Natl Acad Sci U S A *111*, 8287–8292. 10.1073/pnas.1402436111.

43. Perniss, A., Liu, S., Boonen, B., Keshavarz, M., Ruppert, A.-L., Timm, T., Pfeil, U., Soultanova, A., Kusumakshi, S., Delventhal, L., et al. (2020). Chemosensory Cell-Derived Acetylcholine Drives Tracheal Mucociliary Clearance in Response to Virulence-Associated Formyl Peptides. Immunity *52*, 683-699.e11. 10.1016/j.immuni.2020.03.005.

44. Hollenhorst, M.I., Jurastow, I., Nandigama, R., Appenzeller, S., Li, L., Vogel, J., Wiederhold, S., Althaus, M., Empting, M., Altmüller, J., et al. (2020). Tracheal brush cells release acetylcholine in response to bitter tastants for paracrine and autocrine signaling. FASEB J *34*, 316–332. 10.1096/fj.201901314RR.

45. Sam, C., and Bordoni, B. (2023). Physiology, Acetylcholine. In StatPearls (StatPearls Publishing).

46. Hubel, K.A. (1976). Intestinal ion transport: effect of norepinephrine, pilocarpine, and atropine. Am J Physiol *231*, 252–257. 10.1152/ajplegacy.1976.231.1.252.

47. Hirota, C.L., and McKay, D.M. (2006). Cholinergic regulation of epithelial ion transport in the mammalian intestine. Br J Pharmacol *149*, 463–479. 10.1038/sj.bjp.0706889.

48. Birchenough, G.M.H., Johansson, M.E.V., Gustafsson, J.K., Bergström, J.H., and Hansson, G.C. (2015). New developments in goblet cell mucus secretion and function. Mucosal Immunol *8*, 712–719. 10.1038/mi.2015.32.

49. Garcia, M.A.S., Yang, N., and Quinton, P.M. (2009). Normal mouse intestinal mucus release requires cystic fibrosis transmembrane regulator–dependent bicarbonate secretion. J Clin Invest *119*, 2613–2622. 10.1172/JCI38662.

50. Jk, G., A, E., D, A., Me, J., He, N., K, T., H, H., H, S., and Gc, H. (2012). Bicarbonate and functional CFTR channel are required for proper mucin secretion and link cystic fibrosis with its mucus phenotype. The Journal of experimental medicine *209*. 10.1084/jem.20120562.

51. Specian, R.D., and Neutra, M.R. (1980). Mechanism of rapid mucus secretion in goblet cells stimulated by acetylcholine. J Cell Biol *85*, 626–640. 10.1083/jcb.85.3.626.

52. Dolan, B., Ermund, A., Martinez-Abad, B., Johansson, M.E.V., and Hansson, G.C. (2022). Clearance of small intestinal crypts involves goblet cell mucus secretion by intracellular granule rupture and enterocyte ion transport. Sci Signal *15*, eabl5848. 10.1126/scisignal.abl5848.

53. Liu, J., Walker, N.M., Ootani, A., Strubberg, A.M., and Clarke, L.L. (2015). Defective goblet cell exocytosis contributes to murine cystic fibrosis–associated intestinal disease. J Clin Invest *125*, 1056–1068. 10.1172/JCI73193.

54. Zhao, A., McDermott, J., Urban, J.F., Gause, W., Madden, K.B., Yeung, K.A., Morris, S.C., Finkelman, F.D., and Shea-Donohue, T. (2003). Dependence of IL-4, IL-13, and nematode-induced alterations in murine small intestinal smooth muscle contractility on Stat6 and enteric nerves. J Immunol *171*, 948–954. 10.4049/jimmunol.171.2.948.

55. Sanderson, B.E., and Ogilvie, B.M. (1971). A study of acetylcholinesterase throughout the life cycle of Nippostrongylus brasiliensis. Parasitology *62*, 367–373. 10.1017/s0031182000077519.

56. Blackburn, C.C., and Selkirk, M.E. (1992). Characterisation of the secretory acetylcholinesterases from adult Nippostrongylus brasiliensis. Mol Biochem Parasitol *53*, 79–88. 10.1016/0166-6851(92)90009-9.

57. Lawrence, C.E., and Pritchard, D.I. (1993). Differential secretion of acetylcholinesterase and proteases during the development of Heligmosomoides polygyrus. Int J Parasitol *23*, 309–314. 10.1016/0020-7519(93)90004-i.

58. Yajima, T., Inoue, R., Matsumoto, M., and Yajima, M. (2011). Non-neuronal release of ACh plays a key role in secretory response to luminal propionate in rat colon. J Physiol *589*, 953–962. 10.1113/jphysiol.2010.199976.

59. Chu, C., Parkhurst, C.N., Zhang, W., Zhou, L., Yano, H., Arifuzzaman, M., and Artis, D. (2021). The ChAT-acetylcholine pathway promotes group 2 innate lymphoid cell responses and anti-helminth immunity. Sci Immunol *6*, eabe3218. 10.1126/sciimmunol.abe3218.

60. Roberts, L.B., Schnoeller, C., Berkachy, R., Darby, M., Pillaye, J., Oudhoff, M.J., Parmar, N., Mackowiak, C., Sedda, D., Quesniaux, V., et al. (2021). Acetylcholine production by group 2 innate lymphoid cells promotes mucosal immunity to helminths. Sci Immunol *6*, eabd0359. 10.1126/sciimmunol.abd0359.

61. Ramirez, V.T., Godinez, D.R., Brust-Mascher, I., Nonnecke, E.B., Castillo, P.A., Gardner, M.B., Tu, D., Sladek, J.A., Miller, E.N., Lebrilla, C.B., et al. (2019). T-cell derived acetylcholine aids host defenses during enteric bacterial infection with Citrobacter rodentium. PLOS Pathogens *15*, e1007719. 10.1371/journal.ppat.1007719.

62. Reardon, C., Duncan, G.S., Brüstle, A., Brenner, D., Tusche, M.W., Olofsson, P.S., Rosas-Ballina, M., Tracey, K.J., and Mak, T.W. (2013). Lymphocyte-derived ACh regulates local innate but not adaptive immunity. Proceedings of the National Academy of Sciences *110*, 1410–1415. 10.1073/pnas.1221655110.

63. Clarke, L.L. (2009). A guide to Ussing chamber studies of mouse intestine. Am J Physiol Gastrointest Liver Physiol *296*, G1151-1166. 10.1152/ajpgi.90649.2008.

64. Frizzell, R.A., and Hanrahan, J.W. (2012). Physiology of epithelial chloride and fluid secretion. Cold Spring Harb Perspect Med *2*, a009563. 10.1101/cshperspect.a009563.

65. Herbert, D.R., Yang, J.-Q., Hogan, S.P., Groschwitz, K., Khodoun, M., Munitz, A., Orekov, T., Perkins, C., Wang, Q., Brombacher, F., et al. (2009). Intestinal epithelial cell secretion of RELM-beta protects against gastrointestinal worm infection. J Exp Med *206*, 2947–2957. 10.1084/jem.20091268.

66. Horsnell, W.G.C., Cutler, A.J., Hoving, J.C., Mearns, H., Myburgh, E., Arendse, B., Finkelman, F.D., Owens, G.K., Erle, D., and Brombacher, F. (2007). Delayed goblet cell hyperplasia, acetylcholine receptor expression, and worm expulsion in SMC-specific IL-4Ralpha-deficient mice. PLoS Pathog *3*, e1. 10.1371/journal.ppat.0030001.

67. Akiho, H., Blennerhassett, P., Deng, Y., and Collins, S.M. (2002). Role of IL-4, IL-13, and STAT6 in inflammation-induced hypercontractility of murine smooth muscle cells. Am J Physiol Gastrointest Liver Physiol *282*, G226-232. 10.1152/ajpgi.2002.282.2.G226.

68. Cooke, H.J. (1998). “Enteric Tears”: Chloride Secretion and Its Neural Regulation. News Physiol Sci *13*, 269–274.

69. Xue, J., Askwith, C., Javed, N.H., and Cooke, H.J. (2007). Autonomic nervous system and secretion across the intestinal mucosal surface. Auton Neurosci *133*, 55–63. 10.1016/j.autneu.2007.02.001.

70. Cox, M.A., Bassi, C., Saunders, M.E., Nechanitzky, R., Morgado-Palacin, I., Zheng, C., and Mak, T.W. (2020). Beyond neurotransmission: acetylcholine in immunity and inflammation. J Intern Med *287*, 120–133. 10.1111/joim.13006.

71. Mashimo, M., Moriwaki, Y., Misawa, H., Kawashima, K., and Fujii, T. (2021). Regulation of Immune Functions by Non-Neuronal Acetylcholine (ACh) via Muscarinic and Nicotinic ACh Receptors. Int J Mol Sci *22*, 6818. 10.3390/ijms22136818.

72. Haber, A.L., Biton, M., Rogel, N., Herbst, R.H., Shekhar, K., Smillie, C., Burgin, G., Delorey, T.M., Howitt, M.R., Katz, Y., et al. (2017). A single-cell survey of the small intestinal epithelium. Nature *551*, 333–339. 10.1038/nature24489.

73. Schütz, B., Ruppert, A.-L., Strobel, O., Lazarus, M., Urade, Y., Büchler, M.W., and Weihe, E. (2019). Distribution pattern and molecular signature of cholinergic tuft cells in human gastro-intestinal and pancreatic-biliary tract. Sci Rep *9*, 17466. 10.1038/s41598-019-53997-3.

74. Deng, J., Tan, L.H., Kohanski, M.A., Kennedy, D.W., Bosso, J.V., Adappa, N.D., Palmer, J.N., Shi, J., and Cohen, N.A. (2021). Solitary chemosensory cells are innervated by trigeminal nerve endings and autoregulated by cholinergic receptors. Int Forum Allergy Rhinol *11*, 877–884. 10.1002/alr.22695.

75. Lips, K.S., Wunsch, J., Zarghooni, S., Bschleipfer, T., Schukowski, K., Weidner, W., Wessler, I., Schwantes, U., Koepsell, H., and Kummer, W. (2007). Acetylcholine and molecular components of its synthesis and release machinery in the urothelium. Eur Urol *51*, 1042–1053. 10.1016/j.eururo.2006.10.028.

76. Nadjsombati, M.S., Niepoth, N., Webeck, L.M., Kennedy, E.A., Jones, D.L., Baldridge, M.T., Bendesky, A., and Moltke, J. von (2022). Genetic mapping reveals

Pou2af2-dependent tuning of tuft cell differentiation and intestinal type 2 immunity. 2022.10.19.512785. 10.1101/2022.10.19.512785.

77. von Moltke, J., Ji, M., Liang, H.-E., and Locksley, R.M. (2016). Tuft-cell-derived IL-25 regulates an intestinal ILC2-epithelial response circuit. Nature *529*, 221–225. 10.1038/nature16161.

78. Gustafsson, J.K., Ermund, A., Johansson, M.E.V., Schütte, A., Hansson, G.C., and Sjövall, H. (2012). An ex vivo method for studying mucus formation, properties, and thickness in human colonic biopsies and mouse small and large intestinal explants. Am J Physiol Gastrointest Liver Physiol *302*, G430-438. 10.1152/ajpgi.00405.2011.

79. Stockinger, S., Albers, T., Duerr, C.U., Ménard, S., Pütsep, K., Andersson, M., and Hornef, M.W. (2014). Interleukin-13-mediated paneth cell degranulation and antimicrobial peptide release. J Innate Immun *6*, 530–541. 10.1159/000357644.

80. Banks, M.R., and Farthing, M.J.G. (2002). Fluid and electrolyte transport in the small intestine. Curr Opin Gastroenterol *18*, 176–181. 10.1097/00001574-200203000-00004.

81. Browning, J.G., Hardcastle, J., Hardcastle, P.T., and Redfern, J.S. (1978). Localization of the effect of acetylcholine in regulating intestinal ion transport. J Physiol *281*, 15–27. 10.1113/jphysiol.1978.sp012406.

82. Geubelle, P., Gilissen, J., Dilly, S., Poma, L., Dupuis, N., Laschet, C., Abboud, D., Inoue, A., Jouret, F., Pirotte, B., et al. (2017). Identification and pharmacological characterization of succinate receptor agonists. Br J Pharmacol *174*, 796–808. 10.1111/bph.13738.

83. Vanoye, C.G., Altenberg, G.A., and Reuss, L. (1999). Inhibition of P-glycoprotein-mediated transport by a hydrophobic contaminant in commercial gluconate salts. Am J Physiol *276*, C1439-1442. 10.1152/ajpcell.1999.276.6.C1439.

84. Harrington, A.M., Hutson, J.M., and Southwell, B.R. (2010). Cholinergic neurotransmission and muscarinic receptors in the enteric nervous system. Prog Histochem Cytochem *44*, 173–202. 10.1016/j.proghi.2009.10.001.

85. Xiong, Z., Zhu, X., Geng, J., Xu, Y., Wu, R., Li, C., Fan, D., Qin, X., Du, Y., Tian, Y., et al. (2022). Intestinal Tuft-2 cells exert antimicrobial immunity via sensing bacterial metabolite N-undecanoylglycine. Immunity *55*, 686-700.e7. 10.1016/j.immuni.2022.03.001.

86. Keshavarz, M., Faraj Tabrizi, S., Ruppert, A.-L., Pfeil, U., Schreiber, Y., Klein, J., Brandenburger, I., Lochnit, G., Bhushan, S., Perniss, A., et al. (2022). Cysteinyl leukotrienes and acetylcholine are biliary tuft cell cotransmitters. Sci Immunol *7*, eabf6734. 10.1126/sciimmunol.abf6734.

87. Lee, R.J., Kofonow, J.M., Rosen, P.L., Siebert, A.P., Chen, B., Doghramji, L., Xiong, G., Adappa, N.D., Palmer, J.N., Kennedy, D.W., et al. (2014). Bitter and sweet taste receptors regulate human upper respiratory innate immunity. J. Clin. Invest. *124*, 1393–1405. 10.1172/JCI72094.

88. Zhu, H., Aryal, D.K., Olsen, R.H.J., Urban, D.J., Swearingen, A., Forbes, S., Roth, B.L., and Hochgeschwender, U. (2016). Cre-dependent DREADD (Designer Receptors Exclusively Activated by Designer Drugs) mice. Genesis *54*, 439–446. 10.1002/dvg.22949.

89. Chen, X., Choo, H., Huang, X.-P., Yang, X., Stone, O., Roth, B.L., and Jin, J. (2015). The first structure-activity relationship studies for designer receptors exclusively activated by designer drugs. ACS Chem Neurosci *6*, 476–484. 10.1021/cn500325v.

90. Barilli, A., Aldegheri, L., Bianchi, F., Brault, L., Brodbeck, D., Castelletti, L., Feriani, A., Lingard, I., Myers, R., Nola, S., et al. (2021). From High-Throughput Screening to Target Validation: Benzo[d]isothiazoles as Potent and Selective Agonists of Human Transient Receptor Potential Cation Channel Subfamily M Member 5 Possessing In Vivo Gastrointestinal Prokinetic Activity in Rodents. J Med Chem *64*, 5931–5955. 10.1021/acs.jmedchem.1c00065.

91. Virginio, C., Aldegheri, L., Nola, S., Brodbeck, D., Brault, L., Raveglia, L.F., Barilli, A., Sabat, M., and Myers, R. (2022). Identification of positive modulators of TRPM5 channel from a high-throughput screen using a fluorescent membrane potential assay. SLAS Discov *27*, 55–64. 10.1016/j.slasd.2021.10.004.

92. Schütz, B., Jurastow, I., Bader, S., Ringer, C., von Engelhardt, J., Chubanov, V., Gudermann, T., Diener, M., Kummer, W., Krasteva-Christ, G., et al. (2015). Chemical coding and chemosensory properties of cholinergic brush cells in the mouse gastrointestinal and biliary tract. Front Physiol *6*, 87. 10.3389/fphys.2015.00087.

93. McLean, L.P., Smith, A., Cheung, L., Urban, J.F., Sun, R., Grinchuk, V., Desai, N., Zhao, A., Raufman, J.-P., and Shea-Donohue, T. (2016). Type 3 muscarinic receptors contribute to intestinal mucosal homeostasis and clearance of Nippostrongylus brasiliensis through induction of TH2 cytokines. Am J Physiol Gastrointest Liver Physiol *311*, G130-141. 10.1152/ajpgi.00461.2014.

94. Hollenhorst, M.I., Kumar, P., Zimmer, M., Salah, A., Maxeiner, S., Elhawy, M.I., Evers, S.B., Flockerzi, V., Gudermann, T., Chubanov, V., et al. (2022). Taste Receptor Activation in Tracheal Brush Cells by Denatonium Modulates ENaC Channels via Ca2+, cAMP and ACh. Cells *11*, 2411. 10.3390/cells11152411.

95. Banerjee, A., Herring, C.A., Chen, B., Kim, H., Simmons, A.J., Southard-Smith, A.N., Allaman, M.M., White, J.R., Macedonia, M.C., Mckinley, E.T., et al. (2020). Succinate Produced by Intestinal Microbes Promotes Specification of Tuft Cells to Suppress Ileal Inflammation. Gastroenterology *159*, 2101-2115.e5. 10.1053/j.gastro.2020.08.029.

96. Huh, W.J., Roland, J.T., Asai, M., and Kaji, I. (2020). Distribution of duodenal tuft cells is altered in pediatric patients with acute and chronic enteropathy. Biomedical Research *41*, 113–118. 10.2220/biomedres.41.113.

97. Aigbologa, J., Connolly, M., Buckley, J.M., and O'Malley, D. (2020). Mucosal Tuft Cell Density Is Increased in Diarrhea-Predominant Irritable Bowel Syndrome Colonic Biopsies. Front Psychiatry *11*, 436. 10.3389/fpsyt.2020.00436.

98. Fung, C., Fraser, L.M., Barrón, G.M., Gologorsky, M.B., Atkinson, S.N., Gerrick, E.R., Hayward, M., Ziegelbauer, J., Li, J.A., Nico, K.F., et al. (2022). Tuft cells mediate commensal remodeling of the small intestinal antimicrobial landscape. 2022.10.24.512770. 10.1101/2022.10.24.512770.

99. Sa, R., C, L., Am, M., K, L., Kl, T., C, B., S, K., Sk, G., A, N., Jm, A.-G., et al. (2019). CFTR-PTEN-dependent mitochondrial metabolic dysfunction promotes Pseudomonas aeruginosa airway infection. Science translational medicine *11*. 10.1126/scitranslmed.aav4634.

100. Me, K., Cm, M., Jg, G., Sd, P., An, G., R, A., S, Y., Pe, B., Ca, S., Pl, Z., et al. (2022). IL-13-programmed airway tuft cells produce PGE2, which promotes CFTR-dependent mucociliary function. JCI insight *7*. 10.1172/jci.insight.159832.

101. Hofmann, T., Chubanov, V., Gudermann, T., and Montell, C. (2003). TRPM5 is a voltage-modulated and Ca(2+)-activated monovalent selective cation channel. Curr Biol *13*, 1153–1158. 10.1016/s0960-9822(03)00431-7.

102. O'Leary, C.E., Schneider, C., and Locksley, R.M. (2019). Tuft Cells-Systemically Dispersed Sensory Epithelia Integrating Immune and Neural Circuitry. Annu Rev Immunol *37*, 47–72. 10.1146/annurev-immunol-042718-041505.

103. Marillier, R.G., Michels, C., Smith, E.M., Fick, L.C.E., Leeto, M., Dewals, B., Horsnell, W.G.C., and Brombacher, F. (2008). IL-4/IL-13 independent goblet cell hyperplasia in experimental helminth infections. BMC Immunol *9*, 11. 10.1186/1471-2172-9-11.

104. McKenzie, G.J., Bancroft, A., Grencis, R.K., and McKenzie, A.N. (1998). A distinct role for interleukin-13 in Th2-cell-mediated immune responses. Curr Biol *8*, 339–342. 10.1016/s0960-9822(98)70134-4.

105. Miller, H.R., Huntley, J.F., and Wallace, G.R. (1981). Immune exclusion and mucus trapping during the rapid expulsion of Nippostrongylus brasiliensis from primed rats. Immunology *44*, 419–429.

106. Oeser, K., Schwartz, C., and Voehringer, D. (2015). Conditional IL-4/IL-13-deficient mice reveal a critical role of innate immune cells for protective immunity against gastrointestinal helminths. Mucosal Immunol *8*, 672–682. 10.1038/mi.2014.101.

107. Hu, Z., Zhang, C., Sifuentes-Dominguez, L., Zarek, C.M., Propheter, D.C., Kuang, Z., Wang, Y., Pendse, M., Ruhn, K.A., Hassell, B., et al. (2021). Small proline-rich protein 2A is a gut bactericidal protein deployed during helminth infection. Science (New York, N.Y.) *374*, eabe6723. 10.1126/science.abe6723.

108. Wu, D., Ahrens, R., Osterfeld, H., Noah, T.K., Groschwitz, K., Foster, P.S., Steinbrecher, K.A., Rothenberg, M.E., Shroyer, N.F., Matthaei, K.I., et al. (2011). Interleukin-13 (IL-13)/IL-13 receptor alpha1 (IL-13Ralpha1) signaling regulates intestinal epithelial cystic fibrosis transmembrane conductance regulator channel-dependent Cl- secretion. J Biol Chem *286*, 13357–13369. 10.1074/jbc.M110.214965.

109. Darby, M., Schnoeller, C., Vira, A., Culley, F.J., Bobat, S., Logan, E., Kirstein, F., Wess, J., Cunningham, A.F., Brombacher, F., et al. (2015). The M3 muscarinic receptor is required for optimal adaptive immunity to helminth and bacterial infection. PLoS Pathog *11*, e1004636. 10.1371/journal.ppat.1004636.

110. Wyatt, K.D., Sakamoto, K., and Watford, W.T. (2022). Tamoxifen administration induces histopathologic changes within the lungs of Cre-recombinase-negative mice: A case report. Lab Anim *56*, 297–303. 10.1177/00236772211042968.

111. C, S., Dj, T., and Rk, G. (2018). A sticky end for gastrointestinal helminths; the role of the mucus barrier. Parasite immunology *40*. 10.1111/pim.12517.

112. Middelhoff, M., Nienhüser, H., Valenti, G., Maurer, H.C., Hayakawa, Y., Takahashi, R., Kim, W., Jiang, Z., Malagola, E., Cuti, K., et al. (2020). Prox1-positive cells monitor and sustain the murine intestinal epithelial cholinergic niche. Nat Commun *11*, 111. 10.1038/s41467-019-13850-7.

113. Takahashi, T., Shiraishi, A., Murata, J., Matsubara, S., Nakaoka, S., Kirimoto, S., and Osawa, M. (2021). Muscarinic receptor M3 contributes to intestinal stem cell maintenance via EphB/ephrin-B signaling. Life Sci Alliance *4*, e202000962. 10.26508/lsa.202000962.

114. Madden, K.B., Yeung, K.A., Zhao, A., Gause, W.C., Finkelman, F.D., Katona, I.M., Urban, J.F., and Shea-Donohue, T. (2004). Enteric nematodes induce stereotypic STAT6-dependent alterations in intestinal epithelial cell function. J Immunol *172*, 5616–5621. 10.4049/jimmunol.172.9.5616.

115. Morroni, M., Cangiotti, A.M., and Cinti, S. (2007). Brush cells in the human duodenojejunal junction: an ultrastructural study. J Anat *211*, 125–131. 10.1111/j.1469-7580.2007.00738.x.

116. Cheng, X., Voss, U., and Ekblad, E. (2018). Tuft cells: Distribution and connections with nerves and endocrine cells in mouse intestine. Exp Cell Res *369*, 105–111. 10.1016/j.yexcr.2018.05.011.

117. Voehringer, D., Reese, T.A., Huang, X., Shinkai, K., and Locksley, R.M. (2006). Type 2 immunity is controlled by IL-4/IL-13 expression in hematopoietic non-eosinophil cells of the innate immune system. J Exp Med *203*, 1435–1446. 10.1084/jem.20052448.

118. Nadjsombati, M.S., McGinty, J.W., Lyons-Cohen, M.R., Jaffe, J.B., DiPeso, L., Schneider, C., Miller, C.N., Pollack, J.L., Nagana Gowda, G.A., Fontana, M.F., et al. (2018). Detection of Succinate by Intestinal Tuft Cells Triggers a Type 2 Innate Immune Circuit. Immunity *49*, 33-41.e7. 10.1016/j.immuni.2018.06.016.

119. Law, C.W., Chen, Y., Shi, W., and Smyth, G.K. (2014). voom: Precision weights unlock linear model analysis tools for RNA-seq read counts. Genome Biol *15*, R29. 10.1186/gb-2014-15-2-r29.

120. Robinson, M.D., and Oshlack, A. (2010). A scaling normalization method for differential expression analysis of RNA-seq data. Genome Biol *11*, R25. 10.1186/gb-2010-11-3-r25.

121. Robinson, M.D., McCarthy, D.J., and Smyth, G.K. (2010). edgeR: a Bioconductor package for differential expression analysis of digital gene expression data. Bioinformatics *26*, 139–140. 10.1093/bioinformatics/btp616.

122. Ritchie, M.E., Phipson, B., Wu, D., Hu, Y., Law, C.W., Shi, W., and Smyth, G.K. (2015). limma powers differential expression analyses for RNA-sequencing and microarray studies. Nucleic Acids Res *43*, e47. 10.1093/nar/gkv007.

123. Lips, K.S., Volk, C., Schmitt, B.M., Pfeil, U., Arndt, P., Miska, D., Ermert, L., Kummer, W., and Koepsell, H. (2005). Polyspecific Cation Transporters Mediate Luminal Release of Acetylcholine from Bronchial Epithelium. Am J Respir Cell Mol Biol *33*, 79–88. 10.1165/rcmb.2004-0363OC.

124. Wessler, I., and Kirkpatrick, C.J. (2008). Acetylcholine beyond neurons: the non-neuronal cholinergic system in humans. British Journal of Pharmacology *154*, 1558–1571. 10.1038/bjp.2008.185.

125. Sato, A., and Miyoshi, S. (1997). Fine structure of tuft cells of the main excretory duct epithelium in the rat submandibular gland. The Anatomical Record *248*, 325–331. 10.1002/(SICI)1097-0185(199707)248:3<325::AID-AR4>3.0.CO;2-O.

126. Hoover, B., Baena, V., Kaelberer, M.M., Getaneh, F., Chinchilla, S., and Bohórquez, D.V. (2017). The intestinal tuft cell nanostructure in 3D. Sci Rep *7*, 1652. 10.1038/s41598-017-01520-x.

127. Moyat, M., Lebon, L., Perdijk, O., Wickramasinghe, L.C., Zaiss, M.M., Mosconi, I., Volpe, B., Guenat, N., Shah, K., Coakley, G., et al. (2022). Microbial regulation of intestinal motility provides resistance against helminth infection. Mucosal Immunology *15*, 1283–1295. 10.1038/s41385-022-00498-8.

128. Roberts, L.B., Berkachy, R., Wane, M., Patel, D.F., Schnoeller, C., Lord, G.M., Gounaris, K., Ryffel, B., Quesniaux, V., Darby, M., et al. (2022). Differential Regulation of Allergic Airway Inflammation by Acetylcholine. Frontiers in Immunology *13*.

129. Hagen, J., Sarkies, P., and Selkirk, M.E. (2021). Lentiviral transduction facilitates RNA interference in the nematode parasite Nippostrongylus brasiliensis. PLOS Pathogens *17*, e1009286. 10.1371/journal.ppat.1009286.

130. Hagen, J., Ghosh, S., Sarkies, P., and Selkirk, M.E. (2023). Gene editing in the nematode parasite Nippostrongylus brasiliensis using extracellular vesicles to deliver active Cas9/guide RNA complexes. Frontiers in Parasitology *2*.

131. Sankaranarayanan, G., Berriman, M., and Rinaldi, G. (2021). An uneven race: genome editing for parasitic worms. Nat Rev Microbiol *19*, 621–621. 10.1038/s41579-021-00625-5.

132. Abongwa, M., Martin, R.J., and Robertson, A.P. (2017). A BRIEF REVIEW ON THE MODE OF ACTION OF ANTINEMATODAL DRUGS. Acta Vet (Beogr) *67*, 137–152. 10.1515/acve-2017-0013.

133. Hollenhorst, M.I., Jurastow, I., Nandigama, R., Appenzeller, S., Li, L., Vogel, J., Wiederhold, S., Althaus, M., Empting, M., Altmüller, J., et al. (2020). Tracheal brush cells release acetylcholine in response to bitter tastants for paracrine and autocrine signaling. FASEB j. *34*, 316–332. 10.1096/fj.201901314RR.

134. Uddin, M.J., Leslie, J.L., Burgess, S.L., Oakland, N., Thompson, B., Abhyankar, M., Revilla, J., Frisbee, A., Donlan, A.N., Kumar, P., et al. (2022). The IL-33-ILC2 pathway protects from amebic colitis. Mucosal Immunol *15*, 165–175. 10.1038/s41385-021-00442-2.

135. Rozehnal, V., Nakai, D., Hoepner, U., Fischer, T., Kamiyama, E., Takahashi, M., Yasuda, S., and Mueller, J. (2012). Human small intestinal and colonic tissue mounted in the Ussing chamber as a tool for characterizing the intestinal absorption of drugs. European Journal of Pharmaceutical Sciences *46*, 367–373. 10.1016/j.ejps.2012.02.025.

136. Tuft cell–produced cysteinyl leukotrienes and IL-25 synergistically initiate lung type 2 inflammation 10.1126/sciimmunol.abj0474.

137. Knoop, K.A., McDonald, K.G., McCrate, S., McDole, J.R., and Newberry, R.D. (2015). Microbial sensing by goblet cells controls immune surveillance of luminal antigens in the colon. Mucosal Immunol *8*, 198–210. 10.1038/mi.2014.58.

138. Gustafsson, J.K., Davis, J.E., Rappai, T., McDonald, K.G., Kulkarni, D.H., Knoop, K.A., Hogan, S.P., Fitzpatrick, J.A., Lencer, W.I., and Newberry, R.D. (2021). Intestinal goblet cells sample and deliver lumenal antigens by regulated endocytic uptake and transcytosis. Elife *10*, e67292. 10.7554/eLife.67292.

139. Birchenough, G.M.H., Nyström, E.E.L., Johansson, M.E.V., and Hansson, G.C. (2016). A sentinel goblet cell guards the colonic crypt by triggering Nlrp6-dependent Muc2 secretion. Science *352*, 1535–1542. 10.1126/science.aaf7419.

140. Bohórquez, D.V., Shahid, R.A., Erdmann, A., Kreger, A.M., Wang, Y., Calakos, N., Wang, F., and Liddle, R.A. (2015). Neuroepithelial circuit formed by innervation of sensory enteroendocrine cells. 10.1172/JCI78361.

141. Worthington, J.J., Reimann, F., and Gribble, F.M. (2018). Enteroendocrine cells-sensory sentinels of the intestinal environment and orchestrators of mucosal immunity. Mucosal Immunology *11*, 3–20. 10.1038/mi.2017.73.

142. Monosynaptic circuit tracing in vivo through Cre-dependent targeting and complementation of modified rabies virus 10.1073/pnas.1011756107.

143. Tropism for tuft cells determines immune promotion of norovirus pathogenesis 10.1126/science.aar3799.

144. Jung, C., Hugot, J.-P., and Barreau, F. (2010). Peyer's Patches: The Immune Sensors of the Intestine. International Journal of Inflammation *2010*, e823710. 10.4061/2010/823710.

145. Mabbott, N.A., Donaldson, D.S., Ohno, H., Williams, I.R., and Mahajan, A. (2013). Microfold (M) cells: important immunosurveillance posts in the intestinal epithelium. Mucosal Immunology *6*, 666–677. 10.1038/mi.2013.30.

146. Gautron, L., Rutkowski, J.M., Burton, M.D., Wei, W., Wan, Y., and Elmquist, J.K. (2013). Neuronal and nonneuronal cholinergic structures in the mouse gastrointestinal tract and spleen: Reporter Mouse for Peripheral Cholinergic Cells. J. Comp. Neurol. *521*, 3741–3767. 10.1002/cne.23376.

147. Chang, J.E., Buechler, M.B., Gressier, E., Turley, S.J., and Carroll, M.C. (2019). Mechanosensing by Peyer's patch stroma regulates lymphocyte migration and mucosal antibody responses. Nat Immunol *20*, 1506–1516. 10.1038/s41590-019-0505-z.

148. Xu, H., Ding, J., Porter, C.B.M., Wallrapp, A., Tabaka, M., Ma, S., Fu, S., Guo, X., Riesenfeld, S.J., Su, C., et al. (2019). Transcriptional atlas of intestinal immune cells reveals that neuropeptide α-CGRP modulates group 2 innate lymphoid cell responses. Immunity *51*, 696-708.e9. 10.1016/j.immuni.2019.09.004.

149. Matteoli, G., and Boeckxstaens, G.E. (2013). The vagal innervation of the gut and immune homeostasis. Gut *62*, 1214–1222. 10.1136/gutjnl-2012-302550.

150. Zhang, X., Lei, B., Yuan, Y., Zhang, L., Hu, L., Jin, S., Kang, B., Liao, X., Sun, W., Xu, F., et al. (2020). Brain control of humoral immune responses amenable to behavioural modulation. Nature *581*, 204–208. 10.1038/s41586-020-2235-7.

151. Choe, K., Jang, J.Y., Park, I., Kim, Y., Ahn, S., Park, D.-Y., Hong, Y.-K., Alitalo, K., Koh, G.Y., and Kim, P. (2015). Intravital imaging of intestinal lacteals unveils lipid drainage through contractility. 10.1172/JCI76509.